STATE SPACE BASED LOAD FREQUENCY CONTROL OF MULTI-AREA POWER SYSTEMS

KRISHNA PAL SINGH PARMAR

STATE SPACE BASED LOAD FREQUENCY CONTROL OF MULTI-AREA POWER SYSTEMS

A

Thesis Submitted

in Partial Fulfilment of the Requirements

for the Degree of

DOCTOR OF PHILOSOPHY

By

Krishna Pal Singh Parmar

Department of Electronics and Electrical Engineering

Indian Institute of Technology Guwahati

Guwahati - 781 039, INDIA.

October, 2013

Certificate

This is to certify that the thesis entitled "**STATE SPACE BASED LOAD FREQUENCY CONTROL OF MULTI-AREA POWER SYSTEMS**", submitted by **Krishna Pal Singh Parmar** (07610212), a research scholar in the *Department of Electronics & Electrical Engineering, Indian Institute of Technology, Guwahati*, for the award of the degree of **Doctor of Philosophy**, is a record of an original research work carried out by him under my supervision and guidance. The thesis has fulfilled all requirements as per the regulations of the Institute and in my opinion has reached the standard needed for submission. The results embodied in this thesis have not been submitted to any other University or Institute for the award of any degree or diploma.

Dated:

Guwahati.

Prof. Somanath Majhi
Dept. of Electronics & Electrical Engg.
Indian Institute of Technology Guwahati
Guwahati - 781039, Assam, India.

Acknowledgements

I would like to express my sincere gratitude to my supervisor, Prof. Somanath Majhi, for his excellent guidance and support throughout the course for this work. My heartfelt thanks to him for the unlimited support and patience shown to me. I would particularly like to thank for all his help in patiently and carefully correcting all my manuscripts and thesis. I would like to thank my doctoral committee members Prof. P. K. Bora, Prof. C. Mahanta and Dr. H. B. Nemade for sparing their precious time to evaluate the progress of my work. Their suggestions have been valuable. I am thankful to Prof. D. P. Kothari, Director(Research), MVSR Engineering College, Hyderabad, India and former Director i/c, IIT Delhi for guiding me on power system issues and sparing his valuable time to solve my difficulties all the way. I would also like to thank other faculty members for their kind help during my academic studies.

My special thanks to Mr. Sanjib, Mr. Sidananda, Mr. Goswami and all the members of the C&I Laboratory for providing various resources useful in research work. I had a great time with my many friends at IITG, including (but not limited to) Mr. Sanjoy, Mr. Dola, Mr. Govind, Mr. Bajrangbali and Mr Mridul. I thank them for their support and encouragement.

Among those deserving of a special mention is my wife Atri Parmar, who had extended her wholeheartedly support to bring this work into existence. She has been able to take care of my daughter and son extremely well. I thank my daughter Vaidehi and son Vansh for keeping me energetic and reducing my worries. Again, I am grateful to my parents, mother in-law Ms Shyama Baghel and elder brother Mr. R. B. Singh Parmar, whose love and encouragement made this research possible.

I am grateful to Sh. Subodh Garg, Director General, Sh. J. S. S. Rao, Principal Director (CP), Sh. S. K. Choudhary, Principal Director(MS), Ms Manju Mam, Director (MS) and colleagues of NPTI for guiding and helping me on various technical aspects. My special thanks goes to Sh. Manas Ray, former Director, NPTI, Guwahati who helped me to initiate this research work. Finally, I would like to thank the Almighty God for bestowing me this opportunity and showering his blessings on me to come out successful against all odds.

(Krishna Pal Singh Parmar)

Abstract

The main aim of this thesis is to present a state space based load frequency control (LFC) system in conventional and restructured power system environment emphasizing on multi-source power generation (MSPG). An output feedback controller (OFC) is presented with a pragmatic point of view. As full state feedback controllers (FSFCs) require the transfer of information from all parts of the system to a central control facility for processing, which for large scale interconnected power system could prove to be prohibitive, more practical and alternative forms of feedback controllers such as OFCs have been the subject of extensive investigation in the various control engineering applications. As these controllers use only a subset of the state vector for feedback purposes, they are simpler, more practical and easy to implement than the FSFCs. A simple algorithm is presented to optimize the OFC gains. All the power system models presented for LFC study have been simulated using MATLAB Simulation tool and dynamic responses, thereof, are obtained at optimum controller gain settings. The dynamic responses obtained with OFC have been compared with that of FSFC and in most of the cases improved results are obtained.

Most of the researchers worked on LFC of power systems considering thermal unit with non-reheat turbines. In this thesis, the LFC is extended for the conventional power systems with the combinations of non-reheat turbines, reheat turbines and hydro turbine. The control area having MSPG represented by an equivalent of thermal or hydro unit dynamics only may not result in a realistic design of LFC control. Therefore, new power system models with MSPG are presented in this thesis for LFC study in both conventional and restructured power system environment. The LFC system is further improved by considering AC-DC tie lines and thyristor controlled phase shifter (TCPS). Modified LFC of an interconnected power system with MSPG is proposed in restructured power system environment considering all the possible contracts between generation companies (GENECOs) and distribution companies(DISCOs). The LFC of hydro power plants operational in KHOZESTAN, IRAN has also been studied.

The proposed controller performs well on this hydro plant and improves the frequency deviation responses remarkably. The proposed controller shows its capability and flexibility by providing the desirable dynamic responses to all the power system models studied. To examine the robust performance of the OFC, the system parameters and operating load conditions are varied by $\pm 25\%$ from their nominal values to obtain the dynamic responses. The effects of generation rate constraint (GRC) and variation in step load perturbations (SLPs) are also examined. Dynamic responses are obtained by varying the regulation parameter and the most appropriate value is suggested for the power systems with MSPG.

Many research work on LFC systems have been reported in recent years. Still there is much room for further improvement and extensions of such schemes in new power system environment. In this thesis, LFC systems of several new models have been presented and improved dynamic responses are obtained.

CONTENTS

LIST OF FIGURES

LIST OF TABLES

NOMENCLATURE

ACE	Area control error
AGC	Automatic generation control
DISCO	Distribution company
FSFC	Full state feedback controller
GENCO	Generation company
ISE	Integral square error
ITAE	Integral of time weighted absolute error
LFC	Load frequency control
MAIPS	Multi-area interconnected power system
MIMO	Multi-input multi-output
MISO	Multi-input single output
MSPG	Multi-source power generation
OFC	Output feedback controller
OS	Overshoot
PI	Proportional integral controller
PID	Proportional integral and derivative controller
SAPS	Single area power system
SLP	Step load perturbation
ST	Settling time
TAIPS	Two area interconnected power system
TCPS	Thyristor controlled phase shifter
TRANSCO	Transmission company

MATHEMATICAL NOTATIONS

ACE_i	Area control error
P_{rti}	Rated capacity of control area, MW
P_{Li}	Nominal load of control area, MW
f	Nominal system frequency, Hz
Δf_i	Incremental change in frequency of control area, Hz
$Y_g(s)$	Governor dynamics
$Y_t(s)$	Turbine dynamics
$Y_p(s)$	Power system(rotating mass and load) dynamics
$\Delta P_{tie,12}$	Incremental change in actual tie line power flow from control area-1 to 2, pu MW
$\Delta P_{tie,i}$	Total tie line power change between control area-i and all other control areas, pu MW
ΔP_{Di}	Total incremental change in local load of control area, pu MW
ΔP_{mi}	Incremental generation change in turbine power output, pu MW
ΔP_{mki}	Incremental generation change in turbine power output of k^{th} GENCO of area, pu MW
ΔP_{gi}	Incremental change in governor output command, pu MW
ΔP_{vi}	Incremental change in governor valve position, pu MW
ΔP_{ci}	Incremental change in speed changer position, pu MW
ΔP_{cki}	Incremental change in speed changer position of k^{th} GENCO of area, pu MW
D_i	Equivalent system damping coefficient of control area, pu MW/Hz
H_i	Equivalent inertia constant of control area, MW-s/MVA
B_i	Frequency bias parameter of control area, pu MW/Hz
$K_i(s)$	Controller dynamics
$\tilde{K}$	Output feedback controller gain matrix

$\bar{K}$	Full state feedback controller gain matrix
a_{12}	control area capacity ratio
T_{SGi}	Steam turbine speed governor time constant, s
T_{Ti}	Steam turbine time constant, s
T_{PSi}	Power system time constant, s
R_i	Governor speed regulation parameter of control area, Hz/pu MW
R_{ki}	Governor speed regulation parameter of k^{th} GENCO of area, Hz/pu MW
K_{PSi}	Power system gain, Hz/pu MW
K_{Ri}	Steam turbine reheat constant
T_{Ri}	Steam turbine reheat time constant, s
T_{Wi}	Nominal starting time of water in penstock, s
T_{RSi}	Hydro turbine speed governor reset time, s
T_{RHi}	Hydro turbine speed governor transient droop time constant, s
T_{GHi}	Hydro turbine speed governor main servo time constant, s
X_{Gi}	Lead time constant of Gas turbine speed governor, s
Y_{Gi}	Lag time constant of Gas turbine speed governor, s
c_{gi}	Gas turbine valve positioner
b_{gi}	Gas turbine constant of valve positioner, s
T_{Fi}	Gas turbine fuel time constant, s
T_{CRi}	Gas turbine combustion reaction time delay, s
T_{CDi}	Gas turbine compressor discharge volume -time constant, s
α_{ki}	Generation contribution factor of k^{th} GENCO of area
epf_k	Economic participation factor of k^{th} generating unit
cpf_{kl}	Contract participation factor between k^{th} GENCO and $l^{th}DISCO$
T_{12}	Tie line power coefficient between area-1 and area-2
K_{Φ}	Gain constant of TCPS
T_{Φ}	Time constant of TCPS, s
K_{DCi}	Gain constant of HVDC link

T_{DCi}	Time constant of HVDC link, s

Subscripts

i	i^{th} control area
k	k^{th} GENCO
l	l^{th} DISCO
ki	k^{th} GENCO of i^{th} control area

LIST OF PUBLICATIONS

Journal Publications

1. K. P. Singh Parmar, S. Majhi and D. P. Kothari, Optimal Load Frequency Control of an Interconnected Power System, MIT International Journal of Electrical and Instrumentation Engineering, pp 1-5, Vol-1, No.1, 2011

2. K. P. Singh Parmar, S. Majhi and D. P. Kothari, Improvement of Dynamic Performance of LFC of the Two Area Power System: an Analysis using MATLAB, International Journal of Computer Applications, Vol 40, No. 10, pp 28-32, 2012

3. K. P. Singh Parmar, S. Majhi and D. P. Kothari, LFC of an Interconnected Power System with Thyristor Controlled Phase Shifter in the Tie Line, International Journal of Computer Applications, Vol 41, No. 9, pp 27-30, 2012

4. K. P. Singh Parmar, S. Majhi and D. P. Kothari, Load frequency control of a realistic power system with multi-source power generation, International Journal of Electrical Power and Energy Systems (Elsevier), Vol.42, pp 426-33, 2012

5. K. P. Singh Parmar, S. Majhi and D. P. Kothari, LFC of an Interconnected Power System with Multi-source Power Generation in Deregulated Power Environment, International Journal of Electrical Power and Energy Systems (Elsevier), manuscript no. IJEPES-D-12-00804R1 (Revision submitted)

Conference Publications

1. K. P. Singh Parmar, S. Majhi and D. P. Kothari, Multi-Area Load Frequency Control in a Power System Using Optimal Output Feedback Method, IEEE Conf. proceedings, PEDES, New Delhi, India, 2010.

2. K. P. Singh Parmar, S. Majhi and D. P. Kothari, Automatic Generation Control of an Interconnected Hydrothermal Power System, IEEE Conf. proceedings, INDICON, Kolkata, India, 2010.

3. K. P. Singh Parmar, S. Majhi and D. P. Kothari, Automatic Generation Control Strategies: A state of art survey, International Conference on Advances in Electrical and Electronics Engineering (ICAEEE) Proceedings, Moradabad, India, 2011.

CHAPTER 1

INTRODUCTION

1.1 Load frequency control

The automatic generation control(AGC) or LFC problem in power systems has a long history and has been one of the most important topics of research and study of interconnected power systems. In a power system, LFC as an ancillary service plays an important and fundamental role to maintain the power system reliability at an appropriate level. It has gained the importance with the change of power system structure and the growth of size and complexity of interconnected systems [1–9]. The successful operation of interconnected power systems requires the matching of total power generation with total load demand and associated power system losses [2–4]. As the demand deviates from its nominal value with an unpredictable small amount, the operating point of power system changes, and hence, system may experience deviations in nominal system frequency and scheduled tie line power exchanges, which may yield undesirable effects [2, 7, 9, 10]. Maintaining system frequency and tie line power interchanges with neighboring control areas at the scheduled values are the two main objectives of a power system LFC [4, 7, 10–14]. These objectives are met by measuring a control error signal, called the area control error (ACE), which represents the real power imbalance between generation and load [2, 6, 14, 15].

Depending on the type of generating units, and constraints on their range and rate of response to the LFC signals, the actual response time varies from a few seconds to several seconds [14, 16, 17]. In LFC practice, rapidly varying components of system signals are almost unobservable due to filters involved in the process. That is why further reduction in the re-

sponse time of LFC is neither possible nor desired. In practice, the design and performance of an LFC system depend on how generation units respond to control signal. Such control schemes are useful as they are able to maintain a sufficient level of reserved control range and a sufficient level of control rate [17].

Global analysis of the power system markets shows that LFC is one of the most profitable ancillary services of the interconnected power systems. This service is related to the short-term balance of real power and frequency of the power systems and acquires a principal role to enable power exchanges and to provide better conditions for electricity trading [5, 6, 11, 18–22]. The LFC modeling and control scheme have been explained in detail in the Chapter 2.

1.2 Research Background

LFC plays an important role in modern energy management systems. The LFC problem has been extensively studied during the last few decades. Most of the work focused on the LFC of conventional single area or two area power systems. The first attempt in the area of LFC has been to control the frequency of a power system via the flywheel governor of the synchronous machine. This technique was subsequently found to be insufficient, and a supplementary control was included to the governor with the help of a signal directly proportional to the frequency deviation plus its integral. This scheme constitutes the classical approach to the LFC of power systems. Very early works in this important area of LFC have been by Cohn et al. [23–27]. These works were based on tie line bias control strategy. Quazza [28] illustrated non-interactive control considering (i) non-interaction between frequency and tie line powers controls and (ii) each control area taking care of its own load variations. The revolutionary optimal control concept for LFC regulator designs of interconnected power systems was presented by Elgerd [8].

A technique based on coordinated system wide correction of time error and inadvertent interchange was discussed in an LFC study by Cohn [29]. Supplementary controllers were designed to regulate the ACEs to zero effectively. The research work also contributed the design

of LFC based on various control techniques. The power systems are usually large scale systems with complex nonlinear dynamics. However, most of the research work reported so far has been performed by considering linearized models of interconnected power systems. The LFC response for small load perturbations using linearized models of various power system components has been widely accepted [1–10]. The effect of GRC was included in the LFC studies, considering both continuous and discrete power system models [30–34]. Lot of research work has been presented on the modeling of various energy source dynamics for LFC studies of power systems [2, 5–7, 10, 35–38].

The LFC regulator design methods using modern optimal control theory enable the power engineers to design an optimal control system with respect to given performance criterion. Fosha and Elgerd [39] were the first to present their work on optimal LFC regulator design using this concept. A two-area interconnected power system (TAIPS)consisting of two identical power plants of non-reheat thermal turbines was taken for investigations. A new formulation for optimal LFC strategy has been proposed in [40]. The feasibility of an optimal LFC scheme requires the availability of all state variables for feedback. Next, the problem is to reconstruct the unavailable states from the available outputs and controls using an observer.

Considering state reconstruction, many significant contributions have been made [41–46]. Bohn and Miniesy [41] have studied the LFC of a TAIPS by making the use of differential approximation and a Luenberger observer. Exploiting the fact that the nonlinearity of the power system model, namely, the tie line power flow, is measurable, the observer has been designed to give zero asymptotic error, even for the nonlinear model. LFC schemes based on an optimal observer, using a nonlinear transformation [42] and reduced-order system models with a local observer [43] have been reported in the literature. A simple generating unit model oriented towards LFC and the method for its transfer function identification based on a two-stage procedure is presented in [46]. Due to practical difficulties in the implementation of regulators based on feedback of all state variables, suboptimal LFC regulator designs were considered [47–49]. A suboptimal and near-optimal LFC concept using modern control theory is proposed by Moorthy and Aggarwal [47]. The LFC regulator design using Lyapunov's second method and utilizing

minimum settling time theory has been proposed by Shirai [50]. The design of decentralized LFC based on structured singular values is presented in [51].

Various LFC schemes based on two-level [52] and multi-level [53–55] control concepts have been proposed. A two-level suboptimal controller has been suggested by Miniesy and Bohn [52]. However, this approach does not ensure zero steady state error, and hence, a multilevel finite time optimal controller design ensuring zero steady state error has been reported in [53]. The advantage of hierarchical structure is reflected in the fact that even if one of the control levels fails, the system remains in operation.

Keeping in view the accuracy and reliability of digital controllers, researchers have focussed on proposing digital LFC control schemes [56–63]. Ross [56] was probably the first to present a comprehensive direct digital LFC regulator for the power systems. Later, a digital LFC incorporating dynamic control criteria for performance evaluation of digital control system based on field test results was initiated by Ross and Green in [57]. Bohn and Miniesy [41] have analyzed the effect of the sampling period on the system's dynamic response. Kothari and coworkers [62, 64] have studied the LFC in discrete mode. The investigations were carried out with more feasible modeling of LFC strategy, i.e., considering that the system is operating in continuous mode and the controller is operating in discrete mode [64]. In [62], discrete mode LFC of an interconnected power system with reheat turbines considering a new ACE is described. The new ACE is derived from tie line power deviation, frequency deviation, time error, and inadvertent interchanges.

A robust controller design based on the Riccati equation approach has been proposed for the power systems [65, 66]. Later, based on a combination of the robust control approach and an adaptive control technique, a design procedure of a new robust adaptive controller was proposed for power system LFC with system parametric uncertainties [65]. The other research contributions on decentralized robust LFC based on the Riccati equation approach have been recorded in [67]. The design of decentralized robust LFC applying structured singular values is proposed by Yang et al. [68]. It has been shown that when the frequency response based diagonal dominance cannot be achieved, the structured singular values can be applied to design

decentralized LFC to achieve the desired system dynamic performance [68].

Apart from various LFC schemes, adaptive control has been a topic of research for a long time. The task of adaptive control is to make the process under control less sensitive to changes in process parameters and process dynamics. A number of articles have been appeared on adaptive LFC schemes [69–74]. In 1966, Ross [69] described control criteria in LFC and the related practical difficulties encountered in trying to achieve these criteria. The implementation and analysis of an adaptive LFC system on the Hungarian power system has been proposed by Vajk et al. [71]. A multi-area adaptive LFC scheme for LFC of power systems [73] and a reduced-order adaptive LFC for interconnected hydro-thermal power system [74] are reported in the literature.

Many researchers have applied the artificial intelligence and evolutionary algorithms based controllers for the LFC study. In recent years, the advent of modern intelligent methods, such as Artificial neural networks (ANNs), fuzzy logic, Genetic algorithms(GAs), Particle swarm optimization (PSO), PSO-hybrids and Bacterial Foraging(BF)-based optimization has solved the LFC problems [4, 15, 75–81]. Application of the ANN technique based on robust control methodologies for solution of the LFC problem in interconnected power system has appeared in the literatures [75, 76]. Shayeghi and Shayanfar [75] have presented the concept of the H_∞ robust control technique for training of radial biased function (RBF) neural networks for improvement of the performance of the proposed controller under various operating conditions. In Ref. [76], the idea of μ-synthesis control techniques has been used for training an ANN-based LFC controller too. Researches on the LFC problem shows the LFC analysis using the fuzzy proportional plus integral (PI) controller [78, 79].

Application of the optimal control theory to power system has shown that an optimal load frequency controller can improve the dynamic stability of a power system [4]. As state feedback controllers require the transfer of information from all parts of the system to a central control facility for processing, which for large scale interconnected power system could prove to be prohibitive, alternative more practical forms of feedback controllers such as output feedback and decentralized controllers have been the subject of extensive investigation. As these controllers

use only a subset of the state vector for feedback purposes, they are simpler, more practical and easy to implement than the full state feedback controllers [2, 49]. Bettayeb et. al [82] proposed the incorporation of time-weighted linear quadratic regulator state and output feedback control design for power system dynamic stability analysis. Shahnazi et. al [83] presented an output feedback control with disturbance rejection for a class of nonlinear multi-input multi- output (MIMO) systems with unknown but bounded disturbances. An application of linear quadratic Gaussian (LQG) based load frequency controller in a competitive electricity environment is witness of the popularity of state feedback controls [11]. Tyagi and Srivastava [84] presents the design of a decentralized AGC scheme where the controller has been designed by appropriately assigning the eigen-structure of each isolated subsystem via state feedback, satisfying the sufficient conditions for stability.

Most recently many researchers [1, 12, 13, 15, 80, 85–87] have studied the LFC problem of hydro, thermal systems using proportional, integral and derivative (PID) controller, fuzzy controller, decentralized controller and optimal multi input single output (MISO) PID controller based on different algorithms and optimization techniques. The fuzzy PI controller is known to give poor performance in system transient response. Chang et al. [88], obtained the optimum adjustment gains of the integral controller using GAs through performance indices integral square error (ISE) and integral of time of absolute error (ITAE). The premature convergence of GA degrades its efficiency and reduces the search capability. Nanda et al. [15] proposed the LFC using Bacterial Foraging-Based Optimization. PSO is developed through simulation of bird flocking in multi-dimensional space. Like GA, PSO is also less susceptible to getting trapped on local optimum [15, 80]. Mojtaba et al. [85] proposed a robust multi-variable model based predictive control (MPC) for the solution of LFC in a multi-area interconnected power system (MAIPS). The proposed control scheme is designed to consider multi-variable nature of LFC, system uncertainty and generation rate constraint, simultaneously. Alireza et al. [1] studied the LFC of the hydro power system (operational in Iran) using optimal MISO PID controller. Hasan et al. [86] presented the design of sub-optimal AGC regulators based on the constrained feedback control strategy using the feedback of system states. Decentralized load frequency

controller is presented for the LFC of an interconnected thermal power system [13] which uses large number of states for the controller feedback. Challa et al. [89] has presented the analysis and design of controller for two area hydro-thermal-gas AGC system. They have shown that for LFC study, optimal PI state feedback controller is more robust and performs better than conventional genetic algorithm based PI controller. However, this optimal PI state feedback controller uses all the states for feedback purpose which is practically difficult and results in the increased complexity and cost of the controller. Rakhshani et al. [87] have applied reduced-order observer control for two-area LFC system after deregulation. In fact, one of the main observed problems in the control of AGC systems is the limitation to access and measurement of state variables in the real world. So with a practical point of view, an optimal output feedback method, is used to solve this problem [90–94]. In the output feedback method, only the measurable state variables within each control area are required to use for feedback. All these controllers discussed have relative advantages and disadvantages. Shayeghi et al. [95] concluded in the state of art survey on LFC, that there are no rules as to when a particular technique is more suitable for the LFC problem.

Apart from advances in control concepts, there have been many changes during the last decade or more, such as deregulation of the power industry and use of super conducting magnetic energy storage, wind turbines and photovoltaic cells as other sources of electrical energy to the system. In a power system, the instantaneous mismatch between supply and demand of real power for sudden load changes can be reduced by the addition of active power sources with fast response such as battery energy storage (BES), super conducting magnetic energy storage (SMES), capacitive energy storage (CES) and Redox Flow Batteries devices [96–100]. Bhatti and Kothari [101] presented the Variable structure load-frequency control of isolated wind-diesel-micro-hydro hybrid power systems.

Literature survey shows that mostly AC tie lines are used for the interconnection of multi-area power systems and lesser attention is given to AC-DC parallel tie lines [2, 4]. HVDC transmission has emerged due to its various techno-economical advantages. One of the major applications of HVDC transmission is operating a DC link in parallel with an AC link intercon-

necting two control areas to get an improved system dynamic performance with greater stability margins under small disturbances in the system [102,103]. Considerable research work has been carried out on LFC of interconnected power systems connected via HVDC link in parallel with AC link [4, 102–105].

The Flexible AC Transmission Systems (FACTS) devices provide more flexibility in power system operation and control. TCPS is an effective FACTS device for the tie line power flow control of an interconnected power system. The TCPS device is modeled and used in series with tie lines to improve the dynamic performance of LFC of the interconnected power systems by the many researchers [4, 106–109].

The classical LFC based on ACE is difficult to implement in a restructured power system environment. In recent years, several control scenarios based on robust and optimal approaches have been proposed for the AGC system in deregulated power systems. Some research is contained in [5,6,11,18–22,84,110–113]. In the restructured power system environment, vertically integrated system of conventional power system do not exist [20]. In a competitive electricity market, generating companies (GENCOs), distribution companies (DISCOs), transmission companies (TRANSCOs), and power system operator (PSO) [5, 6, 18, 19, 114] are all market players. As there are so many GENCOs and DISCOs in the deregulated power system, a DISCO has the freedom to have a contract with any GENCOs for the transaction of power. A DISCO of one control area can make contract with a GENCO in another control area [19, 20]. For stable and secure operation of a power system, the PSO has to provide a number of ancillary services. One of the ancillary services is the frequency regulation based on the concept of the LFC. The crucial role of LFC system will continue in restructured power system environment with some modifications accounting bilateral transactions and deregulation policy [5]. A detailed discussion on LFC issues in power system operation after deregulation is reported in [20–22].

An LFC system required for Poolco-based transactions described in [20, 112] utilizes an integral controller. A method to find optimal controller gains of this type of controller for a two-area system is proposed in [20]. In [115], B. Tyagi et. al proposed a general model

for multi-area LFC suitable for a competitive electricity environment. LFC work in deregulated power system is reported in [5,11,18–20,84] where they have considered either thermal or hydro system in a control area. In new power system environment, a control area may have variety of sources like hydro, thermal, gas, renewable etc., therefore representing a control area by thermal or hydro system dynamics only may not result in a good design of LFC system [5, 6, 89, 90]. Recently some researchers studied the LFC of conventional power system considering hydro, thermal and gas generating units in each control area [89, 90, 116, 117], however they did not consider the LFC scheme in restructured power system environment.

1.3 Motivation

Global analysis of the power system markets shows that LFC is one of the most profitable ancillary services of the interconnected power systems. LFC is very important topic of research and many researchers studied this problems with various combinations of controllers and power system models. All the controller methods presented in literature for LFC study have their own advantages and disadvantages.

Application of the optimal control theory to power system has shown that an optimal LFC can improve the dynamic stability of a power system. The LFC regulator design techniques using modern optimal control theory enable the power engineers to design an optimal control system with respect to given performance criterion. As state feedback controllers require the transfer of information from all parts of the system to a central control facility for processing, which for large scale inter connected power system could prove to be prohibitive. In the larger systems all the states may not be available for measurement and require large number of sensors. Keeping in view the above, researchers motivated to make application of more promising and practical form of optimal OFC for the study of LFC as this controller uses only a subset of the state vector for feedback purposes, this is simpler, more practical and easy to implement than the full state feedback controller.

Apart from advances in control concepts, there have been many changes during the last

decade or more, such as deregulation of the power industry, use of AC-DC tie lines, FACTS devices etc. Most of the researchers considered either thermal or hydro generating units in a control area. In a real situation, control area may have variety of sources of generations such as hydro, thermal, gas, nuclear, solar, wind etc. The control area having different sources of power generation represented by an equivalent of thermal or hydro unit dynamics only may not result in realistic design of LFC control. Keeping in view the changing power scenario, combination of multi-source generators in a control area with their corresponding generation contribution factors is more realistic for the study of LFC Further, this motivated to include the more realistic combination of multi-source power generation (Thermal, hydro and gas) in a control area. An attempt has been made to study the LFC of various new power system models with MSPG including FACTS devices (TCPS), AC-DC tie lines and restructured power system environment. To demonstrate the performance of controller over a wide range of variation in parameters and load condition is also one of the key factor of motivation.

1.4 Significant contributions of the thesis

Although LFC has been widely addressed, keeping in view the changing power system environment there is still a lot of openings to this work. The thesis has investigated and contributed to the following areas:

- Mathematical modeling and state space forms of conventional power systems and power systems with MSPG are presented
- New power system models with MSPG considering TCPS, AC-DC lines and restructured power system environment are presented for LFC study
- A more practical form of optimal controllers, OFC is presented for LFC study. A simple algorithm is presented to solve the problem using MATLAB code
- OFC is presented for the LFC of TAIPSs (i)thermal-thermal with non-reheat (ii)thermal-thermal with reheat and (iii) hydro-thermal power plants and dynamic responses are com-

pared with FSFC

- OFC is presented for the LFC of (i) SAPS with MSPG (ii) TAIPS with MSPG and dynamic responses are compared with FSFC. LFC of low, medium and high head hydro plants is also studied. Sensitivity analysis is done over a wide range of variation of parameters and load conditions. Effect of GRC and variation in regulation parameter is also analyzed.

- OFC is presented and compared with most recent research work [1] on actual hydro plants and improved dynamic responses are obtained

- OFC is presented for LFC of TAIPS with MSPG considering AC-DC tie lines and improved dynamic responses are obtained

- OFC is presented for LFC of TAIPS with MSPG considering TCPS and improved dynamic responses are obtained

- OFC is presented for LFC of TAIPS with MSPG in restructured power system environment considering various possible contracts between GENCOs and DISCOs.

1.5 Organization of the thesis

The thesis is organized as follows:

Chapter 1 gives a general introduction on LFC problem. The past achievements in the LFC literature are briefly reviewed and the main motivation and significant contributions of the present thesis are summarized.

Chapter 2 presents mathematical modeling and LFC of power systems. The controller design equations and algorithm are presented in brief.

Chapter 3 discusses LFC of conventional power systems. The LFC of (i)Thermal-thermal power system with non-reheat turbines, (ii) Thermal-thermal power system with reheat turbine and (iii) Hydro-thermal power system has been studied and performance of OFC is compared with FSFC.

Chapter 4 proposes LFC of the power systems with MSPG. The LFC of (i) Single area power system with multi-source power generation, (ii) Two area interconnected power system with multi-source power generation (iii) Hydro power plants has been studied.

Chapter 5 is organized in two main sections. Firstly, the LFC of power system with MSPG considering AC-DC tie lines is presented. In the second section, LFC of power system with MSPG considering TCPS is studied.

In chapter 6, LFC of TAIPS with MSPG in restructured power system is presented.

Finally in Chapter 7, general conclusions and suggestions for further work are documented.

CHAPTER 2

MATHEMATICAL MODELING AND LFC OF POWER SYSTEMS

2.1 Introduction

A detailed literature survey on LFC problem has been carried out in the previous chapter. It is understood that the study of the response of power systems to perturbations and operational changes is greatly assisted by mathematical models and computer simulations. Mathematical models involving small perturbations are developed by linearization of the system around a current operating point but the larger disturbances have to be obtained by solving non-linear differential equations. The LFC study is basically based on the small signal analysis. The linearized models of turbines, governors, power systems and associated equations reported in [2, 7, 8, 10, 39] are well accepted and have been used by many researchers for LFC system modeling in isolated and interconnected power systems [4, 13, 81, 85, 86, 95].

In the classical control methodologies, frequency response plots such as Bode and Nyquist diagrams are usually used to obtain the desired gain and phase margins. The investigations carried out using classical control approaches reveal that it often result in relatively large overshoots and transient frequency deviation [9, 10, 34, 118]. Moreover, the settling time of the system frequency deviation is comparatively long. Most recently many researchers [1,12,13,15,80,85–87] have studied the LFC problem of hydro, thermal systems using PID controller, fuzzy controller, decentralized controller and optimal MISO PID controller based on different algorithms and optimization techniques. The fuzzy PI controller is known to give poor performance in system

transient response. Chang et al. [88], obtained the optimum adjustment gains of the integral controller using GAs through performance indices ISE and ITAE. The premature convergence of GA degrades its efficiency and reduces the search capability. Nanda et al. [15] proposed the LFC using Bacterial Foraging-Based Optimization. PSO is developed through simulation of bird flocking in multi-dimensional space. Like GA, PSO is also less susceptible to getting trapped on local optimum [15, 80]. Mojtaba et al. [85] proposed a robust multi-variable model based predictive control (MPC) for the solution of LFC in a multi-area power system. Alireza et al. [1] studied the LFC of the hydro power system (operational in Iran) using optimal MISO PID controller. Hasan et al. [86] presented the design of sub-optimal AGC regulators based on the constrained feedback control strategy using the feedback of system states. Decentralized load frequency controller is presented for the LFC of an interconnected thermal power system [13] which uses large number of states for the controller feedback. Challa et al. [89] has presented the analysis and design of controller for two area hydro-thermal-gas AGC system. They have shown that for LFC study, optimal PI state feedback controller is more robust and performs better than conventional genetic algorithm based PI controller. However, this optimal PI state feedback controller uses all the states for feedback purpose which is practically difficult and results in the increased complexity and cost of the controller. Rakhshani et al. [87] have applied reduced-order observer control for two-area LFC system after deregulation. In fact, one of the main observed problems in the control of AGC systems is the limitation to access and measurement of state variables in the real world. All these controllers discussed have relative advantages and disadvantages. Shayeghi et al. [95] concluded in the state of art survey on LFC that there are no rules as to when a particular technique is more suitable for the LFC problem.

Application of the optimal control theory to power system has shown that an optimal load frequency controller can improve the dynamic stability of a power system [4]. The LFC regulator design techniques using modern optimal control theory enable the power engineers to design an optimal control system with respect to given performance criterion. Fosha and Elgerd [39] were the first to present their work on optimal LFC regulator design using this concept. The feasibility of an optimal LFC scheme requires the availability of all state variables for feedback.

However, these efforts seem unrealistic, since it is difficult to achieve this. Then, the problem is to reconstruct the unavailable states from the available outputs and controls using an observer. Due to practical limitations in the implementation of regulators based on feedback of all state variables, suboptimal AGC regulator designs were considered [47–49].

As state feedback controllers require the transfer of information from all parts of the system to a central control facility for processing, which for large scale inter connected power system could prove to be prohibitive, alternative more practical forms of feedback controllers such as output feedback and decentralized controllers have been the subject of extensive investigation. As these controllers use only a subset of the state vector for feedback purposes, they are simpler, more practical and easy to implement than the full state feedback controllers [2, 49]. Bettayeb et. al [82] investigates the incorporation of time-weighted linear quadratic regulator state and output feedback control design for power system dynamic stability analysis. Shahnazi et. al [83] proposed an output feedback control with disturbance rejection for a class of non-linear MIMO systems with unknown but bounded disturbances. An application of LQG based load frequency controller in a competitive electricity environment is witness of the popularity of state feedback controls [11]. Tyagi and Srivastava [84] presents the design of a decentralized automatic generation control (AGC) scheme where the controller has been designed by appropriately assigning the eigen-structure of each isolated subsystem via state feedback, satisfying the sufficient conditions for stability. Mishra et al. [119] studied LFC using linear quadratic regulator where Kalman estimator is used to estimate the states. The estate estimation increases the complexity and cost of the controller. Amongst various control schemes of state feedback discussed above, the output feedback method [83, 120]seems to be more practical.

Most recent application of state feedback control (optimal control) [11, 82–84, 86, 87, 89, 90, 93, 94, 119] in LFC analysis of power systems shows their popularity and superiority over other controllers. The output feedback controller (OFC) is proposed in this thesis from pragmatic point of view, which uses less number of states as feedback. In the output feedback method, only the output state variables within each control area are required for feedback purpose. The proposed OFC overcomes the drawbacks of full state feedback controller (FSFC).

This chapter presents LFC modeling, associated equations and linearized models of single area power system (SAPS) and multi-area interconnected power systems (MAIPS) in detail. The new LFC model for the MAIPS having multi-source power generation(MSPG) is proposed. The fundamental and secondary LFC loops, concept of tie lines, ACEs are introduced. The controller design steps and algorithm of the OFC are described in detail. FSFC is used for the comparison purpose, however important equations are described in brief for the ready reference. The important steps to solve the LFC problem using proposed OFC are described in last.

2.2 Fundamental LFC loops

The frequency of a power system depends on active power balance. A change in active power demand at one point of a network is reflected in the entire power system by a change in frequency. Therefore, system frequency provides a useful index to indicate the imbalance between the active power generation and load. Any short-term energy imbalance will result in an instantaneous change in system frequency as the disturbance is initially offset by the kinetic energy of the rotating plant. Significant loss in the generation without an adequate system response can produce extreme frequency excursions outside the working range of the plant. Therefore LFC plays an important role to maintain the balance between power generation and frequency [5, 6].

The real power in a power system is being controlled by controlling the mechanical power output of the prime mover. Depending on the type of generation,the prime mover may be a steam turbine,gas turbine, hydro-turbine or diesel engine. In the case of a steam or hydro-turbine,mechanical power is controlled by the opening or closing of valves regulating the input of steam or water flow into the turbine. Steam (or water) input to turbines must be continuously regulated to match real power demand, failing which the machine speed will vary with consequent change in frequency [5, 6, 10].

In addition to a primary frequency control, most of the large synchronous generators are equipped with a supplementary frequency control loop. A schematic block diagram of a synchronous generator equipped with frequency control loops is shown in Fig. 2.1 where, the speed

governor senses the change in speed (frequency) via the primary and supplementary control loops. Very large mechanical forces are needed to position the main valve(or gate) against the high steam (or water) pressure, and these forces are obtained via several stages of hydraulic amplifiers. The hydraulic amplifier provides the necessary mechanical forces to position the main valve against the high-steam (or hydro) pressure, and the speed changer provides a steady-state power output setting for the turbine [5, 6, 10].

The speed governor on each generating unit provides the primary speed control function, and all generating units contribute to the overall change in generation, irrespective of the location of the load change, using their speed governing. However, primary control action is not usually sufficient to restore the system frequency and the supplementary control loop is required to adjust the load reference set point through the speed-changer motor. The supplementary loop performs a feedback via the frequency deviation and adds it to the primary control loop through a dynamic controller. The resulting signal (ΔP_c) is used to regulate the system frequency. In real-world power systems, the dynamic controller is usually a simple integral or proportional integral (PI) controller [2, 5, 6, 10].

As shown in Fig. 2.1, the frequency experiences a transient change (Δf) following a change in load (ΔP_D). Thus, the feedback mechanism comes into play and generates an appropriate signal for the turbine to make generation (ΔP_m), track the load and restore the system frequency [6].

2.3 Frequency response modeling

Power systems have a highly non-linear and time-varying nature. However, for the purpose of frequency control synthesis and analysis in the presence of load disturbances, a simple low-order linearized model is used. In comparison with voltage and rotor angle dynamics, the dynamics affecting frequency response are relatively slow, in the range of seconds to minutes. In this section, a simplified frequency response model for the described schematic block diagram in Fig. 2.1 with one generator unit is described, and then the resulting model is generalized

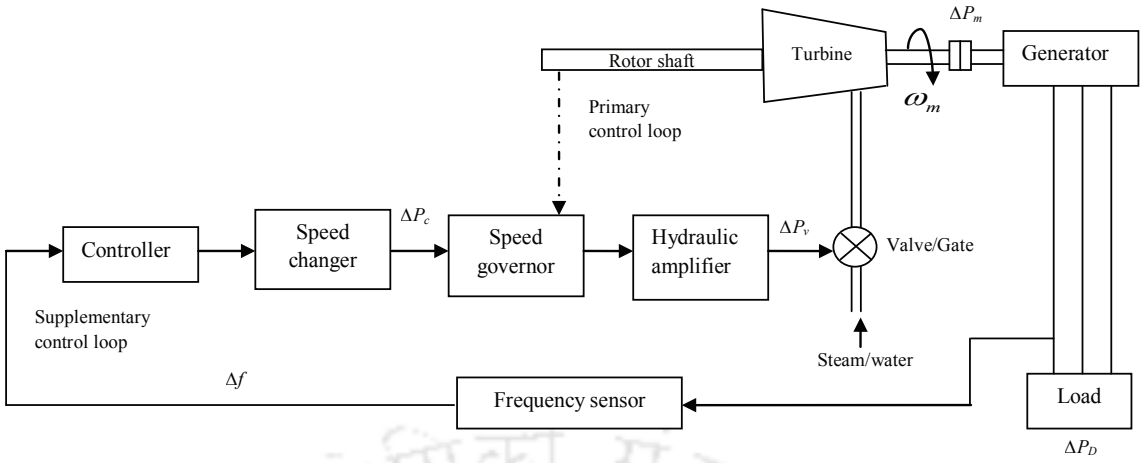

Figure 2.1: Schematic block diagram of a synchronous generator with basic frequency control loops

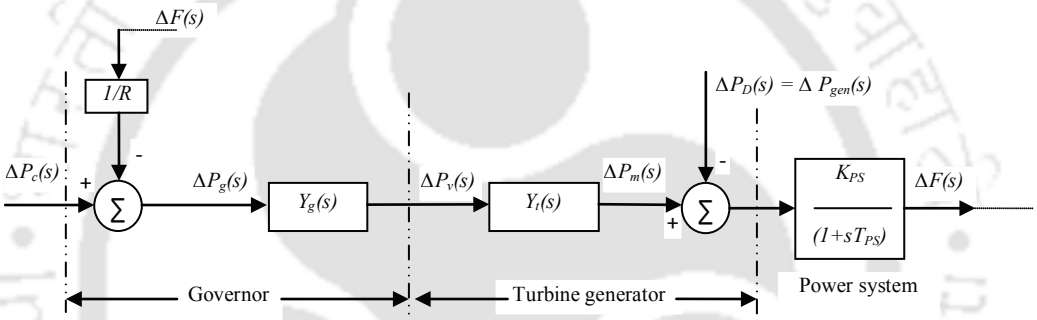

Figure 2.2: Linear model of the primary LFC loop

for multi-area interconnected power system as described in section 2.4. A linear model of the system with primary LFC loop is shown in Fig. 2.2 and its associated equation are presented in this section. An increase in governor command ΔP_g results from increase in ΔP_c and a decrease in Δf. Thus we can write for a small increment

$$\Delta P_g = \Delta P_c - \frac{1}{R}\Delta f \tag{2.1}$$

where

ΔP_g is small change in governor command,

ΔP_c is small change in reference power setting,

and R is the regulation parameter or droop characteristics (Hertz per pu MW). R is defined as the ratio of speed deviation or frequency deviation to change in valve/gate position or

power output. For example 4% R means that 4% frequency deviation causes 100% change in valve/gate position or power output.

Laplace transformation of the equation (2.1) yields

$$\Delta P_g(s) = \Delta P_c(s) - \frac{1}{R}\Delta F(s) \tag{2.2}$$

$Y_g(s)$, the transfer function of speed governor system is given by

$$Y_g(s) = \frac{\Delta P_v(s)}{\Delta P_g(s)} \tag{2.3}$$

The speed governor system transfer function, $Y_g(s)$ depends upon the type of the governing system used in the generating unit. A speed governing system of a steam turbine has the following transfer function [2, 7]:

$$Y_g(s) = \frac{1}{1+sT_{SG}} \tag{2.4}$$

where, T_{SG} is the steam turbine speed governor time constant.

The Turbine power increment ΔP_m depends entirely upon the control valve(or gate) power increment ΔP_v and response characteristics of the turbine.

The turbine transfer function may be given as

$$Y_t(s) = \frac{\Delta P_m(s)}{\Delta P_v(s)} \tag{2.5}$$

The turbine transfer function, $Y_t(s)$ depends upon the type of turbine.

A non-reheat steam turbine has the following transfer function [2, 7]:

$$Y_t(s) = \frac{\Delta P_m(s)}{\Delta P_v(s)} = \frac{1}{1+sT_T} \tag{2.6}$$

where, T_T is steam turbine time constant.

The generator power increment $\Delta P_{gen} = \Delta P_D$ depends entirely upon the changes ΔP_D in the load being fed from the generator, which adjusts its output so as to meet the demand changes. These adjustments are essentially instantaneous certainly in comparison with slow changes in turbine output, and therefore we can set

$$\Delta P_{gen} = \Delta P_D \tag{2.7}$$

Power system (load and machine) transfer function is given by

$$Y_p(s) = \frac{K_{PS}}{1 + sT_{PS}} \tag{2.8}$$

where

$K_{PS} = \frac{1}{D}$ is power system gain, Hz/pu MW,

H is the equivalent inertia constant, MW-s/MVA,

$T_{PS} = \frac{2H}{fD}$ is power system time constant, s

and $D = \frac{\partial P_l}{\partial f}\frac{1}{P_{rt}}$ is Equivalent system damping coefficient, pu MW/Hz.

$\Delta F(s)$ can now be expressed as

$$\Delta F(s) = Y_p(s)\left[\Delta P_m(s) - \Delta P_D(s)\right] \tag{2.9}$$

In fact, the block diagram of a single area power system without supplementary control shown in Fig. 2.2 is based on above equations and results. Now it is necessary that frequency deviations must settle with zero steady state error. To accomplish this supplementary control loop must be closed and the speed changer is manipulated in accordance with some suitable controller action. The signal fed into the controller is referred to as area control error (ACE). The ACE in an isolated(single area) power system may be defined as:

$$ACE = B\Delta f \tag{2.10}$$

where, B is frequency bias parameter, pu MW/Hz.

The speed changer can be commanded by a control signal ΔP_c obtained by a suitable control action on the error signal.

$$\Delta P_c = K(s)ACE \tag{2.11}$$

where, $K(s)$ is the controller.

For an example, Let the controller be integral controller, $K(s) = \frac{-K_I}{s}$ then ΔP_c becomes

$$\Delta P_c = -K_I \int B\Delta f\, dt \tag{2.12}$$

The polarity of integral controller must be chosen negative so as to cause a positive frequency error to give rise to a negative or decrease command. As long as an error remains the controller

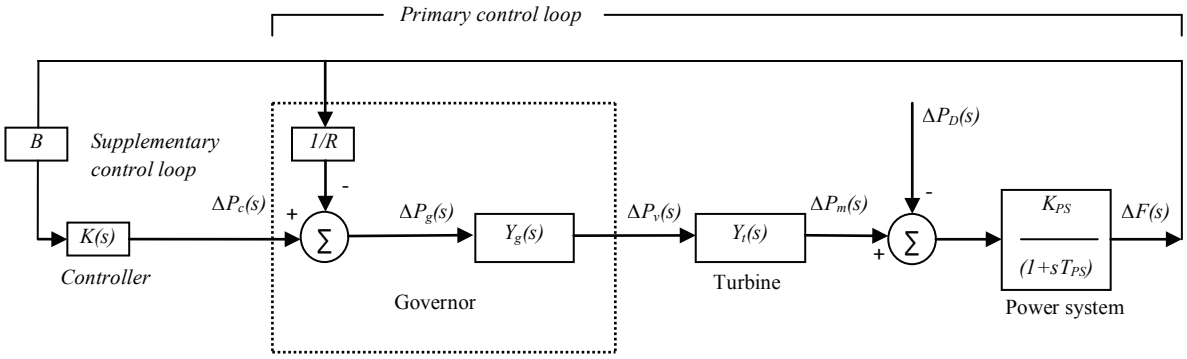

Figure 2.3: Linear model with supplementary LFC loop

output will increase, causing the speed changer to move. The controller output, and thus the speed changer position attains a constant value only when the frequency error has been reduced to zero. The gain constant K_I controls the rate of integration and thus speed of response of loop. A block diagram for an isolated (single area) system with supplementary control is as shown in Fig. 2.3.

2.4 LFC modeling of the MAIPS

In an isolated power system, regulation of tie-line power is not a control issue, and the LFC task is limited to restore the system frequency to the specified nominal value. In order to generalize the described model for interconnected power systems, the control area concept needs to be used, as it is a coherent area consisting of a group of generators and loads, where all the generators respond to changes in load or speed-changer settings, in unison. The frequency is assumed to be the same at all points of a control area. A multi-area power system comprises areas that are interconnected by high voltage transmission lines or tie lines. The trend of frequency measured in each control area is an indicator of the trend of the mismatch power in the interconnection and not in the control area alone. The LFC system in each control area of the multi-area interconnected power systems (MAIPS) should control the interchange power with the other control areas as well as its local frequency [2, 5, 6, 10]. Therefore, the described dynamic LFC system model shown in Fig. 2.3 must be modified by taking into account the tie-line power signal. For

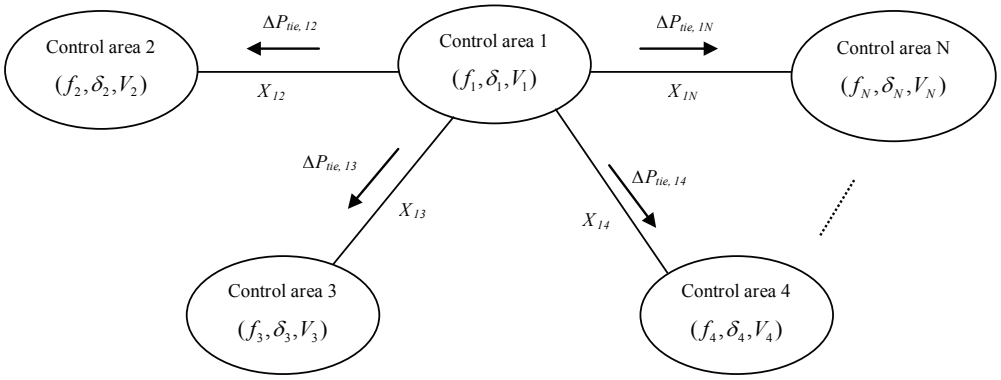

Figure 2.4: N-control areas power system

this purpose, consider Fig. 2.4, which shows a power system with N-control areas. In normal operation the tie line power flow from control area 1 to control area 2 is given by

$$P_{tie,12} = \frac{|V_1||V_2|}{X_{12}} \sin(\delta_1 - \delta_2) \tag{2.13}$$

where X_{12} is the tie-line reactance between control areas 1 and 2,

and δ_1 and δ_2 are the angles of end voltages V_1 and V_2 respectively.

For small deviations in the angles δ_1 and δ_2 the tie line power changes with

$$\Delta P_{tie,12} = \frac{|V_1||V_2|}{X_{12}} \cos(\delta_1 - \delta_2)(\Delta\delta_1 - \Delta\delta_2) \tag{2.14}$$

Synchronizing coefficient T_{12} of a line is defined by

$$T_{12} = \frac{|V_1||V_2|}{X_{12}} \cos(\delta_1 - \delta_2) \tag{2.15}$$

The tie line power deviation then takes on the form

$$\Delta P_{tie,12} = T_{12}(\Delta\delta_1 - \Delta\delta_2) \tag{2.16}$$

The frequency deviation Δf is related to the reference angle $\Delta\delta$ by the formula

$$\Delta\delta = 2\pi \int_0^t \Delta f dt \tag{2.17}$$

By expressing the tie line power deviations in term of Δf, we get

$$\Delta P_{tie,12} = 2\pi T_{12} \left(\int_0^t \Delta f_1 dt - \int_0^t \Delta f_2 dt \right) \tag{2.18}$$

Laplace transformation of the equation (2.18) yields

$$\Delta P_{tie,12}(s) = \frac{2\pi T_{12}}{s}\left(\Delta F_1(s) - \Delta F_2(s)\right) \tag{2.19}$$

Similarly the incremental tie line power flow from control area 2 to area 1 is given by

$$\Delta P_{tie,21} = 2\pi T_{21}\left(\int_0^t \Delta f_2 dt - \int_0^t \Delta f_1 dt\right) \tag{2.20}$$

Taking the Laplace transform of equation (2.20)

$$\Delta P_{tie,21}(s) = \frac{2\pi T_{21}}{s}\left(\Delta F_2(s) - \Delta F_1(s)\right) \tag{2.21}$$

where,

$$T_{21} = \frac{|V_2||V_1|}{X_{12}}\cos(\delta_2 - \delta_1) \tag{2.22}$$

If incremental powers are expressed in pu, then

$$T_{21} = -\frac{P_{rt1}}{P_{rt2}}T_{12} = a_{12}T_{12} \tag{2.23}$$

where

P_{rt1} and P_{rt2} are the rated power of control area 1 and 2 respectively,

and

a_{12} is the control area capacity ratio, defined as: $a_{12} = -\frac{P_{rt1}}{P_{rt2}}$

If losses are neglected and equal area ratings ($P_{rt1} = P_{rt2}$) are taken

$$\Delta P_{tie,21} = a_{12}\Delta P_{tie,12} = -\Delta P_{tie,12} \tag{2.24}$$

similarly, the tie line power change between areas 1 and 3 is given by

$$\Delta P_{tie,13}(s) = \frac{2\pi T_{13}}{s}\left(\Delta F_1(s) - \Delta F_3(s)\right) \tag{2.25}$$

and the tie line power change between control areas 1 and 4 is given by

$$\Delta P_{tie,14}(s) = \frac{2\pi T_{14}}{s}\left(\Delta F_1(s) - \Delta F_4(s)\right) \tag{2.26}$$

Considering equations (2.19), (2.25) and (2.26), the total tie line power change between control area 1 and the other control three areas 2, 3 and 4 can be calculated as

$$\Delta P_{tie,1}(s) = \Delta P_{tie,12}(s) + \Delta P_{tie,13}(s) + \Delta P_{tie,14}(s) = \frac{2\pi}{s}\left(\sum_{j=2,3,4} T_{1j}\Delta F_1(s) - \sum_{j=2,3,4} T_{1j}\Delta F_j(s)\right) \tag{2.27}$$

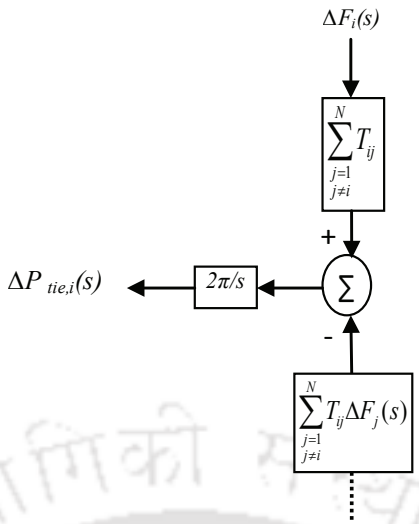

Figure 2.5: Block diagram representation for tie line power change of control area-*i* in an interconnected power system with N-control areas

Similarly, for N-control areas shown in Fig. 2.4, the total tie line power change between control area-*i* and all other control areas is

$$\Delta P_{tie,i}(s) = \sum_{\substack{j=1\\ j\neq i}}^{N} \Delta P_{tie,ij}(s) = \frac{2\pi}{s}\left(\sum_{\substack{j=1\\ j\neq i}}^{N} T_{ij}\Delta F_i(s) - \sum_{\substack{j=1\\ j\neq i}}^{N} T_{ij}\Delta F_j(s) \right) \tag{2.28}$$

Equation (2.28) is represented in the form of a block diagram in Fig. 2.5. The effect of changing the tie line power for an area is equivalent to changing the load of that area. Therefore, the $\Delta P_{tie,i}$ must be added to the mechanical power change ΔP_{mi} and control area load change ΔP_{Di} using an appropriate sign [2, 5, 6, 10]. A combination of block diagrams Figs. 2.3 and 2.5 creates a simplified block diagram for control area-*i* in an N-control area interconnected power system shown in Fig. 2.6. The next point to consider is the supplementary control loop in the presence of a tie line. In the case of an isolated control area, this loop is performed by a feedback from a control area frequency deviation through a simple dynamic controller as shown in Fig. 2.3. In a MAIPS, in addition to regulating area frequency, the supplementary control should maintain the tie line power interchange with neighboring areas at scheduled values. This is generally accomplished by adding a tie line power flow deviation to the frequency deviation in the supplementary feedback loop. A linear combination of frequency and tie line power changes

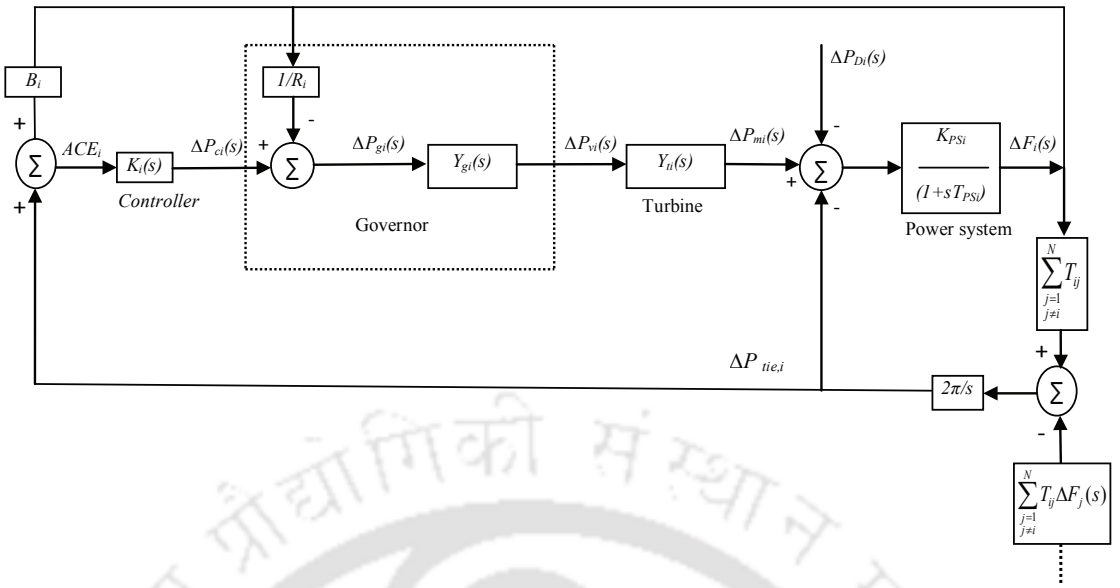

Figure 2.6: Control area-*i* of an interconnected power system with N number of control areas

for control area-*i*, is known as the ACE and can be given as:

$$ACE_i = \Delta P_{tie,i} + B_i \Delta f_i \tag{2.29}$$

B_i is the frequency bias parameter of i^{th} control area. B_i is assumed equal to the frequency bias factor(β_i) [2, 5, 6, 10].

$$B_i = \beta_i = D_i + \frac{1}{R_i} \tag{2.30}$$

The block diagram shown in Fig. 2.6 illustrates how supplementary control is implemented using equation (2.29). The effects of local load changes and interface with other control areas are properly considered as two input signals. Each control area monitors its own tie line power flow and frequency at the area control centre. The ACE signal is computed and allocated to the controller $K(s)$. Finally, the speed changer of i^{th} control area can be commanded by a corresponding control signal ΔP_{ci}. Therefore, it is expected that the supplementary control shown in Fig. 2.6 can ideally meet the basic LFC objectives and maintain area frequency and tie line interchange at scheduled values.

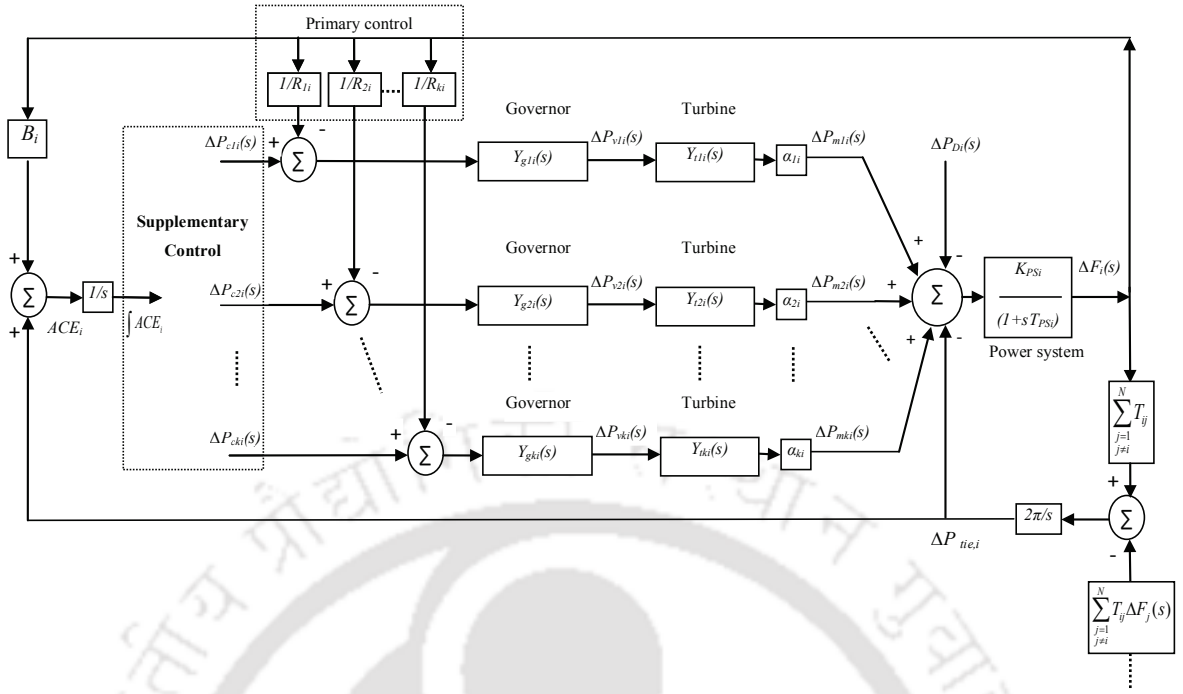

Figure 2.7: Control area-*i* of MAIPS with MSPG and N-number of control areas

2.5 LFC modeling of MAIPS with MSPG

Since the 1970s, the described LFC scheme and power system model in section 2.4 is widely used by researchers for the LFC analysis and synthesis. The far reaching restructuring of the power system industry, application of new technology and concomitant new concepts of operation requires an evaluation and re-examination of this scheme, which is already designed to operate with large and central generating facilities to find ways to maintain, and possibly improve, their efficiency and reliability. Most of the researchers considered either thermal or hydro generating units in a control area. In a real situation, control area may have variety of sources of generations such as hydro, thermal, gas, nuclear, solar, wind etc and the control area having different sources of power generation represented by an equivalent of thermal or hydro unit dynamics only may not result in realistic design of LFC control [6]. Furthermore, in the new power system environment, generators may or may not contribute in the LFC task and contribution factors are not the same for all participant generators [1, 5, 6, 17, 89, 116]. Keeping in view the present power scenario, combination of multi-source generators in a control area with their

corresponding generation contribution factors is more realistic for the study of LFC [89, 116]. In a competitive environment, generation contribution factors are actually time-dependent variables and must be computed dynamically based on bid prices, availability, congestion problems, costs and other related issues. In order to consider the variety of generation dynamics and their contribution rate in the LFC action, the dynamic model of control area-i in Fig. 2.6, can be modified to that shown in Fig. 2.7. From the Fig. 2.7, the total incremental generation change in turbine power outputs of i^{th} area may be given as:

$$\Delta P_{mi}(s) = \sum_{k=1}^{\bar{n}} \Delta P_{mki}(s) \tag{2.31}$$

where, $\bar{n}$ is number of generating units(GENCOs) in the i^{th} control area.

Let the generation contribution factor of k^{th} generating unit in the i^{th} area be defined as α_{ki}. The ΔP_{mki} may now be expressed in terms of $\Delta P_{mi}(s)$ and α_{ki} as:

$$\Delta P_{mki}(s) = \alpha_{ki} \Delta P_{mi}(s) \tag{2.32}$$

From the equation (2.32), it is obvious that ,the sum of generation contribution factors in a control area [5, 6, 89, 116] is equal to 1.

$$\sum_{k=1}^{\bar{n}} \alpha_{ki} = 1 \tag{2.33}$$

where, $0 \leq \alpha_{ki} \leq 1$.

Considering the effect of primary and supplementary controls, the system frequency can be obtained as:

$$\Delta F_i(s) = \frac{K_{PSi}}{(1+sT_{PSi})} \left(\sum_{k=1}^{\bar{n}} \Delta P_{mki}(s) - \Delta P_{Di}(s) - \Delta P_{tie,i}(s) \right) \tag{2.34}$$

and $\Delta P_{mki}(s)$ can be expressed [6, 17, 116] as:

$$\Delta P_{mki}(s) = Y_{gki}(s) Y_{tki}(s) \alpha_{ki} \left(\Delta P_{cki}(s) - \frac{\Delta F_i(s)}{R_{ki}} \right) \tag{2.35}$$

where, $Y_{gki}(s)$ and $Y_{tki}(s)$ are the transfer functions of governing system and turbines of k^{th} generating unit in the i^{th} control area, respectively.

using equations(2.35), the equation(2.34) results as:

$$\Delta F_i(s) = \frac{K_{PSi}}{(1+sT_{PSi})}\left[\sum_{k=1}^{\bar{n}} Y_{gki}(s)Y_{tki}(s)\alpha_{ki}\left(\Delta P_{cki}(s) - \frac{\Delta F_i(s)}{R_{ki}}\right) - \Delta P_{Di}(s) - \Delta P_{tie,i}(s)\right] \quad (2.36)$$

It is assumed that for i^{th} control area, $R_{ki} = R_i$, for ($k = 1$ to $\bar{n}$) and SLP is given in the control area. After knowing the generating units, corresponding $Y_{gki}(s)$ and $Y_{tki}(s)$ can be substituted into equation (2.36) to obtain the frequency response of the i^{th} control area. The LFC study of this kind of model is presented in the chapter 4.

2.6 Controller Design

Probably the most important contribution, optimal control theory has made to the control engineer is the ability to handle a large multivariate control problem with ease. The engineer has only to represent the control system in state variable form and specify the desired performance mathematically in terms of a cost to be minimized. A unique or best controller in the sense of minimizing the cost may be generated by applying well proven theories and techniques. Most recent application of state feedback controllers(optimal control) [11, 82–84, 86, 87, 89, 90, 93, 94, 119] in the LFC analysis of power systems shows their popularity and superiority over other controllers.

In modern control theory approach, control signals are generated by a linear combination of all the system states (full state feedback approach) or a linear combination of states to be controlled/measurable states (output feedback approach) [2, 7, 120]. The OFC is proposed to improve the LFC problem from practical point of view. Practically, it is very difficult and often expensive to measure and to have readily available information about all the states in most of the large power systems. Moreover, the implementation of optimal AGC regulator requires monitoring of all the state variables of the system or state reconstruction, which may be undesirable from cost and complexity considerations [86]. Usually reduced number of state variables or a linear combination thereof is available. The proposed OFC uses less number of feedback states as compared to FSFC, thereby reduces number of sensors, cost and complexities. In this section, FSFC is described in brief for the ready reference and the proposed OFC is explained

in a detail with algorithm.

The statement of the problem in an optimal control theory, may be described in the following state-space form: [1, 2, 7, 39, 119, 120]:

$$\dot{x} = \tilde{A}x + \tilde{B}u \tag{2.37}$$

and

$$y = \tilde{C}x \tag{2.38}$$

where

x is a state vector of the dimension $n \times 1$, n is no. of state variables

u is a control vector of the dimension $m \times 1$, m is no. of control variables

y is an output vector of the dimension $p \times 1$, p is no. of output variables

$\tilde{A}$, $\tilde{B}$ and $\tilde{C}$ are constant matrices with dimensions of $n \times n$, $n \times m$ and $p \times n$, respectively.

The performance of the system is specified in terms of a performance index or cost function(J):

$$J = \frac{1}{2}\int_0^\infty \left(x^T \tilde{Q}x + u^T \tilde{R}u\right) dt \tag{2.39}$$

which is minimized for obtaining parameters of an optimal controller. In the equation (2.39), $\tilde{Q}$ is $n \times n$, symmetric positive semi-definite state cost weighting matrix and $\tilde{R}$ is $m \times m$, symmetric positive semi-definite control cost weighting matrix. The elements of the matrices $\tilde{Q}$ and $\tilde{R}$ may be chosen as per the designer's choice.

The optimal controller law for full state feedback can be defined by [2]

$$u = -\bar{K}x \tag{2.40}$$

The constant gain matrix $\bar{K}$ of the dimension $m \times n$, is obtained from the solution of the matrix Riccati equation

$$\tilde{A}^T P + P\tilde{A} - P\tilde{B}\tilde{R}^{-1}\tilde{B}^T P + \tilde{Q} = 0 \tag{2.41}$$

$$\bar{K} = \tilde{R}^{-1}\tilde{B}^T P \tag{2.42}$$

For stability, all the eigenvalues of the matrix $(\tilde{A} - \tilde{B}\bar{K})$ should have negative real parts. From

equations (2.41) and (2.42), the optimal setting of FSFC gains($\bar{K}$) is obtained. The solution of Riccati equation (2.41) is obtained using the MATLAB function care.m [121, 122].

Let the output feedback control law be defined as

$$u = -\tilde{K}y \tag{2.43}$$

where $\tilde{K}$ is OFC gain matrix of dimension ($m \times p$).

In the optimal control scheme the control inputs are generated by means of feedbacks from the output states with feedback constants to be determined in accordance with optimality criterion. Using equations(2.38) and (2.43), the linear model given by equation (2.37) can be arranged as

$$\dot{x} = (\tilde{A} - \tilde{B}\tilde{K}\tilde{C})x = \tilde{A}_C x \tag{2.44}$$

The performance index given in equation (2.39) can be rewritten as

$$J = \frac{1}{2}\int_0^\infty \left(x^T \left(\tilde{Q} + \tilde{C}^T\tilde{K}^T\tilde{R}\tilde{K}\tilde{C}\right)x\right)dt \tag{2.45}$$

The control problem is now to design the gain matrix $\tilde{K}$ so that J is minimized subject to the following dynamical constraint:

$$\dot{x} = (\tilde{A} - \tilde{B}\tilde{K}\tilde{C})x \tag{2.46}$$

This dynamical optimization problem may be converted into an equivalent static one that is easier to solve. After optimization and simplification, the following optimal gain design equations are obtained [120]:

$$0 = \tilde{A}_c^T\tilde{P} + \tilde{P}\tilde{A}_c + \tilde{C}^T\tilde{K}^T\tilde{R}\tilde{K}\tilde{C} + \tilde{Q} \tag{2.47}$$

$$0 = \tilde{A}_c\tilde{S} + \tilde{S}\tilde{A}_c^T + X \tag{2.48}$$

$$\tilde{K} = \tilde{R}^{-1}\tilde{B}^T\tilde{P}\tilde{S}\tilde{C}^T(\tilde{C}\tilde{S}\tilde{C}^T)^{-1} \tag{2.49}$$

where

$X = E\left\{x(0)x^T(0)\right\}$

If initial states are assumed to be uniformly distributed on the unit sphere, then $X = I$, where

X is $n \times n$, symmetric matrix and I is an identity matrix. In many applications $x(0)$ may not be known, this dependence is typical of output feedback design. It is usual to sidestep this problem by minimizing not the performance index [120] but its expected value ($E\{J\}$) ,

$$E\{J\} = \frac{1}{2}E\left\{x^T(0)\tilde{P}x(0)\right\} = \frac{1}{2}tr(\tilde{P}X) \tag{2.50}$$

The optimal cost can be given by

$$J_0 = \frac{1}{2}tr(\tilde{P}X) \tag{2.51}$$

The equations(2.47) and (2.48) are Lyapunov equations and the equation (2.49) is an equation for the gain $\tilde{K}$. To obtain the output feedback gain $\tilde{K}$ minimizing the J_0, these three coupled equations may be solved simultaneously by iterative techniques [120]. Algorithm to solve these three coupled equations is presented in the section 2.6.1.

2.6.1 Algorithm for OFC

The algorithm for the proposed optimal OFC is as follows:

1.Initialize

Set j=0

set initial value of the gain $\tilde{K}_0$ so that $\tilde{A}_{c,0} = (\tilde{A} - \tilde{B}\tilde{K}_0\tilde{C})$ is asymptotically stable

2. j^{th} iteration

Set $\tilde{A}_{c,j} = (\tilde{A} - \tilde{B}\tilde{K}_j\tilde{C})$

solve Lyapunov equations for $\tilde{P}_j$ and $\tilde{S}_j$

$0 = \tilde{A}_{c,j}^T\tilde{P}_j + \tilde{P}_j\tilde{A}_{c,j} + \tilde{C}^T\tilde{K}_j^T\tilde{R}\tilde{K}_j\tilde{C} + \tilde{Q}$

$0 = \tilde{A}_{c,j}\tilde{S}_j + \tilde{S}_j\tilde{A}_{c,j}^T + X$

solve for $\tilde{K}_j$, where $j \neq 0$

$\tilde{K}_j = \tilde{R}^{-1}\tilde{B}^T\tilde{P}_j\tilde{S}_j\tilde{C}^T(\tilde{C}\tilde{S}_j\tilde{C}^T)^{-1}$

Set

$J_{0,j} = \frac{1}{2}tr(\tilde{P}_jX)$

Evaluate

$\Delta\tilde{K} = \tilde{R}^{-1}\tilde{B}^T\tilde{P}\tilde{S}\tilde{C}^T(\tilde{C}\tilde{S}\tilde{C}^T)^{-1} - \tilde{K}_j$

$\tilde{K}_{j+1} = \tilde{K}_j + \sigma\Delta\tilde{K}$

where σ is chosen so that $\tilde{A}_{c,j+1}$ is asymptotically stable

$J_{0,j+1} = \frac{1}{2}tr(\tilde{P}_{j+1}X) \leq J_{0,j}$

If the values of J_{j+1} and J_j are very close to each other go to step 3

otherwise set $j = j+1$ and go to step 2

3.Terminate

Set $\tilde{K} = \tilde{K}_{j+1}$

and $J_0 = J_{0,j+1}$

Stop

MATLAB code is developed based on the above algorithm to get the optimal value of OFC gains($\tilde{K}$).The Lyapunov equations are solved using MATLAB function lyap.m [121, 122].

2.6.2 Selection of $\tilde{Q}$ and $\tilde{R}$ matrices

The elements of matrices $\tilde{Q}$ and $\tilde{R}$ may be chosen as per the designer's choice [120]. To obtain the desired dynamic response and for the dynamic correction of *ACE* of LFC systems discussed in this thesis, the following design criterion are considered to obtain the matrices $\tilde{Q}$ and $\tilde{R}$ [2, 90, 120, 123]:

1. Excursions of ACEs about their steady values are minimized.
2. Excursions of $\int ACEdt$ about the steady values are minimized.
3. Excursions of control vector about their steady values are minimized.

2.7 Important steps to solve LFC problem

1. Obtain the state equations for the LFC model of the power systems and represent in the state space form.
2. Input the system simulation parameters and data.
3. Compute matrices $\tilde{A}$, $\tilde{B}$ and $\tilde{C}$.

4. Compute matrices $\tilde{Q}$ and $\tilde{R}$ as detailed in 2.6.2 .

5. Obtain the optimal controller gains as described in the section 2.6.

6. Simulate the power system with optimal controllers using MATLAB simulation.

7. Obtain the dynamic responses of the power system following SLPs.

2.8 State-space model of the power systems

State-space model of a LFC dynamical system is a useful representation for the application of the modern/robust control theory. Using appropriate definitions and state variables, the state-space realization of the isolated and interconnected power systems is obtained in the form of equation (2.52) and (2.38) [1, 2, 7, 10, 13, 39, 48, 90, 119].

$$\dot{x} = \tilde{A}x + \tilde{B}u + \tilde{F}w \tag{2.52}$$

where,

$\tilde{F}$ is a disturbance distribution matrix of the dimension $n \times d$,

w is a disturbance vector of the dimension $d \times 1$,

d, is the number of disturbance inputs, and all others terms are same as described in the equations (2.37) and (2.38).

The term ($\tilde{F}w$) represents the disturbance, in way of load demand, to the power system. On the comparison, this power system model described in equation (2.52) is not in the form of the equation (2.37)as desired, for two reasons. In the optimal control theory used, there is no ($\tilde{F}w$) term, and second, the cost function requires the states to be driven to zero for it to have a minimum value. For a SLP in control area-i, the steady state frequency deviations in each control area are required to be zero. But the increased generation in control area-i will by necessity in steady state equal the increased load demand of the area, a non zero quantity, refer Fig. 2.6:

$$\Delta P_{mi} = \Delta P_{Di} \tag{2.53}$$

Some of the other states will also be non-zero [2,8,39,49]. Fosha et al. [39] are probably the first who addressed this dilemma. A simpler way of addressing this dilemma [39, 49] is to redefine the state variables and control variables in terms of their corresponding steady state values.

The i^{th} state variable x_i may be redefined as:

$$x_i^1 \stackrel{\Delta}{=} x_i - x_{iss} \tag{2.54}$$

where $i = 1, 2, ..., n$, and x_{iss} is the steady state value of i^{th} state variable.

Similarly i^{th} control variables may be redefined as:

$$u_i^1 \stackrel{\Delta}{=} u_i - u_{iss} \tag{2.55}$$

where $i = 1, 2, ..., m$, and u_{iss} is the steady state value of i^{th} control variable.

This change of variables puts the system in the form

$$\begin{aligned} \dot{x}^1 &= \tilde{A}x^1 + \tilde{B}u^1 \\ x^1(0) &= -x_{ss} \end{aligned} \tag{2.56}$$

By redefining the states and control variables in terms of their steady state values, only the reference position of the system is shifted [2, 8, 39, 49]. The superscript 1 has been dropped [2,8,39,49] to prevent unnecessary notation problems. The matrices $\tilde{A}$ and $\tilde{B}$ remain unchanged and the equation (2.56) has the form of the equation (2.37).

2.9 Summary

Mathematical modeling of the SAPS, MAIPS and MAIPS with MSPG are described for LFC study. Keeping in view the new power system environment, the concept of MSPG in control area is introduced. In addition to LFC models of SAPS and MAIPS, a new model of MAIPS with MSPG is presented for LFC study. The general form of state-space model of the power systems is explained. The OFC proposed with pragmatic point of view is introduced . The control system design equations and algorithms have been presented.

CHAPTER 3

LFC OF CONVENTIONAL POWER SYSTEMS

3.1 Introduction

LFC modeling and control design of power systems have been presented in detail in chapter 2. Recently, many researchers studied the LFC of conventional power systems considering either thermal-thermal or hydro-thermal systems [9, 12, 13, 107, 124]. Most of the research papers reported in the area of LFC considered the two area interconnected power system with non-reheat type thermal systems. An attempt is made in this chapter to study the LFC of interconnected power systems including reheat type turbines and hydro turbines. The LFC of thermal-thermal with non reheat turbine, thermal-thermal considering reheat turbine and hydro-thermal system is studied using OFC and performance of the proposed OFC has been compared with FSFC.

3.2 TAIPS considering non-reheat turbines

A TAIPS shown in the Fig. 3.1 is considered for the LFC analysis in this section. Each control area of this power system comprises thermal unit with non-reheat turbine. In accordance with modern control terminology ΔP_{c1} and ΔP_{c2} will be referred to as control inputs u_1 and u_2. In the conventional approach u_1 and u_2 were provided by the integral of ACEs [2, 5, 6, 10]. In modern control theory approach u_1 and u_2 will be created by a linear combination of all the system states (full state feedback approach) or output/measurable states(output feedback approach). For formulating the state variable model, the conventional secondary feedback loops are opened and each time constant is represented by a separate block as shown in Fig. 3.1. State variables

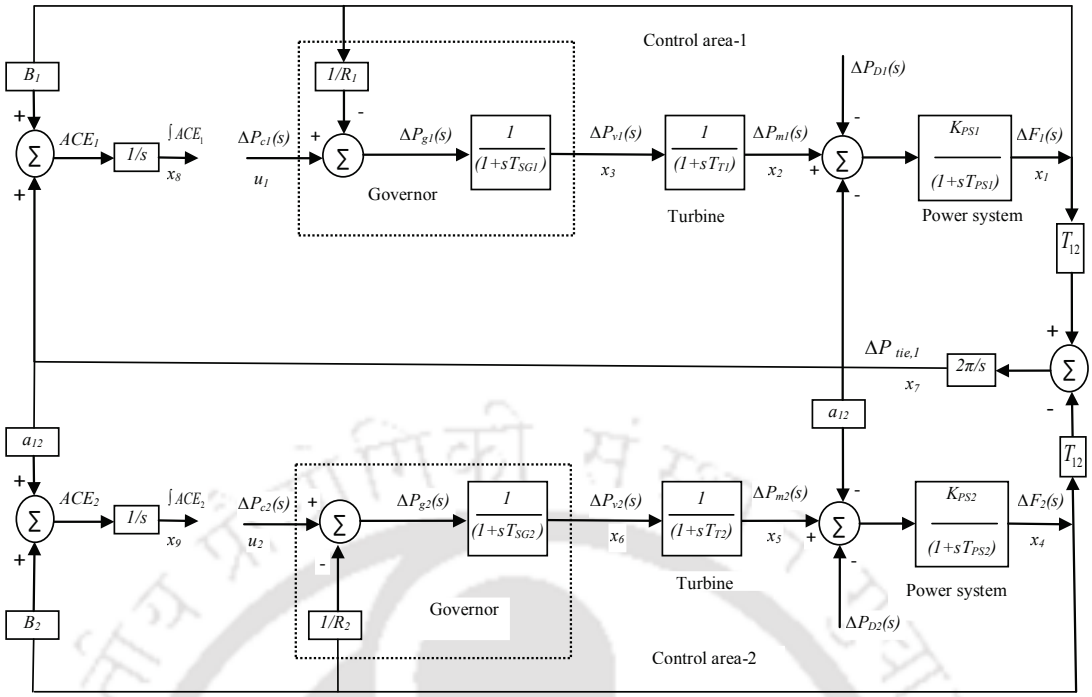

Figure 3.1: TAIPS with non-reheat turbines

are defined as the outputs of all the blocks having either an integrator or a time constant.

3.2.1 State-space Model

The system shown in Fig. 3.1 has nine state variables where $x_1 = \Delta f_1$, $x_4 = \Delta f_2$, $x_2 = \Delta P_{m1}$, $x_5 = \Delta P_{m2}$, $x_8 = \int ACE_1 dt$, $x_9 = \int ACE_2 dt$. The disturbance vector is defined as $w_1 = \Delta P_{D1}$ and $w_2 = \Delta P_{D2}$. After defining all the states as shown in Fig. 3.1, the following differential equations are obtained replacing, s by $\frac{d}{dt}$.

$$\dot{x}_1 = -\frac{1}{T_{PS1}}x_1 + \frac{K_{PS1}}{T_{PS1}}x_2 - \frac{K_{PS1}}{T_{PS1}}x_7 - \frac{K_{PS1}}{T_{PS1}}w_1 \tag{3.1}$$

$$\dot{x}_2 = -\frac{1}{T_{T1}}x_2 + \frac{1}{T_{T1}}x_3 \tag{3.2}$$

$$\dot{x}_3 = -\frac{1}{R_1 T_{SG1}}x_1 - \frac{1}{T_{SG1}}x_3 + \frac{1}{T_{SG1}}u_1 \tag{3.3}$$

$$\dot{x}_4 = -\frac{1}{T_{PS2}}x_4 + \frac{K_{PS2}}{T_{PS2}}x_5 - \frac{a_{12}K_{PS2}}{T_{PS2}}x_7 - \frac{K_{PS2}}{T_{PS2}}w_2 \tag{3.4}$$

$$\dot{x}_5 = -\frac{1}{T_{T2}}x_5 + \frac{1}{T_{T2}}x_6 \tag{3.5}$$

$$\dot{x}_6 = -\frac{1}{R_2 T_{SG2}}x_4 - \frac{1}{T_{SG2}}x_6 + \frac{1}{T_{SG2}}u_2 \tag{3.6}$$

$$\dot{x}_7 = 2\pi T_{12}x_1 - 2\pi T_{12}x_4 \tag{3.7}$$

$$\dot{x}_8 = B_1 x_1 + x_7 \tag{3.8}$$

$$\dot{x}_9 = B_2 x_4 + a_{12}x_7 \tag{3.9}$$

The state equations (3.1)-(3.9) can be organized in the state-space form as described by the equations (2.52) and (2.38) in the chapter 2. For the power system model shown in Fig. 3.1 the associated vectors and matrices are as follows:

state vector, $x = [x_1\ x_2 \ldots\ldots x_9]^T$,

control vector, $u = [u_1\ u_2]^T = [\Delta P_{c1}\ \Delta P_{c2}]^T$

disturbance vector, $w = [w_1\ w_2]^T = [\Delta P_{D1}\ \Delta P_{D2}]^T$

$$\tilde{A} = \begin{bmatrix}
-\frac{1}{T_{PS1}} & \frac{K_{PS1}}{T_{PS1}} & 0 & 0 & 0 & 0 & -\frac{K_{PS1}}{T_{PS1}} & 0 & 0 \\
0 & -\frac{1}{T_{T1}} & \frac{1}{T_{T1}} & 0 & 0 & 0 & 0 & 0 & 0 \\
-\frac{1}{R_1 T_{SG1}} & 0 & -\frac{1}{T_{SG1}} & 0 & 0 & 0 & 0 & 0 & 0 \\
0 & 0 & 0 & -\frac{1}{T_{PS2}} & \frac{K_{PS2}}{T_{PS2}} & 0 & -a_{12}\frac{K_{PS2}}{T_{PS2}} & 0 & 0 \\
0 & 0 & 0 & 0 & -\frac{1}{T_{T2}} & \frac{1}{T_{T2}} & 0 & 0 & 0 \\
0 & 0 & 0 & -\frac{1}{R_2 T_{SG2}} & 0 & -\frac{1}{T_{SG2}} & 0 & 0 & 0 \\
2\pi T_{12} & 0 & 0 & -2\pi T_{12} & 0 & 0 & 0 & 0 & 0 \\
B_1 & 0 & 0 & 0 & 0 & 0 & 1 & 0 & 0 \\
0 & 0 & 0 & B_2 & 0 & 0 & a_{12} & 0 & 0
\end{bmatrix}$$

$$\tilde{B}^T = \begin{bmatrix}
0 & 0 & \frac{1}{T_{SG1}} & 0 & 0 & 0 & 0 & 0 & 0 \\
0 & 0 & 0 & 0 & 0 & \frac{1}{T_{SG2}} & 0 & 0 & 0
\end{bmatrix}$$

and

$$\tilde{F}^T = \begin{bmatrix} -\frac{K_{PS1}}{T_{PS1}} & 0 & 0 & 0 & 0 & 0 & 0 & 0 & 0 \\ 0 & 0 & 0 & -\frac{K_{PS2}}{T_{PS2}} & 0 & 0 & 0 & 0 & 0 \end{bmatrix}$$

The matrix $\tilde{C}$ is defined as

$$\tilde{C} = \begin{bmatrix} 1 & 0 & 0 & 0 & 0 & 0 & 0 & 0 & 0 \\ 0 & 0 & 0 & 1 & 0 & 0 & 0 & 0 & 0 \\ 0 & 0 & 0 & 0 & 0 & 0 & 0 & 1 & 0 \\ 0 & 0 & 0 & 0 & 0 & 0 & 0 & 0 & 1 \end{bmatrix}$$

The performance index J is given in equation(2.39), the matrices $\tilde{Q}$ and $\tilde{R}$ are defined for this problem using the design considerations given in the section 2.6.2. Excursions of $ACEs$ $(x_7 + B_1x_1,\ a_{12}x_7 + B_2x_4)$, $\int ACEdt(x_8, x_9)$ and control vectors(u_1, u_2) about their steady values are minimized and J can be written as:

$$J = \frac{1}{2}\int_0^\infty \left[(x_7 + B_1x_1)^2 + (a_{12}x_7 + B_2x_4)^2 + \left(x_8^2 + x_9^2\right) + \left(u_1^2 + u_2^2\right)\right]dt \tag{3.10}$$

From the equation (3.10), the matrices $\tilde{Q}$ and $\tilde{R}$ can be recognized as:

$$\tilde{Q} = \begin{bmatrix} B_1^2 & 0 & 0 & 0 & 0 & 0 & B_1 & 0 & 0 \\ 0 & 0 & 0 & 0 & 0 & 0 & 0 & 0 & 0 \\ 0 & 0 & 0 & 0 & 0 & 0 & 0 & 0 & 0 \\ 0 & 0 & 0 & B_2^2 & 0 & 0 & a_{12}B_2 & 0 & 0 \\ 0 & 0 & 0 & 0 & 0 & 0 & 0 & 0 & 0 \\ 0 & 0 & 0 & 0 & 0 & 0 & 0 & 0 & 0 \\ B_1 & 0 & 0 & a_{12}B_2 & 0 & 0 & (1+a_{12}^2) & 0 & 0 \\ 0 & 0 & 0 & 0 & 0 & 0 & 0 & 1 & 0 \\ 0 & 0 & 0 & 0 & 0 & 0 & 0 & 0 & 1 \end{bmatrix}$$

$$\tilde{R} = \begin{bmatrix} 1 & 0 \\ 0 & 1 \end{bmatrix}$$

3.2.2 Simulation results and discussion

The procedure described in the section 2.7 is followed. The system parameters and data are given in Table 3.1. The optimum gains of OFC and FSC are obtained. The computer simulations are carried out with the optimum controller gain settings. MATLAB control system toolbox [121] is used to simulate the power system and to obtain dynamic responses of the system for

1% SLP in the control area 1.

Table. 3.1: Simulation parameters of TAIPS considering non-reheat turbines

Parameter	Value
$P_{rt1} = P_{rt2}$	2000 MW
f	60Hz
$H_1 = H_2$	5 MW-s/MVA
$D_1 = D_2$	0.00833 puMW/Hz
$T_{SG1} = T_{SG2}$	0.08s
$T_{T1} = T_{T2}$	0.5s
$R_1 = R_2$	2.4 Hz/puMW
$T_{PS1} = T_{PS2}$	20s
$K_{PS1} = K_{PS2}$	120 s
$B_1 = B_2$	0.425
a_{12}	-1
$2\pi T_{12}$	0.215

The following computational results are obtained:

$$\tilde{A} = \begin{bmatrix} -0.0500 & 6.0000 & 0 & 0 & 0 & 0 & -6.0000 & 0 & 0 \\ 0 & -2.0000 & 2.0000 & 0 & 0 & 0 & 0 & 0 & 0 \\ -5.2083 & 0 & -12.5000 & 0 & 0 & 0 & 0 & 0 & 0 \\ 0 & 0 & 0 & -0.0500 & 6.0000 & 0 & 6.0000 & 0 & 0 \\ 0 & 0 & 0 & 0 & -2.0000 & 2.0000 & 0 & 0 & 0 \\ 0 & 0 & 0 & -5.2083 & 0 & -12.5000 & 0 & 0 & 0 \\ 0.2150 & 0 & 0 & -0.2150 & 0 & 0 & 0 & 0 & 0 \\ 0.4250 & 0 & 0 & 0 & 0 & 0 & 1.0000 & 0 & 0 \\ 0 & 0 & 0 & 0.4250 & 0 & 0 & -1.0000 & 0 & 0 \end{bmatrix}$$

$$\tilde{B}^T = \begin{bmatrix} 0 & 0 & 12.5000 & 0 & 0 & 0 & 0 & 0 & 0 \\ 0 & 0 & 0 & 0 & 0 & 12.5000 & 0 & 0 & 0 \end{bmatrix}$$

$$\tilde{Q} = \begin{bmatrix} 0.1806 & 0 & 0 & 0 & 0 & 0 & 0.4250 & 0 & 0 \\ 0 & 0 & 0 & 0 & 0 & 0 & 0 & 0 & 0 \\ 0 & 0 & 0 & 0 & 0 & 0 & 0 & 0 & 0 \\ 0 & 0 & 0 & 0.1806 & 0 & 0 & -0.4250 & 0 & 0 \\ 0 & 0 & 0 & 0 & 0 & 0 & 0 & 0 & 0 \\ 0 & 0 & 0 & 0 & 0 & 0 & 0 & 0 & 0 \\ 0.4250 & 0 & 0 & -0.4250 & 0 & 0 & 2.0000 & 0 & 0 \\ 0 & 0 & 0 & 0 & 0 & 0 & 0 & 1.0000 & 0 \\ 0 & 0 & 0 & 0 & 0 & 0 & 0 & 0 & 1.0000 \end{bmatrix}$$

$$\tilde{R} = \begin{bmatrix} 1 & 0 \\ 0 & 1 \end{bmatrix}$$

Table. 3.2: Dynamic response comparison in terms of peak overshoot (OS)

	Peak OS of Δf_1(Hz)	Peak OS of Δf_2(Hz)	Peak OS of $\Delta P_{tie,1}$(pu MW)
FSFC	-0.02785	-0.01917	-0.004937
OFC	-0.02582	-0.008737	-0.004061
% reduction in Peak OS	7.28	54.42	17.74

Table. 3.3: Dynamic response comparison in terms of ST

	ST of Δf_1(s)	ST of Δf_2(s)	ST of $\Delta P_{tie,1}$(s)
FSFC	24.55	26	23.84
OFC	17.73	18	16.23
% reduction in ST	27.78	30.76	31.92

The optimum gains of FSFC $\bar{K}$ and OFC $\tilde{K}$ are obtained as:

$$\bar{K} = \begin{bmatrix} 0.4048 & 0.9424 & 0.1408 & -0.0320 & -0.0683 & -0.0096 & -0.2615 & 1.0000 & 0.0000 \\ -0.0320 & -0.0683 & -0.0096 & 0.4048 & 0.9424 & 0.1408 & 0.2615 & 0.0000 & 1.0000 \end{bmatrix}$$

$$\tilde{K} = \begin{bmatrix} 0.1120 & 0.0319 & 0.5646 & 0.0928 \\ 0.0319 & 0.1120 & 0.0928 & 0.5646 \end{bmatrix}$$

Dynamic responses of the system are obtained for 1% SLP in the control area 1. The dynamic responses are shown in Fig. 3.2. It is observed that the OFC gives better dynamic responses having relatively smaller peak overshoot and lesser settling time with zero steady state error as compared to that of FSFC. The quantitative comparison is made in Table 3.2 and 3.3 where percentage improvement in the peak OS of Δf_1, Δf_2 and $\Delta P_{tie,1}$ is 7.28, 54.42, and 17.74, respectively and percentage improvement in the settling time of Δf_1, Δf_2 and $\Delta P_{tie,1}$ is 27.78, 30.76, and 31.92, respectively.

3.3 TAIPS considering reheat and non-reheat turbines

In this section LFC of an interconnected power system as shown in the Fig. 3.3 is presented. The reheat turbine is considered in control area 1. The procedure described in the section2.7 is adopted. The system parameters and data are given in Table 3.4. The power system has 10 state variables. State variables x_1, x_5, x_9 and x_{10} are taken as output feedback states. The optimum gains of OFC and FSFC are obtained. The computer simulations are carried out with

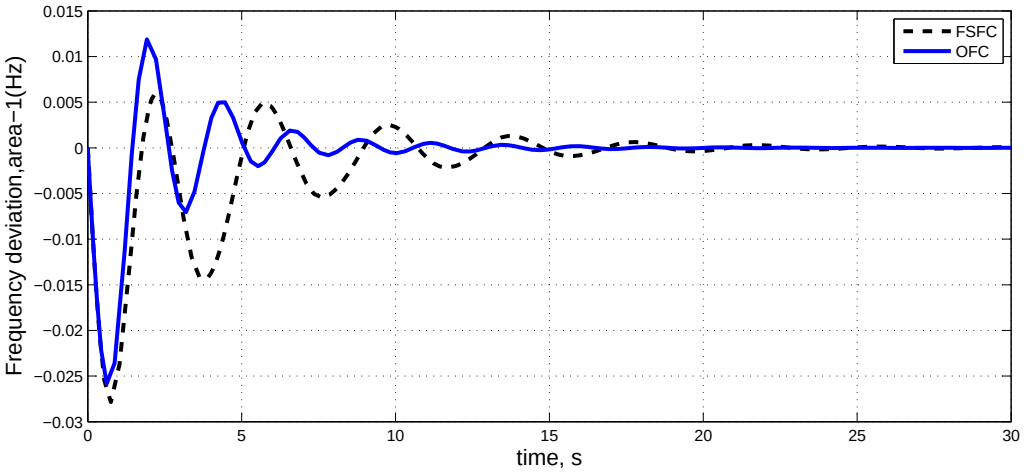

(a) Frequency deviation response of control area 1

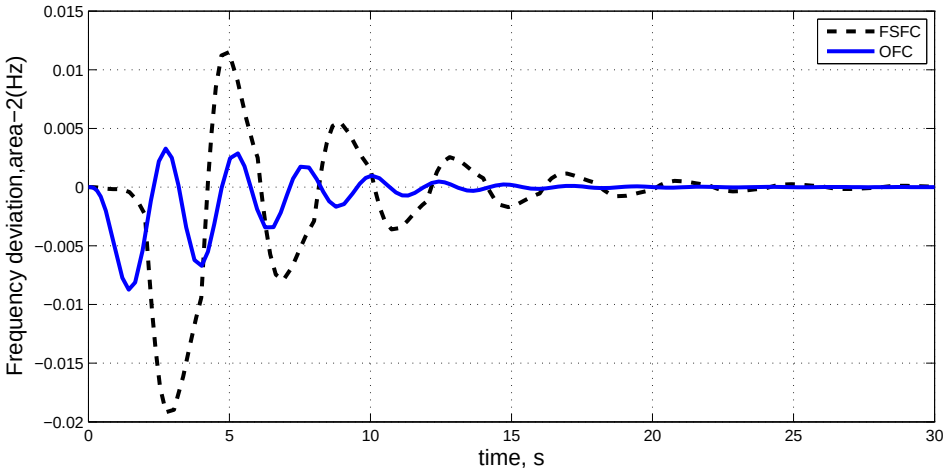

(b) Frequency deviation response of control area 2

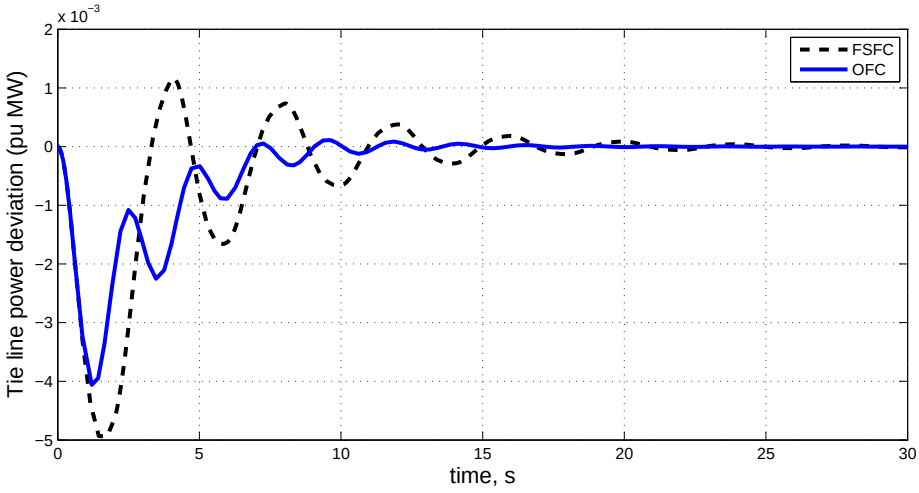

(c) Tie line power deviation response

Figure 3.2: Dynamic responses of TAIPS with non-reheat turbines

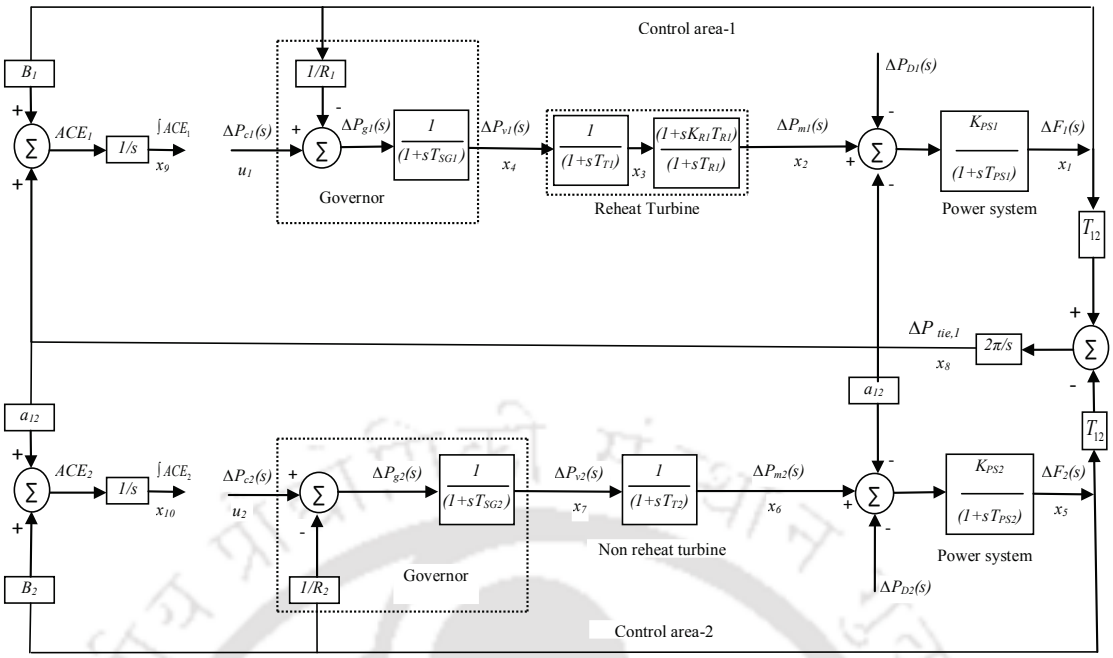

Figure 3.3: TAIPS considering reheat and non-reheat turbines

the optimum controller gain settings. MATLAB control system toolbox [121] is used to simulate the power system and to obtain dynamic responses of the system for 1% SLP in the control area 1.

3.3.1 Simulation results and discussion

The following computational results are obtained:

$$\tilde{A}=\begin{bmatrix} -0.0500 & 6.0000 & 0 & 0 & 0 & 0 & 0 & -6.0000 & 0 & 0 \\ 0 & -3.3333 & 3.3333 & 0 & 0 & 0 & 0 & 0 & 0 & 0 \\ -2.6042 & 0 & -0.1000 & -6.1500 & 0 & 0 & 0 & 0 & 0 & 0 \\ -5.2083 & 0 & 0 & -12.5000 & 0 & 0 & 0 & 0 & 0 & 0 \\ 0 & 0 & 0 & 0 & -0.0500 & 6.0000 & 0 & 6.0000 & 0 & 0 \\ 0 & 0 & 0 & 0 & 0 & -3.3333 & 3.3333 & 0 & 0 & 0 \\ 0 & 0 & 0 & 0 & -12.5000 & 0 & -12.5000 & 0 & 0 & 0 \\ 0.5450 & 0 & 0 & 0 & -0.5450 & 0 & 0 & 0 & 0 & 0 \\ 0.4250 & 0 & 0 & 0 & 0 & 0 & 0 & 1.0000 & 0 & 0 \\ 0 & 0 & 0 & 0 & 0.4250 & 0 & 0 & -1.0000 & 0 & 0 \end{bmatrix}$$

$$\tilde{B}^T=\begin{bmatrix} 0 & 0 & 0.5000 & 1.0000 & 0 & 0 & 0 & 0 & 0 & 0 \\ 0 & 0 & 0 & 0 & 0 & 0 & 1.0000 & 0 & 0 & 0 \end{bmatrix}$$

Table. 3.4: Simulation parameters of TAIPS considering reheat and non-reheat turbines

Parameter	Value
$P_{rt1} = P_{rt2}$	2000 MW
f	60Hz
$H_1 = H_2$	5 MW-s/MVA
$D_1 = D_2$	0.00833 puMW/Hz
$T_{SG1} = T_{SG2}$	0.08s
$T_{T1} = T_{T2}$	0.3s
K_{R1}	0.5
T_{R1}	10s
$R_1 = R_2$	2.4 Hz/puMW
$K_{PS1} = K_{PS2}$	120 s
$T_{PS1} = T_{PS2}$	20s
$B_1 = B_2$	0.425
a_{12}	-1
$2\pi T_{12}$	0.545

and the matrix $\tilde{C}$ is defined as

$$\tilde{C} = \begin{bmatrix} 1 & 0 & 0 & 0 & 0 & 0 & 0 & 0 & 0 & 0 \\ 0 & 0 & 0 & 0 & 1 & 0 & 0 & 0 & 0 & 0 \\ 0 & 0 & 0 & 0 & 0 & 0 & 0 & 0 & 1 & 0 \\ 0 & 0 & 0 & 0 & 0 & 0 & 0 & 0 & 0 & 1 \end{bmatrix}$$

$$\tilde{Q} = \begin{bmatrix} 0.1806 & 0 & 0 & 0 & 0 & 0 & 0 & 0.4250 & 0 & 0 \\ 0 & 0 & 0 & 0 & 0 & 0 & 0 & 0 & 0 & 0 \\ 0 & 0 & 0 & 0 & 0 & 0 & 0 & 0 & 0 & 0 \\ 0 & 0 & 0 & 0 & 0 & 0 & 0 & 0 & 0 & 0 \\ 0 & 0 & 0 & 0 & 0.1806 & 0 & 0 & -0.4250 & 0 & 0 \\ 0 & 0 & 0 & 0 & 0 & 0 & 0 & 0 & 0 & 0 \\ 0 & 0 & 0 & 0 & 0 & 0 & 0 & 0 & 0 & 0 \\ 0.4250 & 0 & 0 & 0 & -0.4250 & 0 & 0 & 2.0000 & 0 & 0 \\ 0 & 0 & 0 & 00 & 0 & 0 & 0 & 1.0000 & 0 & \\ 0 & 0 & 0 & 0 & 0 & 0 & 0 & 0 & 0 & 1.0000 \end{bmatrix}$$

$$\tilde{R} = \begin{bmatrix} 1 & 0 \\ 0 & 1 \end{bmatrix}$$

The optimum gains of FSFC $\bar{K}$ and OFC $\tilde{K}$ are obtained as:

$$\bar{K} = \begin{bmatrix} 0.2106 & 0.3836 & 7.0445 & -3.4432 & -0.0093 & -0.0259 & -0.0075 & -0.0751 & 0.9649 & -0.2627 \\ -0.0313 & -0.0414 & -0.6459 & 0.3155 & 0.1080 & 0.2079 & 0.0553 & -0.2854 & 0.2627 & 0.9649 \end{bmatrix}$$

$$\tilde{K} = \begin{bmatrix} 0.0533 & -0.0948 & 0.8087 & -0.2321 \\ 0.0717 & -0.0424 & 0.2888 & 0.9435 \end{bmatrix}$$

Dynamic responses of the system are obtained for 1% SLP in the control area 1. The dynamic responses are shown in Fig. 3.4. It is observed that the OFC gives better dynamic responses having relatively smaller peak overshoot and lesser settling time with zero steady state error as compared to that of FSFC. The quantitative comparison is made in Table 3.5 and 3.6 where percentage improvement in the peak OS of Δf_2 and $\Delta P_{tie,1}$ is 6.84 and 24.08, respectively and percentage improvement in the settling time of Δf_1, Δf_2 and $\Delta P_{tie,1}$ is 7.96, 3.47 and 16.00, respectively.

Table. 3.5: Dynamic response comparison in terms of peak overshoot (OS)

	Peak OS of Δf_1(Hz)	Peak OS of Δf_2(Hz)	Peak OS of $\Delta P_{tie,1}$(pu MW)
FSFC	-0.02487	-0.01695	-0.01034
OFC	-0.02487	-0.01579	-0.00785
% reduction in Peak OS	0	6.84	24.08

Table. 3.6: Dynamic response comparison in terms of ST

	ST of Δf_1(s)	ST of Δf_2(s)	ST of $\Delta P_{tie,1}$(s)
FSFC	24.22	25.9	27.05
OFC	22.29	25	22.72
% reduction in ST	7.96	3.47	16.00

3.4 Hydro-thermal interconnected power system

In this section LFC of an interconnected Hydro-thermal power system as shown in Fig. 3.5 is presented. The procedure described in the section 2.7 is adopted. The simulation parameters are given in Table 3.7. The power system has 11 state variables. State variables x_1, x_5, x_{10} and x_{11} are taken as output feedback states. The optimum gains of OFC and FSFC are obtained. The computer simulations are carried out with the optimum controller gain settings. MATLAB control system toolbox [121] is used to simulate the power system and to obtain dynamic responses of the system for 1% SLP in the control area 1.

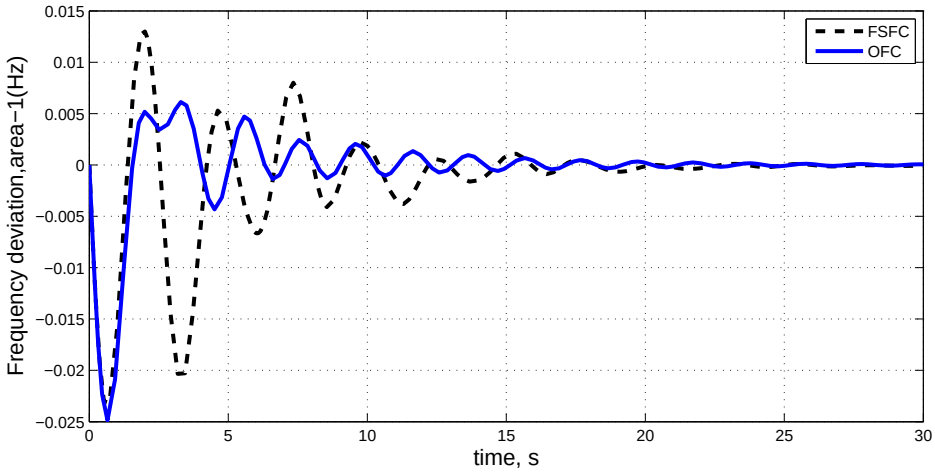

(a) Frequency deviation response of control area 1

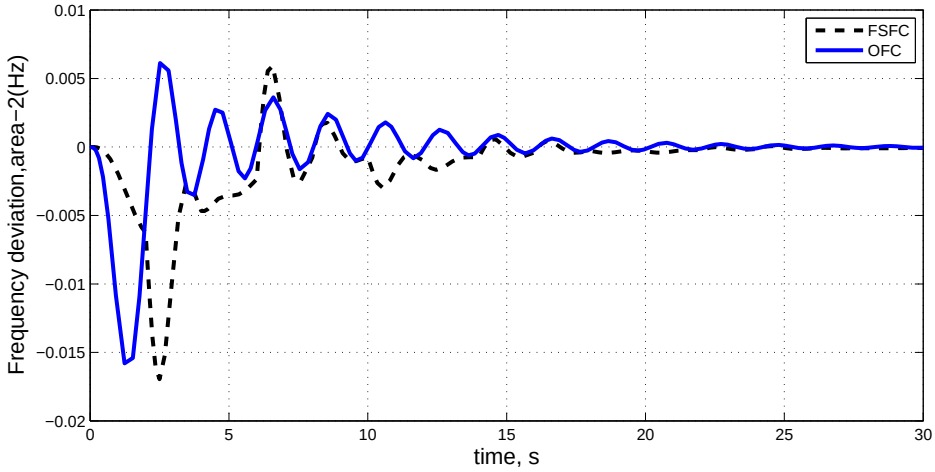

(b) Frequency deviation response of control area 2

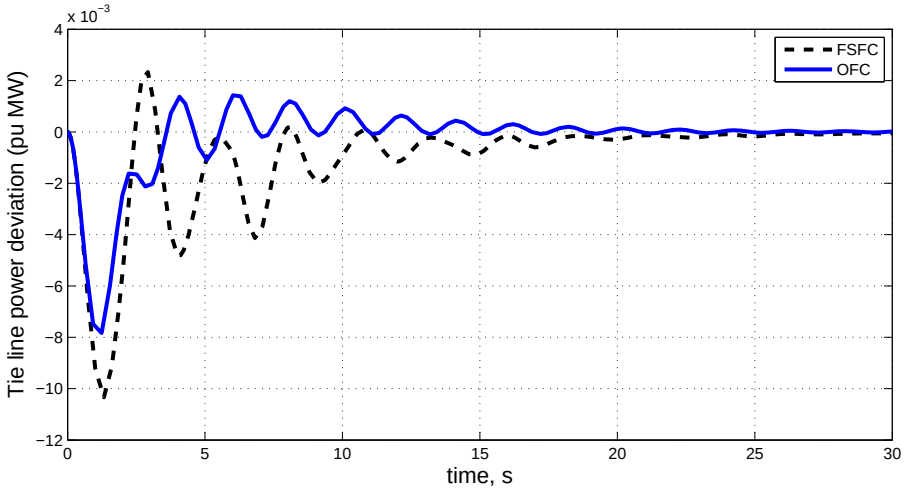

(c) Tie line power deviation response

Figure 3.4: Dynamic responses of TAIPS with reheat and non-reheat turbine

Table. 3.7: Simulation parameters of hydro-thermal interconnected power system

Parameter	Value
$P_{rt1} = P_{rt2}$	2000 MW
f	60Hz
$H_1 = H_2$	5 MW-s/MVA
$D_1 = D_2$	0.00833 puMW/Hz
T_{SG1}	0.08s
T_{T1}	0.3s
K_{R1}	0.5
T_{R1}	10s
T_{GH2}	0.3s
T_{RS2}	5s
T_{RH2}	28.75s
T_{W2}	0.3s
$R_1 = R_2$	2.4 Hz/puMW
$T_{PS1} = T_{PS2}$	20s
$K_{PS1} = K_{PS2}$	120 s
$B_1 = B_2$	0.425
a_{12}	-1
$2\pi T_{12}$	0.215

3.4.1 Simulation results and discussion

The following computational results are obtained:

$$\tilde{A}=\begin{bmatrix}
-0.0500 & 6.0000 & 0 & 0 & 0 & 0 & 0 & 0 & -6.0000 & 0 & 0\\
0 & -3.3333 & 3.3333 & 0 & 0 & 0 & 0 & 0 & 0 & 0 & 0\\
-5.2083 & 0 & -0.1000 & -6.1500 & 0 & 0 & 0 & 0 & 0 & 0 & 0\\
-10.4167 & 0 & 0 & -12.5000 & 0 & 0 & 0 & 0 & 0 & 0 & 0\\
0 & 0 & 0 & 0 & -0.0500 & 6.0000 & 0 & 0 & 6.0000 & 0 & 0\\
0 & 0 & 0 & 0 & 0.9662 & -6.6667 & 6.7362 & 1.0899 & 0 & 0 & 0\\
0 & 0 & 0 & 0 & -0.4831 & 0 & -0.0348 & -0.5449 & 0 & 0 & 0\\
0 & 0 & 0 & 0 & -2.7778 & 0 & 0 & -3.3333 & 0 & 0 & 0\\
0.2150 & 0 & 0 & 0 & -0.2150 & 0 & 0 & 0 & 0 & 0 & 0\\
0.8417 & 0 & 0 & 0 & 0 & 0 & 0 & 0 & 1.0000 & 0 & 0\\
0 & 0 & 0 & 0 & 0.8417 & 0 & 0 & 0 & -1.0000 & 0 & 0
\end{bmatrix}$$

$$\tilde{B}=\begin{bmatrix}
0 & 0 & 0.5000 & 1.0000 & 0 & 0 & 0 & 0 & 0 & 0 & 0\\
0 & 0 & 0 & 0 & 0 & -0.3478 & 0.1739 & 1.0000 & 0 & 0 & 0
\end{bmatrix}$$

and the matrix $\tilde{C}$ is defined as

$$\tilde{C}=\begin{bmatrix}
1 & 0 & 0 & 0 & 0 & 0 & 0 & 0 & 0 & 0 & 0\\
0 & 0 & 0 & 0 & 1 & 0 & 0 & 0 & 0 & 0 & 0\\
0 & 0 & 0 & 0 & 0 & 0 & 0 & 0 & 0 & 1 & 0\\
0 & 0 & 0 & 0 & 0 & 0 & 0 & 0 & 0 & 0 & 1
\end{bmatrix}$$

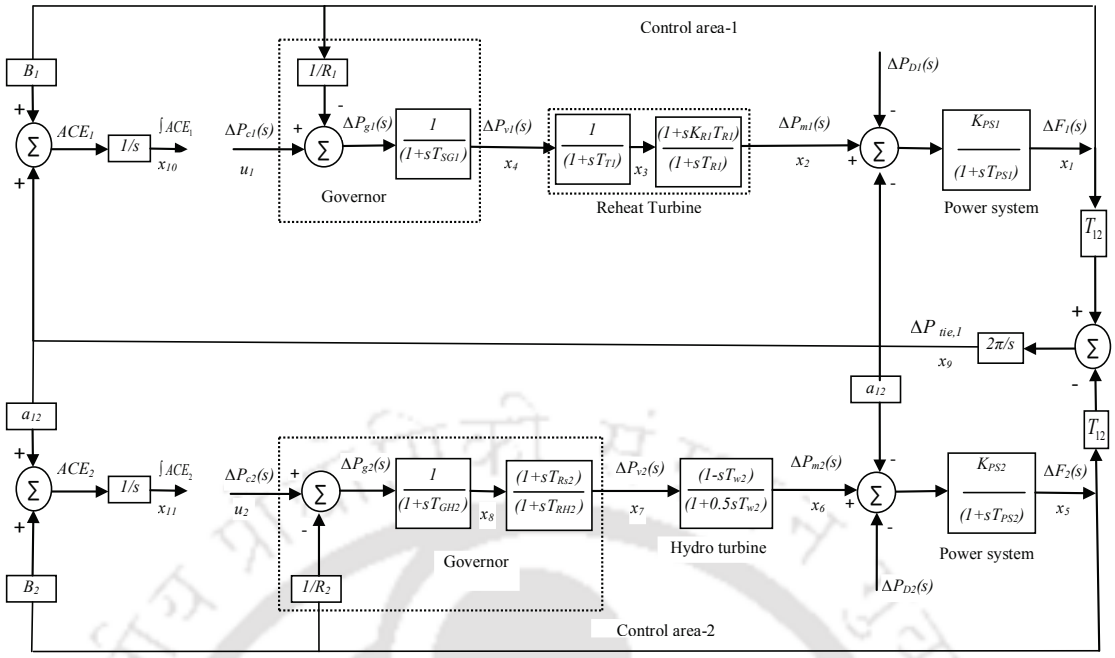

Figure 3.5: Hydro-thermal interconnected power system

$$\tilde{Q} = \begin{bmatrix} 0.7084 & 0 & 0 & 0 & 0 & 0 & 0 & 0 & 0.8417 & 0 & \\ 0 & 0 & 0 & 0 & 0 & 0 & 0 & 0 & 0 & 0 & 0 \\ 0 & 0 & 0 & 0 & 0 & 0 & 0 & 0 & 0 & 0 & 0 \\ 0 & 0 & 0 & 0 & 0 & 0 & 0 & 0 & 0 & 0 & 0 \\ 0 & 0 & 0 & 0 & 0.7084 & 0 & 0 & 0 & -0.8417 & 0 & 0 \\ 0 & 0 & 0 & 0 & 0 & 0 & 0 & 0 & 0 & 0 & 0 \\ 0 & 0 & 0 & 0 & 0 & 0 & 0 & 0 & 0 & 0 & 0 \\ 0 & 0 & 0 & 0 & 0 & 0 & 0 & 0 & 0 & 0 & 0 \\ 0.8417 & 0 & 0 & 0 & -0.8417 & 0 & 0 & 0 & 2.0000 & 0 & 0 \\ 0 & 0 & 0 & 0 & 0 & 0 & 0 & 0 & 0 & 1.0000 & 0 \\ 0 & 0 & 0 & 0 & 0 & 0 & 0 & 0 & 0 & 0 & 1.0000 \end{bmatrix}$$

$$\tilde{R} = \begin{bmatrix} 1 & 0 \\ 0 & 1 \end{bmatrix}$$

The optimal gains of FSFC $\bar{K}$ and OFC $\tilde{K}$ are obtained as:

$$\bar{K} = \begin{bmatrix} 0.2713 & 0.5047 & 7.1418 & -3.4754 & 0.0370 & 0.0432 & 1.1489 & -0.1458 & 0.0062 & 0.9974 & 0.0721 \\ 0.2007 & 0.2805 & 1.1920 & -0.5571 & 0.3878 & 0.4157 & 11.3685 & -1.5619 & 2.7044 & -0.0721 & 0.9974 \end{bmatrix}$$

$$\tilde{K} = \begin{bmatrix} 0.0462 & 0.0770 & 0.7861 & 0.1915 \\ -0.5856 & 0.0934 & 0.2036 & 0.4272 \end{bmatrix}$$

Dynamic responses of the system are obtained for 1% SLP in the control area 1. The dy-

Table. 3.8: Dynamic response comparison in terms of peak overshoot (OS)

	Peak OS of Δf_1(Hz)	Peak OS of Δf_2(Hz)	Peak OS of $\Delta P_{tie,1}$(pu MW)
FSFC	-0.02385	-0.03695	-0.004937
OFC	-0.02385	-0.02583	-0.003258
% reduction in Peak OS	0	30.09	34.00

Table. 3.9: Dynamic response comparison in terms of ST

	ST of Δf_1(s)	ST of Δf_2(s)	ST of $\Delta P_{tie,1}$(s)
FSFC	50	50	50
OFC	16.85	18.91	43.34
% reduction in ST	66.30	62.18	13.32

namic responses are shown in Fig. 3.6. It is observed that the OFC gives better dynamic responses having relatively smaller peak overshoot and lesser settling time with zero steady state error as compared to that of FSFC. The quantitative comparison is made in Table 3.8 and 3.9 where percentage improvement in the peak OS of Δf_2 and $\Delta P_{tie,1}$ is 30.09 and 34.00, respectively and percentage improvement in the settling time(ST) of Δf_1, Δf_2 and $\Delta P_{tie,1}$ is 66.3, 62.18, and 13.32, respectively. Moreover the dynamic responses obtained with FSFC are more oscillatory. The proposed OFC competes well and thus the dynamic responses obtained satisfy the LFC requirements.

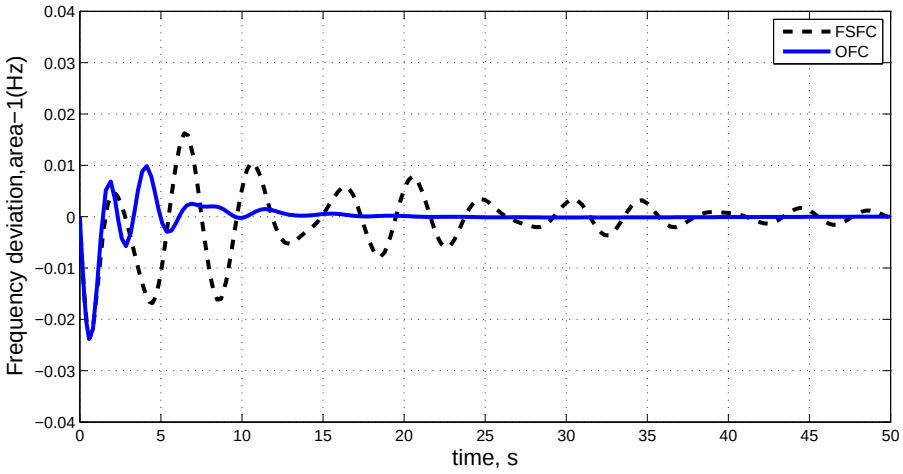

(a) Frequency deviation response of control area 1

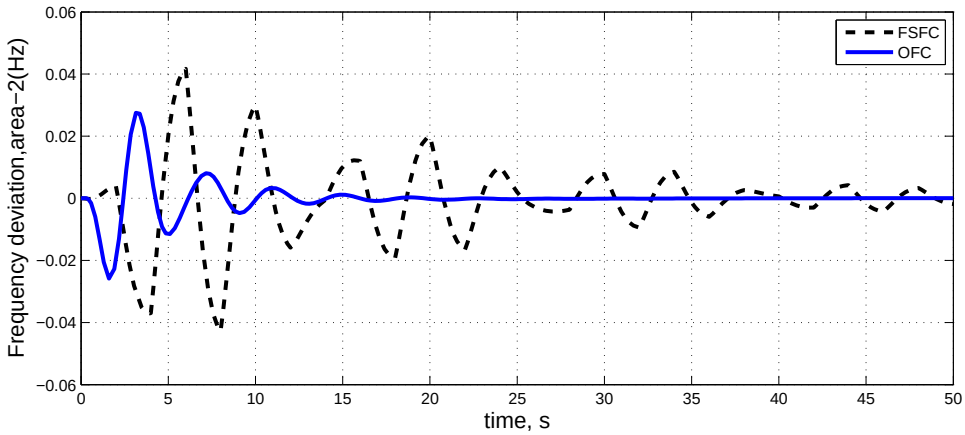

(b) Frequency deviation response of control area 2

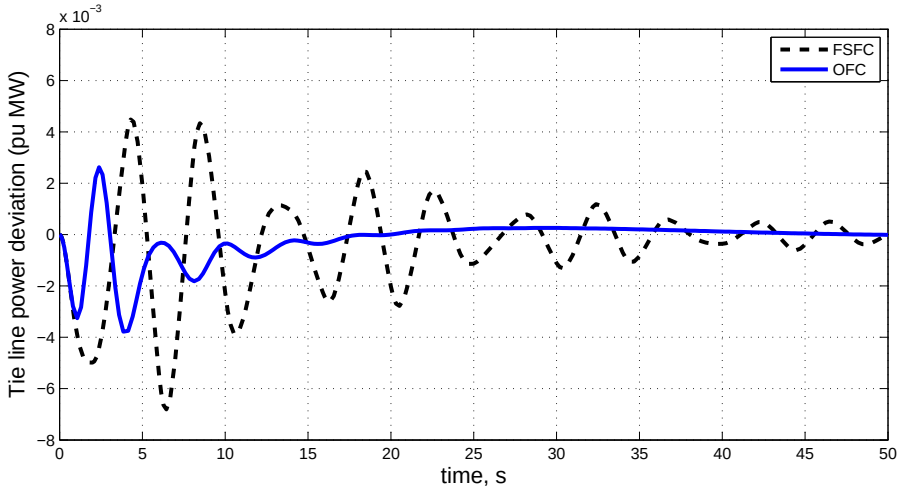

(c) Tie line power deviation response

Figure 3.6: Dynamic response of hydro-thermal interconnected power system

3.5 Summary

The LFC of various TAIPSs has been studied using OFC. The combinations of non-reheat, reheat and hydro turbines are taken to demonstrate the suitability of OFC for LFC of inter-connected power systems with variety. The Dynamic responses obtained with OFC have been compared with that of FSFC. The dynamic responses are obtained for thermal-thermal with non-reheat turbine, thermal-thermal considering reheat turbine and hydro-thermal interconnected power systems. It has been found that dynamic responses obtained with proposed OFC are comparatively better and competes well with FSFC, satisfying the LFC requirements. The OFC is presented from pragmatic point of view which uses less number of states as feedback, thereby reducing the controller cost and complexities.

CHAPTER 4

LFC OF POWER SYSTEMS WITH MULTI-SOURCE POWER GENERATION

4.1 Introduction

LFC is an important function in modern Energy management systems. Most of the researchers considered either thermal or hydro generating units in a control area [1, 9, 13, 15, 124]. In a real situation, control area may have variety of sources of generations such as hydro, thermal, gas, nuclear, solar, wind etc. The control area having different sources of power generation represented by an equivalent of thermal or hydro unit dynamics only may not result in realistic design of LFC control [6,89,116]. Furthermore, in the new power system environment, generators may or may not contribute in the LFC task and contribution factors are not the same for all participant generators [1,5,6,17,89,116]. Keeping in view the present power scenario, combination of multi-source generators in a control area with their corresponding generation contribution factors is more realistic for the study of LFC [89, 116]. In a competitive environment, generation contribution factors are actually time-dependent variables and must be computed dynamically based on bid prices, availability, congestion problems, costs and other related issues.

Most recently the LFC of power systems with MSPG is reported [89, 116, 117]. Challa et al. [89] has presented the analysis and design of controller for two area hydro-thermal-gas LFC system. They have shown that for LFC study, optimal PI state feedback controller is more robust and performs better than conventional genetic algorithm based PI controller. However, this optimal PI state feedback controller uses all the states for feedback purpose which is practically

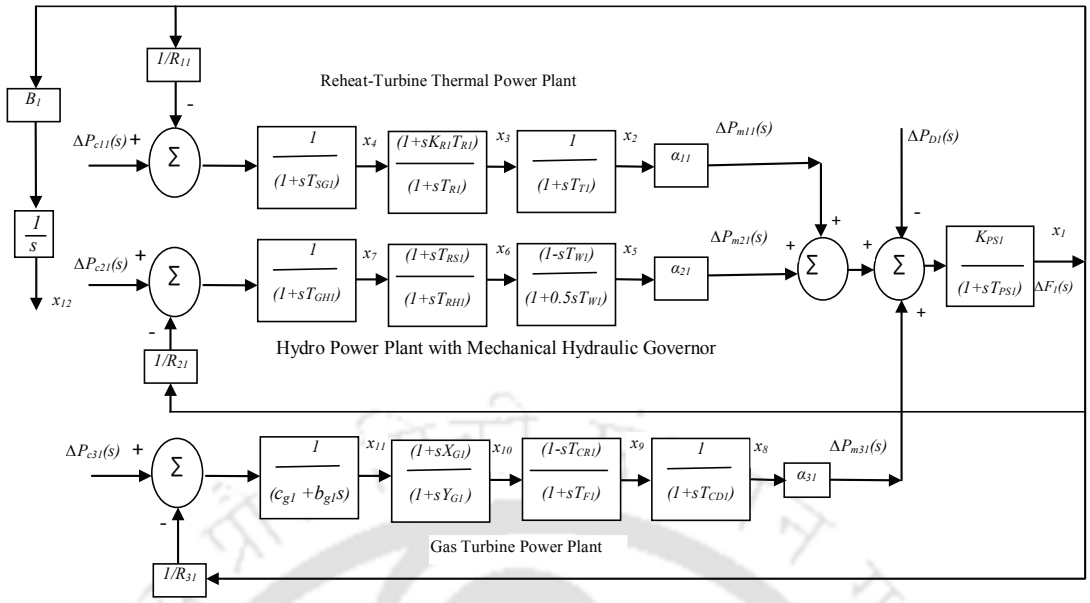

Figure 4.1: Block diagram of the single area Power System comprising Reheat-Thermal, Hydro and Gas generating units

difficult and results in the increased complexity and cost of the controller.

Keeping in view the above, two power system models (i) single area power system with MSPG and (ii) TAIPS with MSPG are presented for LFC analysis. Each control area of the power systems includes dynamics of thermal-reheat turbine, hydro and gas based power plants. The OFC is extended to these systems with pragmatic point of view as it uses less number of states and results in reduced cost and complexity. An extensive analysis is done considering the various effects of variation in system parameters and load conditions. To show the effectiveness of the proposed controller on the actual power system, the LFC of hydro power plants [1] has also been presented.

4.2 Single area power system with MSPG

The Single area power system (SAPS) with MSPG proposed for study comprises reheat-thermal, hydro and gas generating units. The linearized models of governors, reheat-turbines, hydro turbines, gas turbines described in [7, 10, 35–37, 116, 125], are taken for simulation of the power system shown in Fig. 4.1. The simulation parameters and data are given in Table 4.1. The nom-

inal load of the area is taken 1840 MW. The system has $n = 12$ state variables where $x_1 = \Delta f_1$ and $x_{12} = \int ACE\,dt = \int B_1 \Delta f_1 dt$. The power system can be described in the state space form given by the equations (2.52) and (2.38). The associated vectors and matrices are as follows:

state vector, $x = [x_1\ x_2\ .....x_{12}]^T$,

control vector, $u = [u_1\ u_2\ u_3]^T = [\Delta P_{c11}\ \Delta P_{c21}\ \Delta P_{c31}]^T$

disturbance vector, $w = [w_1] = [\Delta P_{D1}]$.

$$\tilde{A} = \begin{bmatrix}
-\frac{1}{T_{PS1}} & \frac{K_{PS1}\alpha_{11}}{T_{PS1}} & 0 & 0 & \frac{K_{PS1}\alpha_{21}}{T_{PS1}} & 0 & 0 & \frac{K_{PS1}\alpha_{31}}{T_{PS1}} & 0 & 0 & 0 & 0 \\
0 & \frac{-1}{T_{T1}} & \frac{1}{T_{T1}} & 0 & 0 & 0 & 0 & 0 & 0 & 0 & 0 & 0 \\
\frac{-K_{R1}}{T_{SG1}R_{11}} & 0 & -\frac{1}{T_{R1}} & \frac{1}{T_{R1}} - \frac{K_{R1}}{T_{SG1}} & 0 & 0 & 0 & 0 & 0 & 0 & 0 & 0 \\
\frac{-1}{T_{SG1}R_{11}} & 0 & 0 & -\frac{1}{T_{SG1}} & 0 & 0 & 0 & 0 & 0 & 0 & 0 & 0 \\
\frac{2T_{RS1}}{T_{RH1}T_{GH1}R_{21}} & 0 & 0 & 0 & -\frac{2}{T_{W1}} & \frac{2}{T_{W1}} + \frac{2}{T_{RH1}} & \frac{2T_{RS1}}{T_{RH1}T_{GH1}} - \frac{2}{T_{RH1}} & 0 & 0 & 0 & 0 & 0 \\
\frac{-T_{RS1}}{T_{RH1}T_{GH1}R_{21}} & 0 & 0 & 0 & 0 & -\frac{1}{T_{RH1}} & \frac{1}{T_{RH1}} - \frac{T_{RS1}}{T_{RH1}T_{GH1}} & 0 & 0 & 0 & 0 & 0 \\
\frac{-1}{T_{GH1}R_{21}} & 0 & 0 & 0 & 0 & 0 & -\frac{1}{T_{GH1}} & 0 & 0 & 0 & 0 & 0 \\
0 & 0 & 0 & 0 & 0 & 0 & 0 & -\frac{1}{T_{CD1}} & \frac{1}{T_{CD1}} & 0 & 0 & 0 \\
\frac{T_{CR1}X_{G1}}{T_{F1}R_{31}Y_{G1}b_{g1}} & 0 & 0 & 0 & 0 & 0 & 0 & 0 & -\frac{1}{T_{F1}} & \frac{1}{T_{F1}} + \frac{T_{CR1}}{T_{F1}Y_{G1}} & \frac{T_{CR1}X_{G1}c_{g1}}{T_{F1}Y_{G1}b_{g1}} - \frac{T_{CR1}}{T_{F1}Y_{G1}} & 0 \\
\frac{-X_{G1}}{R_{31}Y_{G1}b_{g1}} & 0 & 0 & 0 & 0 & 0 & 0 & 0 & 0 & -\frac{1}{Y_{G1}} & \frac{1}{Y_{G1}} - \frac{X_{G1}c_{g1}}{Y_{G1}b_{g1}} & 0 \\
\frac{-1}{R_{31}b_{g1}} & 0 & 0 & 0 & 0 & 0 & 0 & 0 & 0 & 0 & -\frac{c_{g1}}{b_{g1}} & 0 \\
B_1 & 0 & 0 & 0 & 0 & 0 & 0 & 0 & 0 & 0 & 0 & 0
\end{bmatrix}$$

$$\tilde{B}^T = \begin{bmatrix}
0 & 0 & \frac{K_{R1}}{T_{SG1}} & \frac{1}{T_{SG1}} & 0 & 0 & 0 & 0 & 0 & 0 & 0 & 0 \\
0 & 0 & 0 & 0 & -\frac{2T_{RS1}}{T_{RH1}T_{GH1}} & \frac{T_{RS1}}{T_{RH1}T_{GH1}} & \frac{1}{T_{GH1}} & 0 & 0 & 0 & 0 & 0 \\
0 & 0 & 0 & 0 & 0 & 0 & 0 & 0 & -\frac{X_{G1}T_{CR1}}{T_{F1}Y_{G1}b_{g1}} & \frac{X_{G1}}{Y_{G1}b_{g1}} & \frac{1}{b_{g1}} & 0
\end{bmatrix}$$

$$\tilde{F}^T = \begin{bmatrix} -\frac{K_{PS1}}{T_{PS1}} & 0 & 0 & 0 & 0 & 0 & 0 & 0 & 0 & 0 & 0 & 0 \end{bmatrix}$$

and the output matrix $\tilde{C}$ is defined as

$$\tilde{C} = \begin{bmatrix} 0 & 0 & 0 & 0 & 0 & 0 & 0 & 0 & 0 & 0 & 0 & 1 \end{bmatrix}$$

The performance index J is given in equation(2.39), the matrices $\tilde{Q}$ and $\tilde{R}$ are defined for this problem using the design criterion given in the section 2.6.2. Excursions of ACE ($B_1 x_1$), $\int ACE\,dt$ (x_{12}) and control vectors(u_1, u_2, u_3) about their steady values are minimized and J can be written as:

$$J = \frac{1}{2}\int_0^\infty \left[(B_1 x_1)^2 + (x_{12})^2 + \left(u_1^2 + u_2^2 + u_3^2\right)\right] dt \tag{4.1}$$

From the equation (4.1), the matrices $\tilde{Q}$ and $\tilde{R}$ can be recognized as:

$$\tilde{Q}=\begin{bmatrix} {B_1}^2 & 0 & 0 & 0 & 0 & 0 & 0 & 0 & 0 & 0 & 0 & 0 \\ 0 & 0 & 0 & 0 & 0 & 0 & 0 & 0 & 0 & 0 & 0 & 0 \\ 0 & 0 & 0 & 0 & 0 & 0 & 0 & 0 & 0 & 0 & 0 & 0 \\ 0 & 0 & 0 & 0 & 0 & 0 & 0 & 0 & 0 & 0 & 0 & 0 \\ 0 & 0 & 0 & 0 & 0 & 0 & 0 & 0 & 0 & 0 & 0 & 0 \\ 0 & 0 & 0 & 0 & 0 & 0 & 0 & 0 & 0 & 0 & 0 & 0 \\ 0 & 0 & 0 & 0 & 0 & 0 & 0 & 0 & 0 & 0 & 0 & 0 \\ 0 & 0 & 0 & 0 & 0 & 0 & 0 & 0 & 0 & 0 & 0 & 0 \\ 0 & 0 & 0 & 0 & 0 & 0 & 0 & 0 & 0 & 0 & 0 & 0 \\ 0 & 0 & 0 & 0 & 0 & 0 & 0 & 0 & 0 & 0 & 0 & 0 \\ 0 & 0 & 0 & 0 & 0 & 0 & 0 & 0 & 0 & 0 & 0 & 0 \\ 0 & 0 & 0 & 0 & 0 & 0 & 0 & 0 & 0 & 0 & 0 & 1 \end{bmatrix}$$

and

$$\tilde{R}=\begin{bmatrix} 1 & 0 & 0 \\ 0 & 1 & 0 \\ 0 & 0 & 1 \end{bmatrix}$$

4.2.1 Simulation results and discussion

The optimal gain of the proposed OFC is obtained as

$$\tilde{K}=\begin{bmatrix} 0.1514 \\ 0.0131 \\ 0.0708 \end{bmatrix}$$

Dynamic responses of the system are obtained for 1% SLP in the area through MATLAB simulation. The frequency deviation response is depicted in Fig. 4.2. It has been observed that the OFC gives better frequency deviation response having relatively smaller peak overshoot and lesser settling time with zero steady state error as compared to the FSFC. As given in Table 4.2, percentage improvement in peak OS and settling time with OFC is becoming 6.38 and 61.66, respectively. Some steady state error remains if there is no controller in the supplementary loop. The output power deviation responses of thermal, hydro and gas units are shown in Fig. 4.3. The generators respond to accommodate the change in area load by increasing their corresponding generations. The power generations with OFC in action, attains desirable steady values to match the local area load change. The effects of generation rate constraints, selection of regulation parameters and sensitivity analysis are discussed in sections (4.2.2), (4.2.3) and

(4.2.4), respectively.

Table. 4.1: Simulation parameters of SAPS with MSPG

Parameters	Value
P_{rt1}	2000 MW
P_{L1}	1840 MW
$f_1 = f$	60 Hz
H_1	5 MW-s/MVA
D_1	0.0153 pu MW/Hz
K_{PS1}	65.2174 Hz/pu MW
T_{PS1}	10.8696 s
T_{SG1}	0.08 s
T_{T1}	0.3 s
T_{CD1}	0.2 s
B_1	1
K_{R1}	0.3
T_{R1}	10 s
T_{W1}	1 s
T_{RS1}	5 s
T_{RH1}	28.75 s
T_{GH1}	0.2 s
X_{G1}	0.6 s
Y_{G1}	1 s
c_{g1}	1
b_{g1}	0.05 s
T_{F1}	0.23 s
T_{CR1}	0.01s
$R_1 = R$	2.4 Hz/pu MW
α_{11}	0.543478
α_{21}	0.326084
α_{31}	0.130438

4.2.2 Effect of generation rate constraint

In most of the research papers, the effect of restriction on the rate of change of power generation is not considered [8, 19, 39, 86, 91, 92]. In power systems having steam plants and hydro plants, power generation can change only at a specified maximum rate [2, 81, 85, 124–126]. Most of the reheat units have a generation rate around 3 percent/minute. Some have a GRC between 5 and 10 percent/min. For testing further the effectiveness of the proposed controller, the GRC for thermal and hydro units is taken into account in the computer simulation model. GRC for hydro unit: for raise 270 percent/minute (0.045pu/s) and for lower 360 percent/minute (0.06pu/s) is

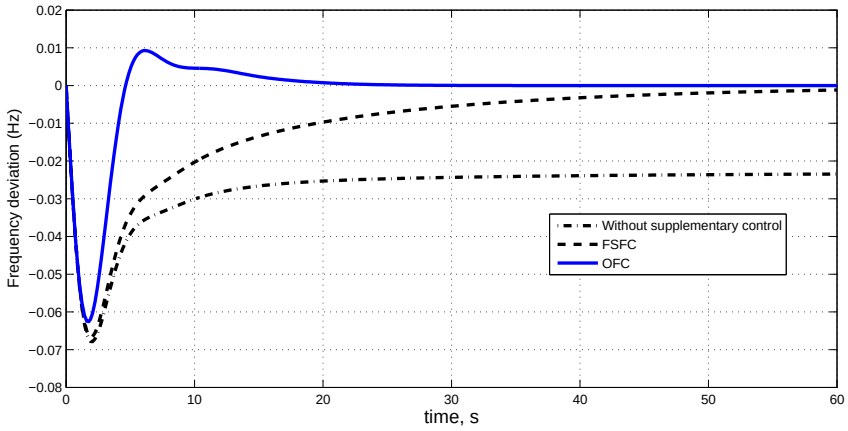

Figure 4.2: Frequency deviation response to 1% SLP in the area

Table. 4.2: Dynamic response comparison of a SAPS

	Peak OS of $\Delta f_1(Hz)$	ST of $\Delta f_1(s)$
FSFC	-0.0668	60
OFC	-0.06242	23
% reduction	6.38	61.66

considered and GRC for reheat turbine thermal unit: for raise and lower 10 percent/minute (0.0017pu/s) is considered for study. The proposed power system is simulated with and without the above GRC limits [9,81,114,123] in thermal and hydro power generating units. The turbine model considering GRC is shown in Fig. 4.5. An attempt is made to show that how does the proposed controller designed on linearized models behave if non-linearity is introduced. The effect of GRC on the frequency deviation response of the area obtained with OFC at nominal load is shown in the Fig. 4.4. There is a little increase in peak OS, however settling time remains same. The frequency deviations settles with zero steady state erro. It has been observed that proposed controller performs well and can accommodate the effect of GRC. Therefore, dynamic response of the system with GRC satisfies LFC problem requirement.

4.2.3 Effect of governor speed regulation parameter (R)

Fig. 4.6 shows the frequency deviation response to 1% load perturbation in the area at nominal load with R varying from 1% to 8%. It is assumed that $R_{ki} = R_i$ and $R_i = R$. It has been observed

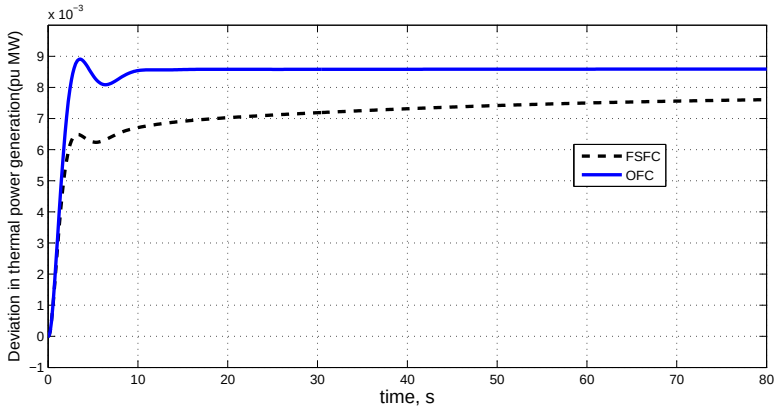

(a) Thermal power generation deviation response

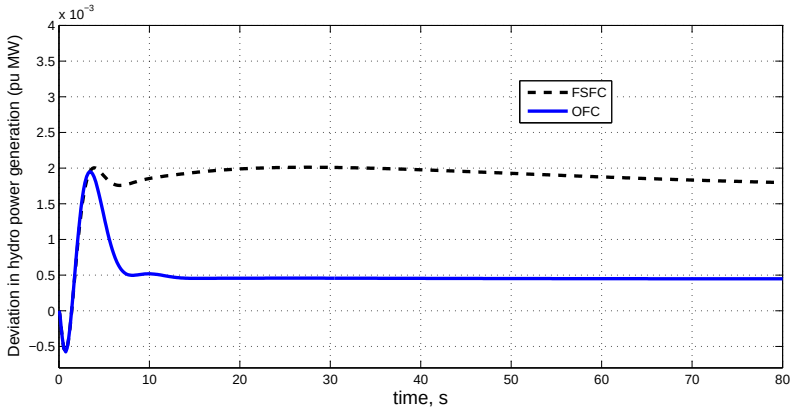

(b) Hydro power generation deviation response

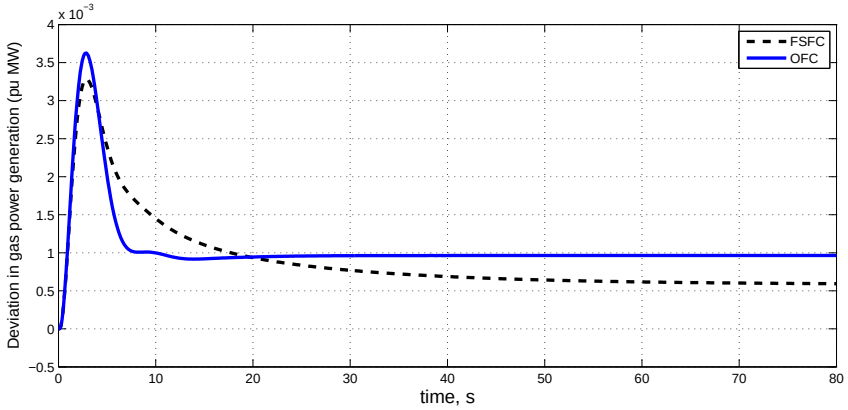

(c) Gas power generation deviation response

Figure 4.3: Power generation deviation responses to 1% SLP in the area

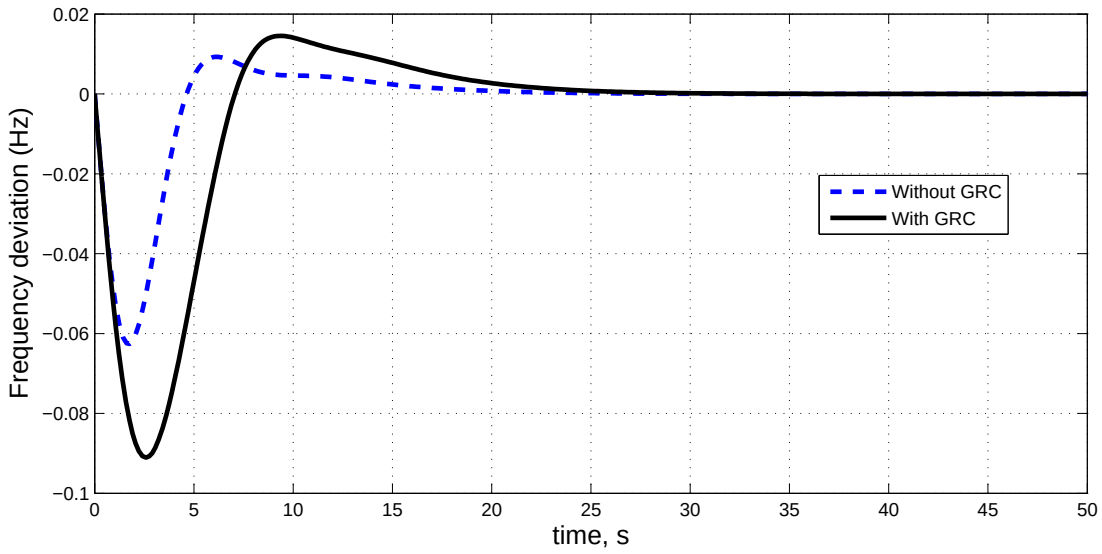

Figure 4.4: Frequency deviation response to 1% SLP in the area considering GRC

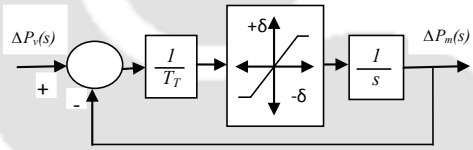

Figure 4.5: Block diagram of a non-linear turbine(GRC)

that for higher values of *R* i.e. 6% and 8%, the peak overshoot and settling time increases; if we further increase the value of *R*, the system gives larger frequency deviation oscillations and settling time. For lower values of *R* i.e. 1% and 2% the system becomes more oscillatory and results in increased cost of governors [15]. Therefore, there should be a compromise between the governor cost and dynamic performance. Findings reveal that there is no need of going for the lower values and the higher values of *R*, since medium value of *R* with corresponding optimum controller gains can be preferred to provide better dynamic response. Therefore *R*=4% taken for the LFC of the proposed system.

4.2.4 Sensitivity analysis

Lesser attention has been paid to this aspect of LFC problem. Most recently Debbarma et al. [114] carried out the sensitivity analysis for LFC using BF technique based fractional-order

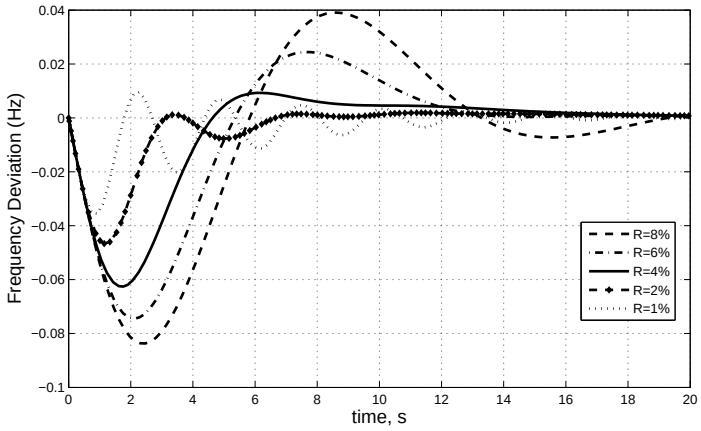

Figure 4.6: Frequency deviation response to 1% SLP in the area with variation in R from 1% to 8%

Table. 4.3: Sensitivity Analysis

Parameter variation	% change	Optimal output feedback controller gains			Performance index J_0
		$\tilde{K}_{11}$	$\tilde{K}_{21}$	$\tilde{K}_{31}$	
All nominal	0	0.1514	0.0131	0.0708	0.414996
Loading	+25	0.1537	0.0142	0.0719	0.406347
condition	−25	0.1491	0.0119	0.0696	0.424447
T_{SG}	+25	0.1496	0.0130	0.0708	0.419149
T_{SG}	−25	0.1532	0.0131	0.0708	0.410883
T_{GH}	+25	0.1510	0.0126	0.0706	0.416183
T_{GH}	−25	0.1519	0.0136	0.0711	0.413668
T_R	+25	0.1540	0.0151	0.0758	0.41860
T_R	−25	0.1482	0.0107	0.0643	0.409793
T_T	+25	0.1454	0.0126	0.0706	0.429905
T_T	−25	0.1577	0.0135	0.0709	0.400242
T_{RH}	+25	0.1515	0.0103	0.0713	0.414982
T_{RH}	−25	0.1508	0.0175	0.0698	0.417074
T_W	+25	0.1503	0.0051	0.0698	0.426905
T_W	−25	0.1526	0.0221	0.0718	0.402864
T_{CD}	+25	0.1521	0.0218	0.0694	0.406546
T_{CD}	−25	0.1531	0.0224	0.0743	0.399133

PID controller. Sensitivity analysis is carried out to demonstrate the robustness of the optimum OFC gains (at nominal condition) for wide changes in system parameters and loading condition from their nominal values. The system parameters and operating load condition are varied by ±25% from their nominal values, taking one at a time. Table 4.3 gives the optimum controller gain settings for varied system parameters and operating load condition using optimal OFC. Dynamic responses are presented in Figs.4.7 and 4.8 for each changed conditions with their corresponding $\tilde{K}$ and further compared with the responses obtained with $\tilde{K}$ at nominal condition. Critical examination of all the responses clearly reveals that responses are more and less same.

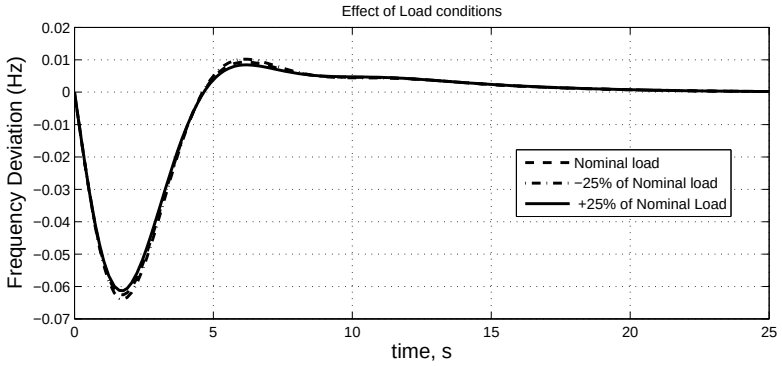

Figure 4.7: Frequency deviation response with variation in load conditions

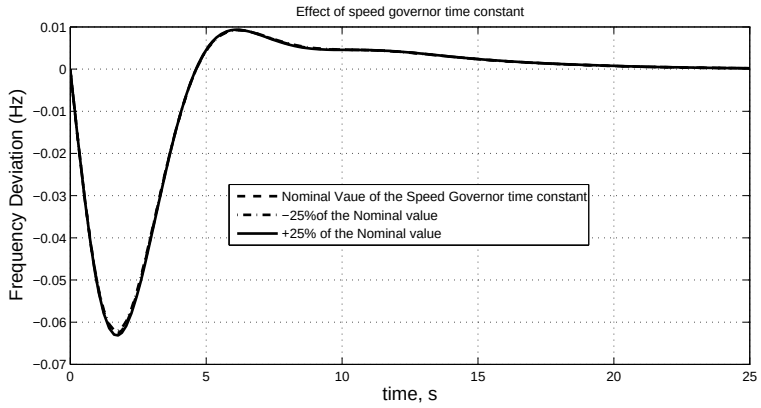

Figure 4.8: Frequency deviation response with variation in speed governor time constant

Only two number of responses are shown in Figs.4.7 and 4.8 to justify the statement. Thus, $\tilde{K}$ obtained at nominal parameter and nominal loading condition need not be reset for wide changes in the system loading or system parameters.

4.3 Two-area interconnected power system with MSPG

Having studied the LFC of SAPS with MSPG, the work has been extended for interconnected power systems. The TAIPS simulated in this study is shown in Fig. 4.9 which comprises reheat-thermal, hydro and gas generating units in each control area. The simulation parameters and data are given in Table 4.4. The nominal load of the control area is taken 1640 MW. The power system has 25 state variables. State variables x_1, x_{12}, x_{24} and x_{25} are taken as output feedback

Table. 4.4: Simulation parameters of TAIPS with MSPG

Parameters	Value
$P_{rt1} = P_{rt2}$	2000 MW
$P_{L1} = P_{L1}$	1640 MW
f	60 Hz
$H_1 = H_2$	5 MW-s/MVA
$D_1 = D_2$	0.0137 pu MW/Hz
$K_{PS1} = K_{PS2}$	73.1707 Hz/pu MW
T_{12}	0.0433
$T_{PS1} = T_{PS2}$	12.1951 s
$T_{SG1} = T_{SG2}$	0.08 s
$T_{T1} = T_{T2}$	0.3 s
$T_{CD1} = T_{CD2}$	0.2 s
$B_1 = B_2$	0.4303
a_{12}	- 1
$K_{R1} = K_{R2}$	0.3
$T_{R1} = T_{R2}$	10 s
$T_{W1} = T_{W2}$	1 s
$T_{RS1} = T_{RS2}$	5 s
$T_{RH1} = T_{RH2}$	28.75 s
$T_{GH1} = T_{GH2}$	0.2 s
$X_{G1} = X_{G2}$	0.6 s
$Y_{G1} = Y_{G2}$	1 s
$c_{g1} = c_{g2}$	1
$b_{g1} = c_{g2}$	0.05 s
$T_{F1} = T_{F2}$	0.23 s
$T_{CR1} = T_{CR2}$	0.01s
$R_1 = R_2$	2.4 Hz/pu MW
$\alpha_{11} = \alpha_{12}$	0.579268
$\alpha_{21} = \alpha_{22}$	0.274390
$\alpha_{31} = \alpha_{32}$	0.146342

states. The power system can be described in the state space form given by the equations (2.52) and (2.38). The associated vectors and matrices are as follows:

state vector, $x = [x_1\ x_2 \ldots\ldots x_{25}]^T$

control vector, $u = [u_1\ u_2\ u_3\ u_4\ u_5\ u_6]^T = [\Delta P_{c11}\ \Delta P_{c21}\ \Delta P_{c31}\ \Delta P_{c12}\ \Delta P_{c22}\ \Delta P_{c32}]^T$

disturbance vector, $w = [w_1\ w_2]^T = [\Delta P_{D1}\ \Delta P_{D2}]^T$.

and the constant matrices $\tilde{A}$, $\tilde{B}$ and $\tilde{C}$, the disturbance matrix $\tilde{F}$ and design matrices $\tilde{Q}$ and $\tilde{R}$ are given in Appendix A.1.

The regulation parameter R is taken 4% for all and for the TAIPS, $\Delta P_{tie,1} = \Delta P_{tie,12}$. The optimum gains of FSFC and optimal OFC have been obtained by running the MATLAB codes

generated on the basis of method described in the controller design section 2.6. MATLAB control system toolbox [121] is used to simulate the power system and to obtain dynamic responses of the system for 1% SLPs in the control area-1. The MATLAB Simulations are run with the optimum controller gains.

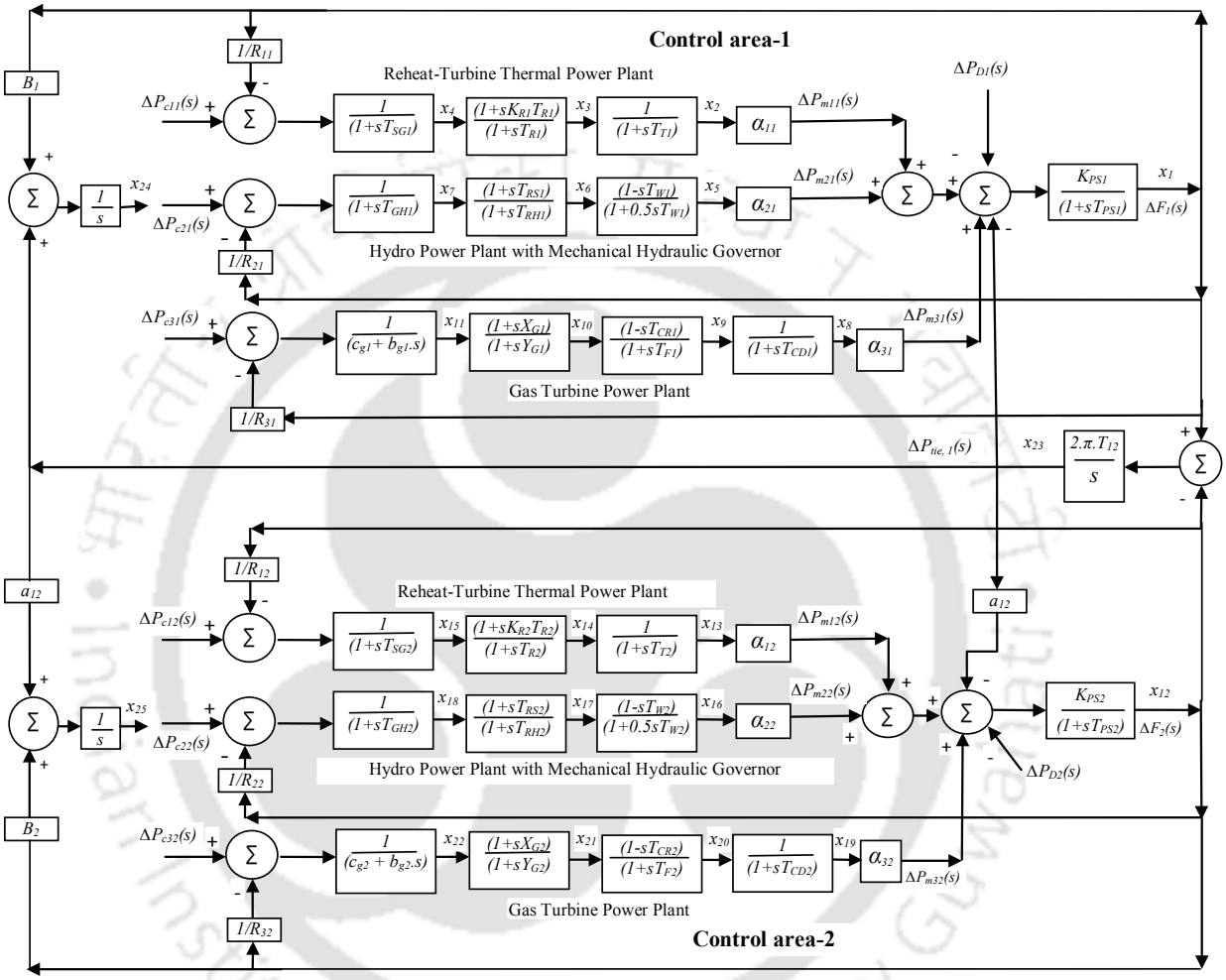

Figure 4.9: TAIPS comprising reheat-thermal, hydro and gas generating units in each control area

4.3.1 Simulation results and discussion

The optimum value of the $\tilde{K}$ for the proposed OFC corresponding to nominal system parameters is obtained as:

$$\tilde{K} = \begin{bmatrix} 0.4202 & -0.0936 & 0.3233 & 0.0808 \\ -0.1634 & -0.0039 & -0.0386 & -0.0522 \\ 0.1622 & -0.0597 & 0.1340 & 0.0207 \\ 0.0719 & 0.8219 & -0.1455 & 0.3840 \\ -0.0469 & -0.6530 & -0.1181 & -0.4162 \\ 0.0473 & 0.3588 & -0.0074 & 0.2008 \end{bmatrix}$$

Dynamic responses of the system are obtained for 1% SLP in the control area-1 through computer simulation. The frequency deviation and tie line power deviation responses are shown in Fig. 4.10. It is observed that the OFC gives better dynamic response having relatively smaller peak overshoot and lesser settling time with zero steady state error as compared to the FSFC. The dynamic response of the power system considering low, medium and high head hydro turbines is as shown in Fig. 4.11. The results show that frequency and tie line power deviations are more and less same for low and high head hydro turbines. The settling time increases in the case of medium head turbine. However OFC shows its suitability for low, medium and high head hydro plants and gives satisfactory dynamic responses.

4.3.2 Effect of GRC

In this section, the performance of the proposed OFC is evaluated considering GRC in power system simulation model. GRC for Hydro unit: for raise 0.045 pu/s and for lower 0.06 pu/s is considered and GRC for reheat turbine thermal unit: 0.0017 pu/s is considered for study. The power system is simulated with and without the above GRC limits in thermal and hydro power generating units in each area. The effect of GRC on the dynamic responses is shown in the Fig. 4.12. The critical examination of dynamic responses reveals that GRC results in increased peak overshoot, however settling time remains same for this particular power system model. The proposed controller accommodates the effect of GRC and gives dynamic responses satisfying

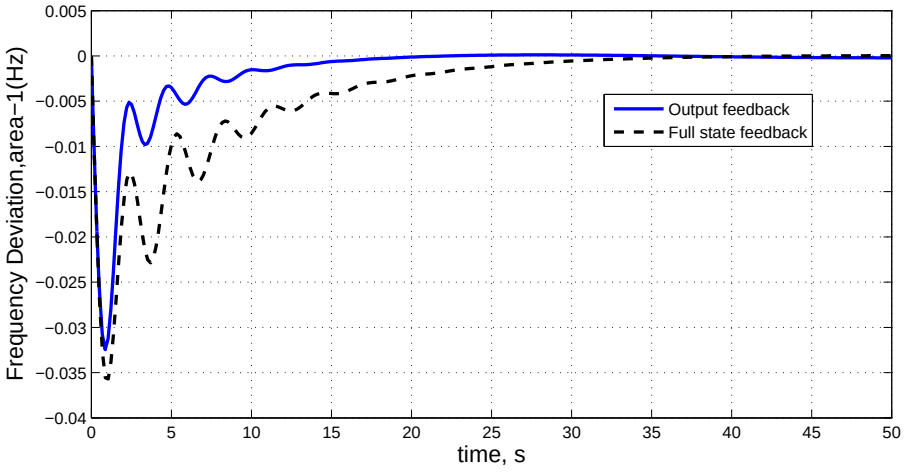

(a) Frequency deviation response of area-1

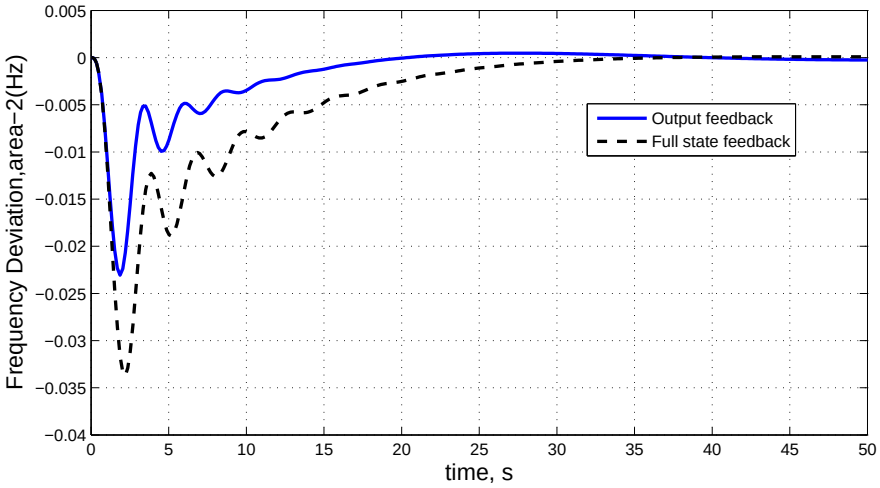

(b) Frequency deviation response of area-2

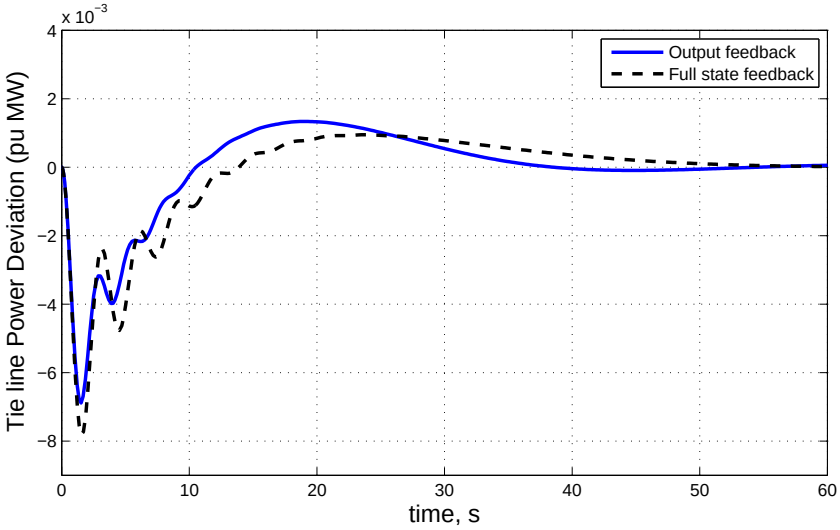

(c) Tie line power deviation response

Figure 4.10: Comparison of frequency and tie line power deviation responses for 1% SLP

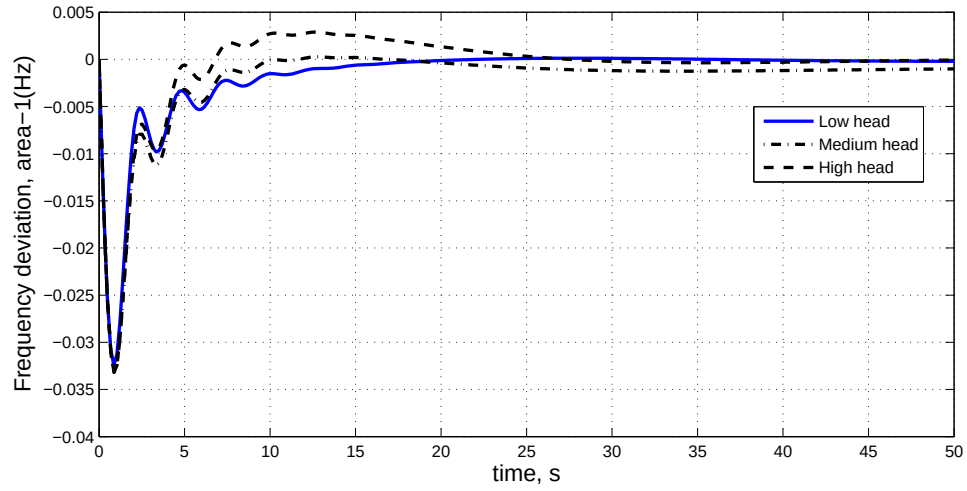

(a) Frequency deviation response of area-1

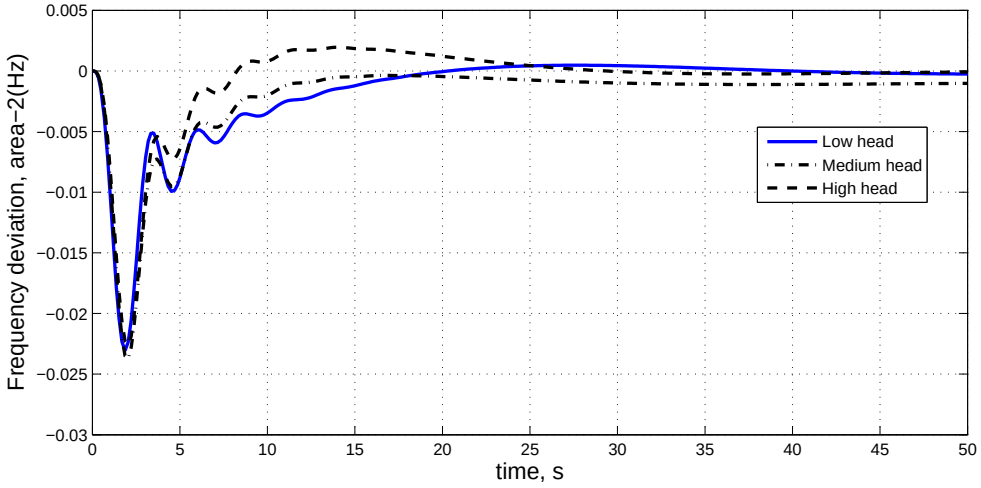

(b) Frequency deviation response of area-2

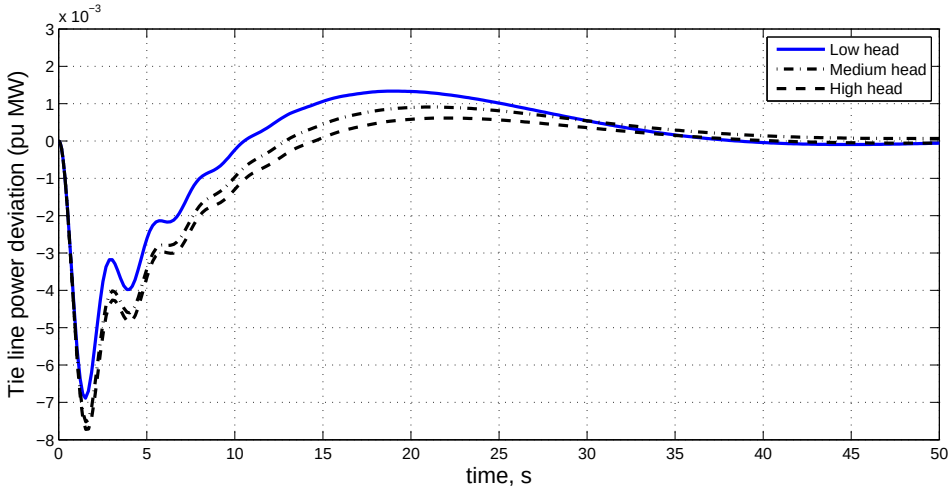

(c) Tie line power deviation response

Figure 4.11: Frequency and tie line power deviation responses with low, medium and high head hydro turbines

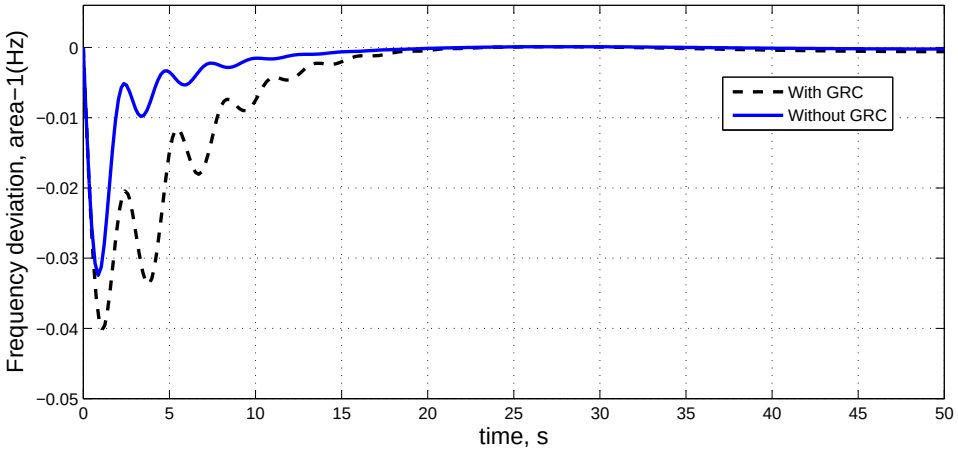

(a) Frequency deviation response of area-1

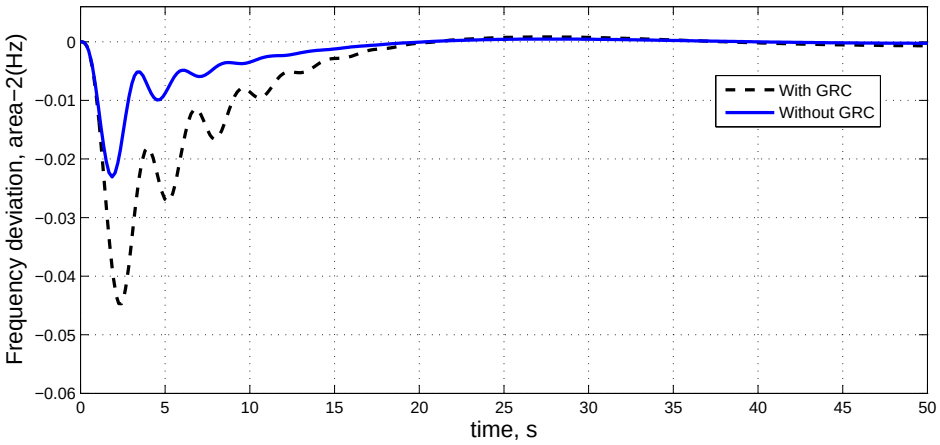

(b) Frequency deviation response of area-2

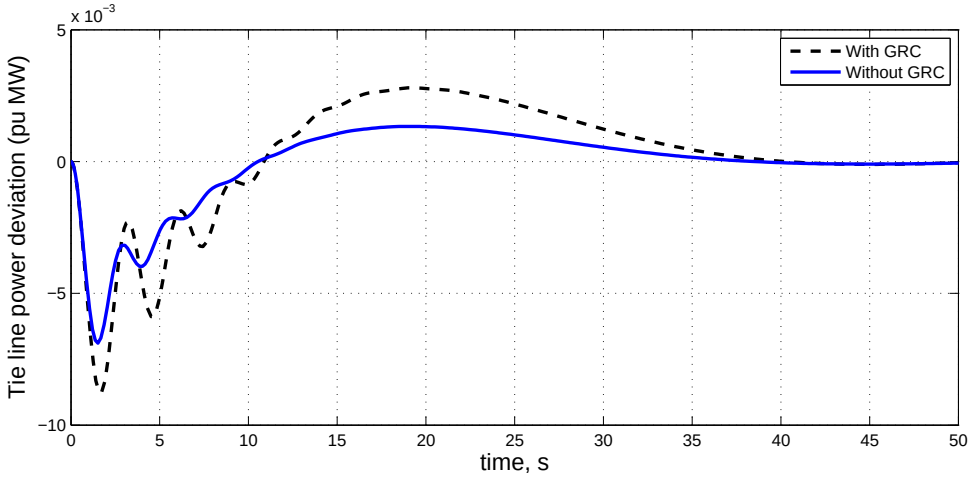

(c) Tie line power deviation response

Figure 4.12: Dynamic responses considering the GRC

LFC problem requirements. It shows that optimal OFC designed for linearized models, may perform well even if GRCs are considered.

4.3.3 Selection of governor speed regulation parameter(R)

Fig. 4.13 shows the dynamic response to 1% SLP in the control area-1 with R varying from 2% to 6%. It is assumed that $R_{ki} = R_i$ and for equal area $R_i = R$. It is observed that for higher values of R i.e. 5% and 6%, the peak overshoot and settling time increases; if we further increase the value of R, the system gives larger peak overshoots and settles with larger settling time. The dynamic response for 3% to 4% value of R results with smaller peak overshoot and lesser settling time. For further lower values of R the system dynamic response becomes more oscillatory. Findings reveal that there is no need of going for the lower values and the higher values of R, since medium value of R with corresponding optimum controller gains can be preferred to provide better dynamic response of LFC. For this power system R is chosen 4% which yields improved results.

4.3.4 Effect of variation in load disturbance

In fact, LFC deals with small level disturbances in the power system. In most of the studies, 1% SLP is taken for the study of LFC problem. In real situations, the load disturbances also vary. In this case, system dynamic responses are obtained for the wide range of SLP varying from 1% to 5% in control area 1. Dynamic responses for different SLPs are shown in Fig. 4.14. It is concluded that for SLP varying from 1% to 5%, the first peak overshoot increases with increase in the level of SLP and settling time remains approximately same with zero steady state error. The proposed OFC acts fast to settle the deviations in the frequency and tie line power. Therefore, the proposed controller satisfy the LFC problem requirement for wide variation of load disturbance.

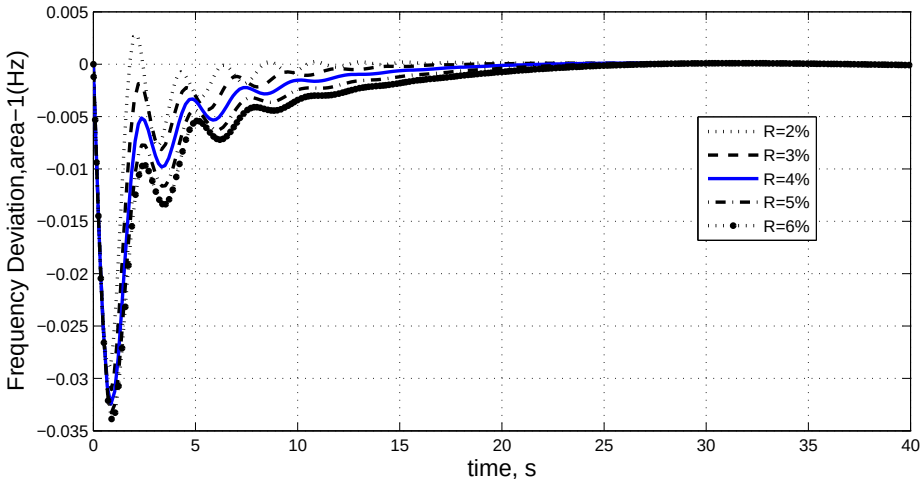

(a) Frequency deviation response of area-1

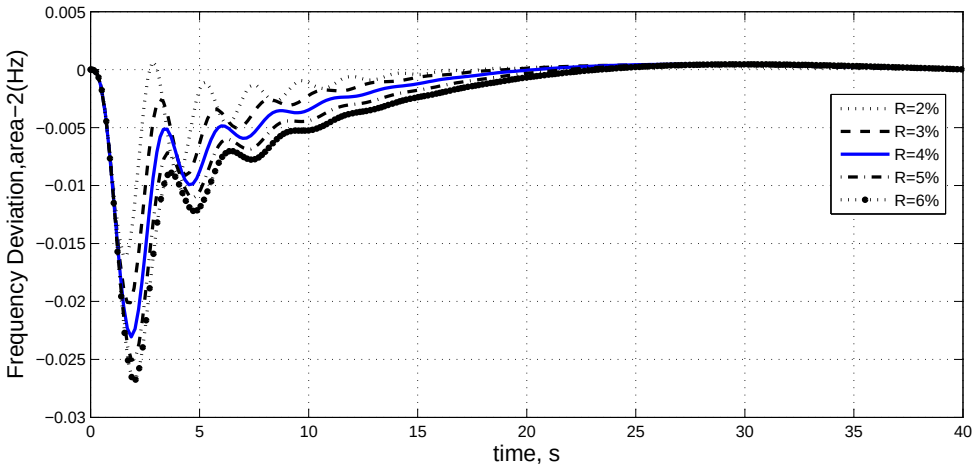

(b) Frequency deviation response of area-2

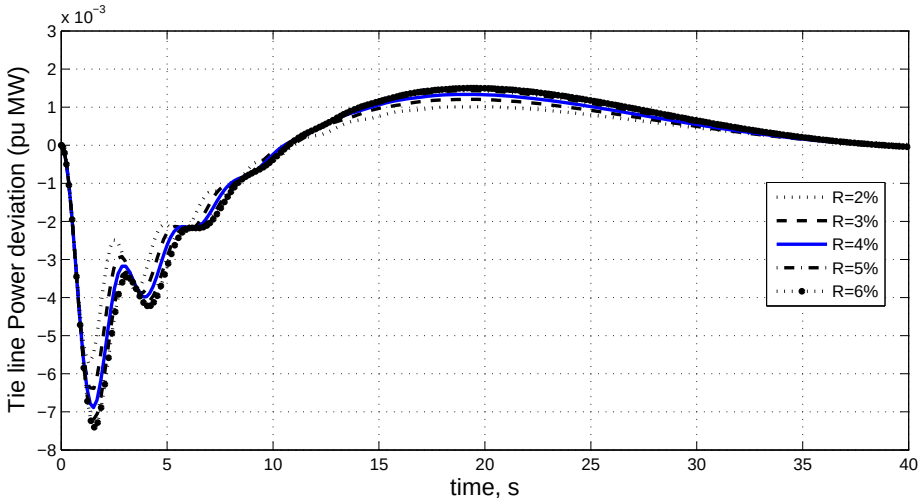

(c) Tie line power deviation response

Figure 4.13: Effect of the *R* on dynamic responses

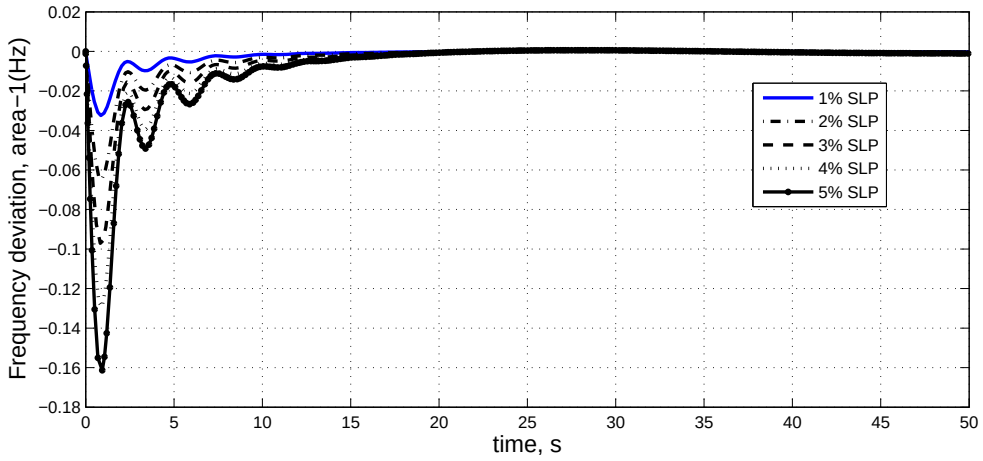

(a) Frequency deviation response of area-1

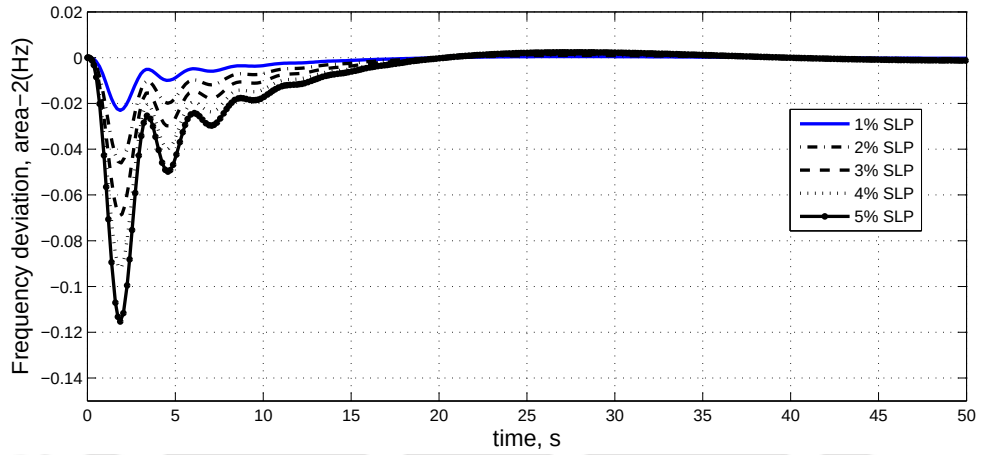

(b) Frequency deviation response of area-2

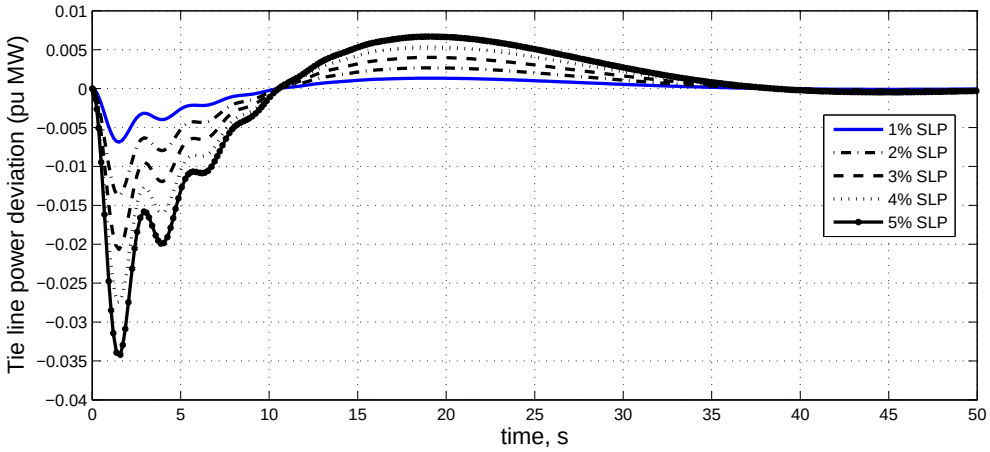

(c) Tie line power deviation response

Figure 4.14: Frequency and tie line power deviation responses for SLPs in area-1, varying from 1% to 5%

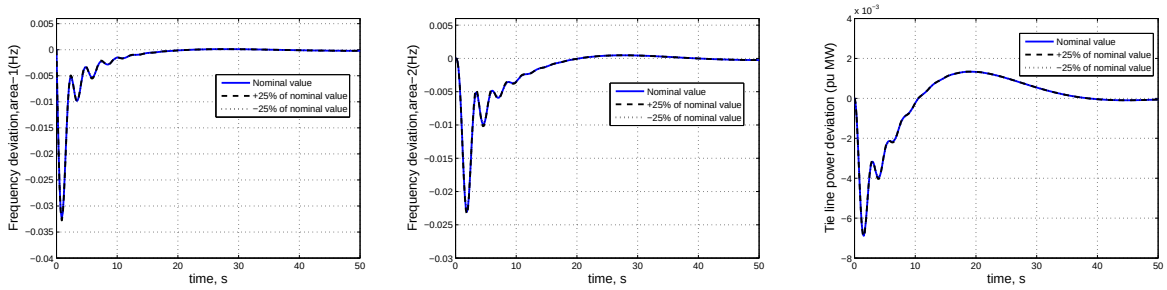

(a) Frequency deviation response of area-1 (b) Frequency deviation response of area-2 (c) Tie line power deviation response

Figure 4.15: Effect of variation in steam turbine speed governor time constant(T_{SG}) on dynamic responses

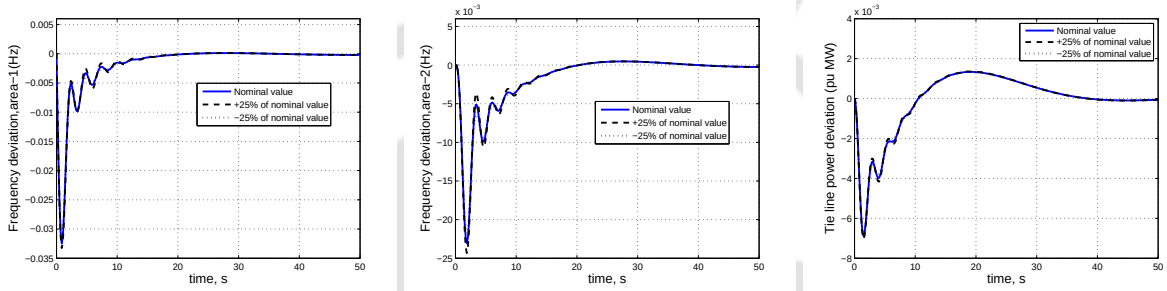

(a) Frequency deviation response of area-1 (b) Frequency deviation response of area-2 (c) Tie line power deviation response

Figure 4.16: Effect of variation in steam turbine time constant(T_T) on dynamic responses

4.3.5 Sensitivity analysis

The system parameters and operating load condition are varied by ±25% from their nominal values, taking one at a time. Dynamic responses for variation in system parameters and load condition are shown in Figs.(4.15)-(4.22). An extensive analysis is done to examine the effect of variation in system parameters and load conditions. Investigations reveal that the dynamic responses hardly change when system parameters and operating load condition are changed by ±25% from their nominal values with the optimum controller gains once set. It is evident that OFC accommodates for the wide range of variations in system parameters and load condition from their nominal values. The settling time and peak overshoot of the dynamic responses under these varied conditions are more and less same with zero steady state error.

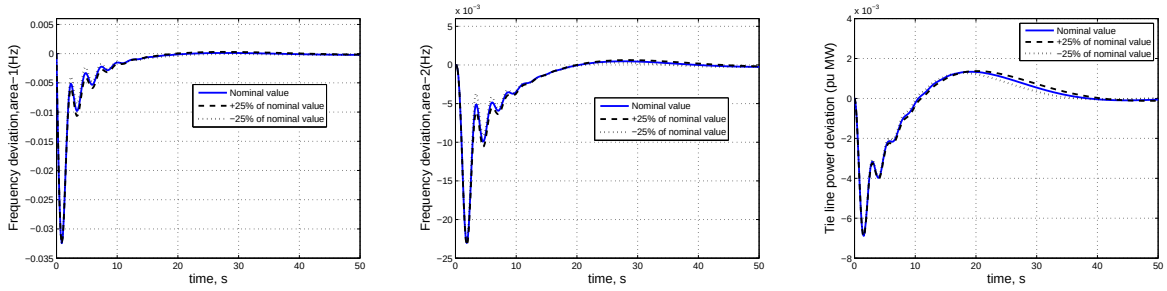

(a) Frequency deviation response of area-1 (b) Frequency deviation response of area-2 (c) Tie line power deviation response

Figure 4.17: Effect of variation in steam turbine reheat time constant(T_R) on dynamic responses

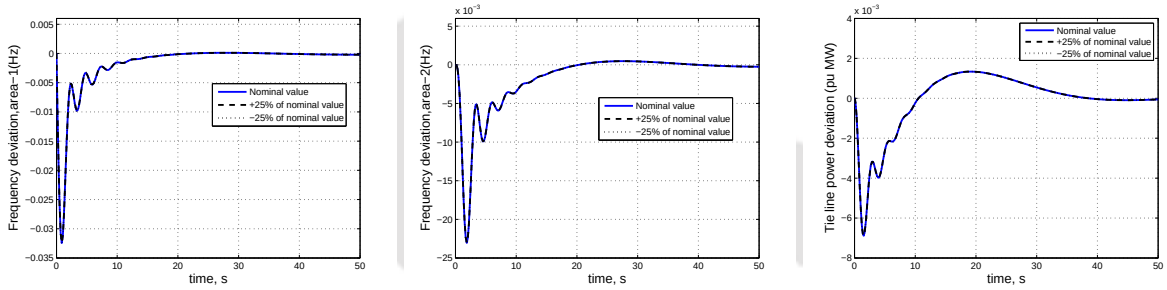

(a) Frequency deviation response of area-1 (b) Frequency deviation response of area-2 (c) Tie line power deviation response

Figure 4.18: Effect of variation in hydro turbine speed governor main servo time constant(T_{GH}) on dynamic responses

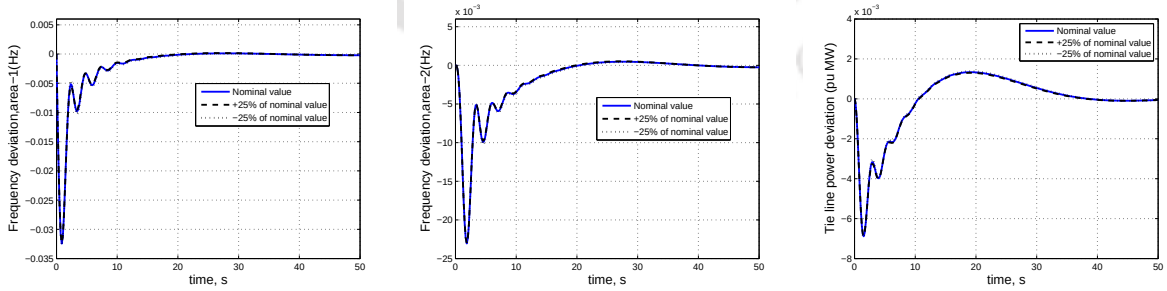

(a) Frequency deviation response of area-1 (b) Frequency deviation response of area-2 (c) Tie line power deviation response

Figure 4.19: Effect of variation in hydro turbine speed governor transient droop time constant(T_{RH}) on dynamic responses

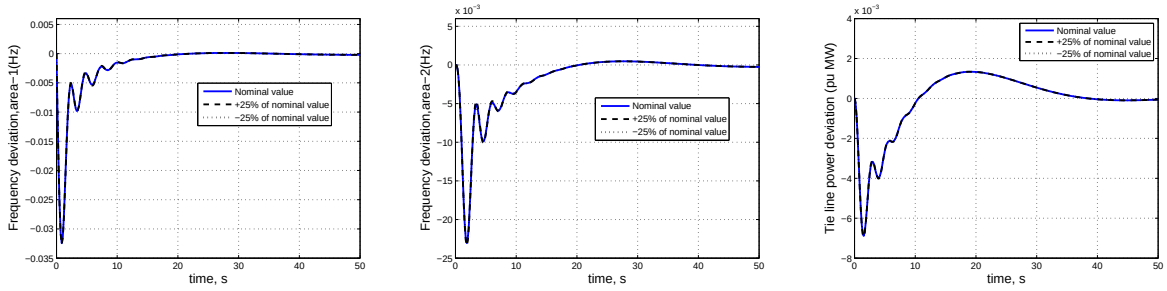

(a) Frequency deviation response of area-1 (b) Frequency deviation response of area-2 (c) Tie line power deviation response

Figure 4.20: Effect of variation in gas turbine compressor discharge volume time constant (T_{CD}) on dynamic responses

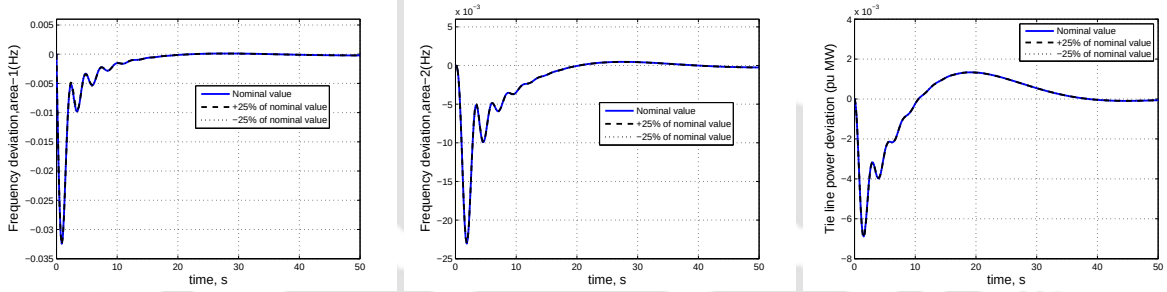

(a) Frequency deviation response of area-1 (b) Frequency deviation response of area-2 (c) Tie line power deviation response

Figure 4.21: Effect of variation in nominal starting time of water in penstock (T_W) on dynamic responses

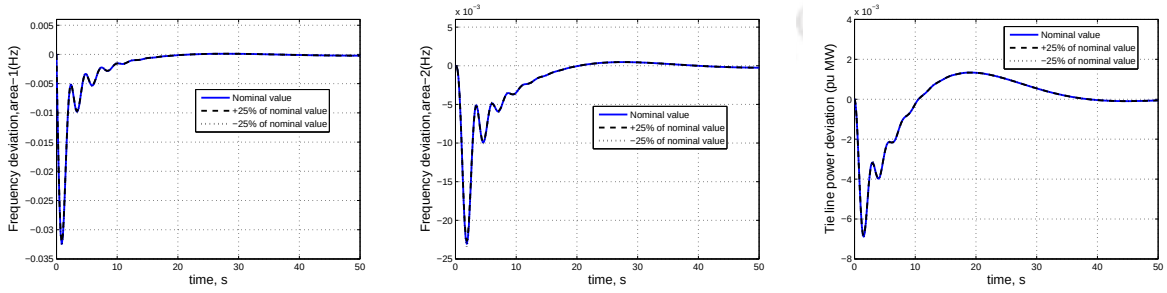

(a) Frequency deviation response of area-1 (b) Frequency deviation response of area-2 (c) Tie line power deviation response

Figure 4.22: Effect of variation in nominal area load on dynamic responses

4.4 LFC of hydro power plants

To ensure the good performance of the proposed optimal OFC on an actual power system, hydro power plants operational in KHOZESTAN (a province in southwest of Iran) [1] are taken as an additional case study in this section. Dez output power is 520 MW whereas Karoon3 output power is 1000 MW operational and 2000 MW nominal. The control area is linked to other control areas of an interconnected power system. The control area includes Karoon3 and Dez hydro power plants where variation of area load and interaction of other control areas are considered as two disturbances in control area.

Most recently (2012), Alireza et al. [1] studied the LFC of this operational plant using a robust optimal MISO PID controller where the tuning of PID controller is stated as an optimization problem in which a combination of quadratic index and maximal complex/real ratio of the closed loop poles is minimized subject to some constraints on characteristic matrix Eigenvalues.

For analysis, their system dynamics, system parameter values, load disturbance conditions and assumptions are considered here. For clarity and sake of comparison, nomenclature of system parameters in this section are kept same as in [1]. Block diagram of a control area including two hydro power plants [1] is referred for formulating the state equations. The block diagram of the interconnected power system is reproduced [1] for ready reference and shown in the Fig. 4.24. Refering equations (2.37) and (2.38), in this case study n=7, m=1 and p=3, where the state vector is $x = [\Delta f\ \Delta P_{tie}\ \Delta P_{tK}\ \Delta P_{tD}\ \Delta P_{gK}\ \Delta P_{gD}\ \int ACE]^T$ and the output state vector is $y = [\Delta f\ \Delta P_{tie}\ \int ACE]^T$.

The system parameters [1] taken to run the MATLAB Simulation are $T_{tK} = 0.32s$, $T_{tD} = 0.24s$, $D = 0.0534puMW/Hz$, $R_D = R_K = 0.467Hz/puMW$, $\beta = 4.334puMW/Hz$ and $T_{gK} = T_{gD} = 11s$. System dynamic responses are obtained with optimal OFC gains for two different situations based on the two types of the present disturbances in the system. In the first situation, the effects of load disturbances in the area itself are examined, w_1 is taken as shown in Fig. 4.24(a) and $w_2 = 0$, whereas in the second situation, the effects of disturbances due to neighboring interconnected control areas are examined which affect the area under control, w_2 is taken

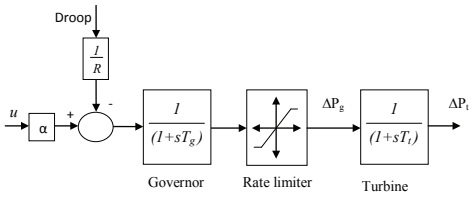

(a) Block diagram of a Genco

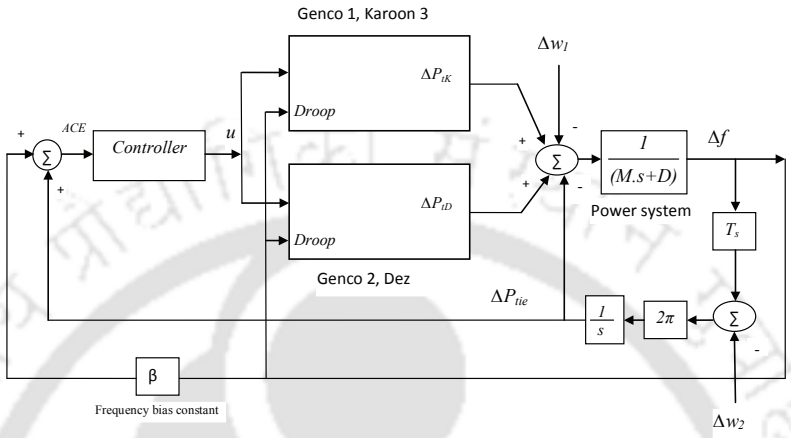

(b) Block diagram of a control area including two hydro power plants

Figure 4.23: Model of hydro power plants operational in KHOZESTAN (Iran), [1]

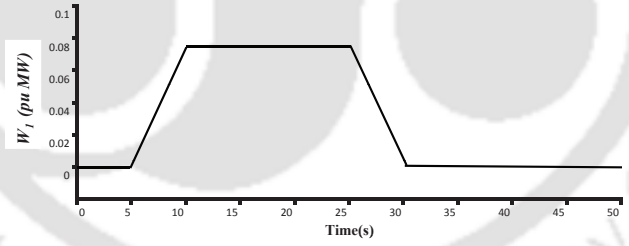

(a)

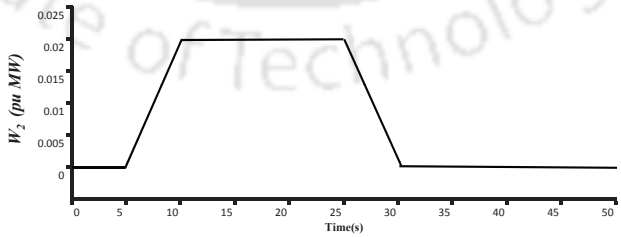

(b)

Figure 4.24: (a)Area load disturbance w_1, first situation (b) Disturbance due to neighboring interconnected control areas w_2, second situation [1]

as shown in Fig.4.24(b) and $w_1 = 0$. The load disturbance patterns taken in both the situations are reproduced from [1].

Fig. 4.25 shows the dynamic responses obtained using proposed OFC controller. As compared, the trajectories of deviation in frequency and tie line power are more and less same. Peak overshoots in frequency deviations observed at each time instant of load changes are improved remarkably and reduction is becoming more than 80%. The improvement in settling time is also observed.

Like MISO PID controller, the proposed controller also guarantees the good performance, such as frequency deviation elimination and disturbance attenuation as well as robustness under area load changes or frequency variation of interconnected areas scenarios. As compared, the peak overshoots in frequency deviation responses obtained with proposed controller are very less resulting in remarkable improvement in the frequency deviation response which is the most important parameter. It is observed that frequency and tie line power settles very fast with zero steady state error. Therefore, the proposed OFC controller satisfies the LFC requirements.

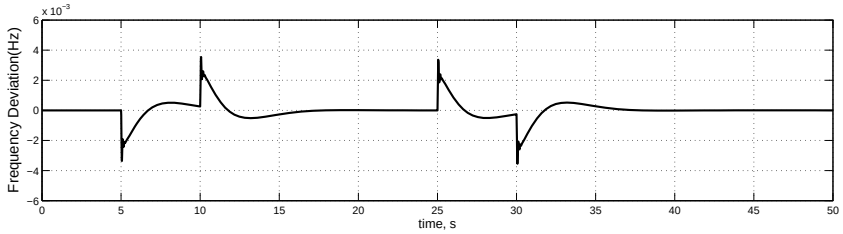

(a) Frequency deviation response for first situation

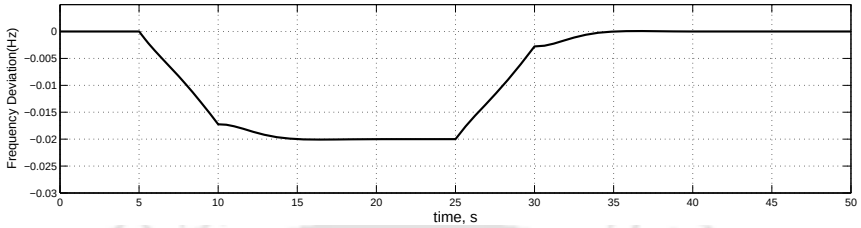

(b) Frequency deviation response for second situation

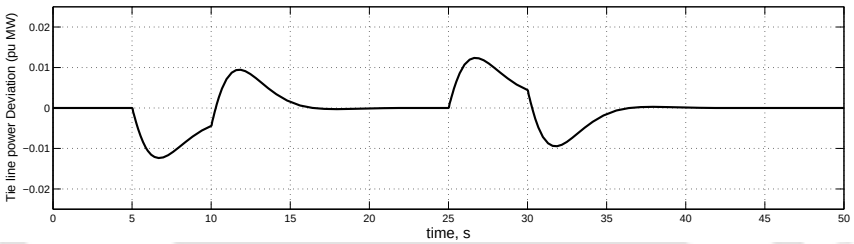

(c) Tie line Power deviation response for the first situation

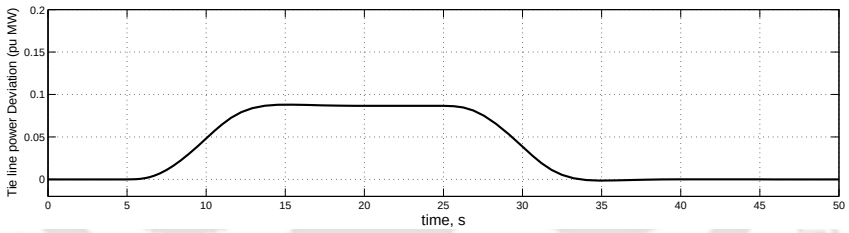

(d) Tie line Power deviation response for the second situation

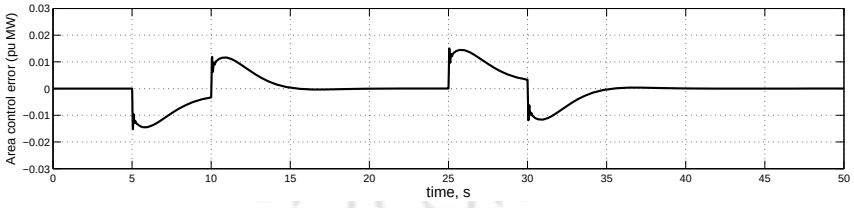

(e) Area control error for the first situation

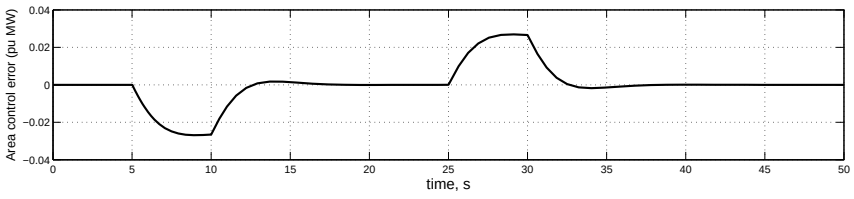

(f) Area control error for the second situation

Figure 4.25: Dynamic responses of hydro power plants operational in KHOZESTAN (Iran)

4.5 Summary

The performance of the proposed controller is demonstrated on the multi-source power systems and its dynamic responses are compared with FSFC. The OFC gives better dynamic response having relatively smaller peak overshoot and lesser settling time with zero steady state error as compared to that of FSFC. The effect of GRC on dynamic response is discussed. The critical examination of dynamic responses reveals that GRC results in increased peak overshoot, however settling time remains same for this particular power system model. Investigations reveal that it is better to prefer the medium value of R i.e. 4% with corresponding optimum controller gains to provide better dynamic response of LFC for the proposed system. The dynamic responses are obtained for 1% to 5% SLPs. It is observed that for SLP varying from 1% to 5%, the first peak overshoot increases with increase in the level of SLP and settling time remains approximately same with zero steady state error. The sensitivity analysis reveals that the optimum values of controller gains obtained for nominal system parameters and load condition are quite insensitive to wide parameter variation $\pm 25\%$. Hence for all practical purposes, the controller is quite robust. The LFC of hydro power plants operational in Iran has also been studied. The proposed controller performs well on this system and improves the frequency deviation responses remarkably. Like MISO PID controller, the proposed controller also guarantees the good performance, such as frequency deviation elimination and disturbance attenuation as well as robustness under area load changes or frequency variation of interconnected areas scenarios. The simulation results show that proposed control strategy is very effective and guarantees good performance. In fact, this method provides a control system that satisfies the load frequency control requirements with a credible dynamic response.

CHAPTER 5

LFC OF POWER SYSTEMS CONSIDERING AC-DC TIE LINES AND TCPS

5.1 Introduction

Electric power systems are interconnected to make the systems more reliable and robust. In a multi-area system, power generations and loads are coordinated with each other through the tie lines among the control areas [2, 10]. An electrical power system consists of many generating units and many loads while its total load demand varies continuously throughout the day. LFC is one of the important control problems in the interconnected power system design and operation, and is becoming more significant now due to the increasing size, changing structure, emerging multi-energy sources and new uncertainties, challenges, environmental constraints, and complexity of power systems [3, 6]. Literature survey shows that mostly AC tie lines are used for the interconnection of MAIPSs and lesser attention is given to AC-DC parallel tie lines [2, 32]. HVDC transmission system is finding more space in the transmission system due to its various techno-economical advantages. One of the major applications of HVDC transmission is operating a DC link in parallel with an AC link interconnecting two control areas to get an improved system dynamic performance with greater stability margins under small perturbations in the system [102, 103, 127, 128]. Some research work is reported on LFC of interconnected power systems connected via HVDC link in parallel with AC link [4, 127]. The idea of LFC of an interconnected power system with a DC tie line in parallel with an AC tie line [77, 102, 127, 128] is extended for the study of LFC of the TAIPS with MSPG as shown in Figs. 5.1 and 5.2.

The Flexible AC Transmission Systems (FACTS) devices provide more flexibility in power system operation and control. Thyristor controlled phase shifter (TCPS) is an effective FACTS device for the tie line power flow control of an interconnected power system. The TCPS device is modeled and used in series with tie lines to improve the dynamic performance of LFC of the interconnected power systems [106, 108].

Literature survey shows that most of the researchers applied optimal control theory on thermal-thermal power systems with AC tie lines only [8, 39, 49, 81, 114, 124]. Optimal controllers have been used in LFC as secondary controllers, but there is hardly any literature that compares performances of optimal controllers for the power system with and without DC tie lines [4]. Some researchers have studied the LFC of thermal-thermal or hydro-thermal power systems considering TCPS but there is hardly any research work that applies optimal OFC strategy for the LFC of the interconnected power systems with MSPG considering TCPS [4,93,106]. Therefore, there is a scope to study the LFC with MSPG and TCPS.

This chapter presents the LFC study of the interconnected power system considering AC-DC parallel tie line and TCPS. An attempt is made to improve the dynamical response of the LFC problem from a practical point of view by considering the OFC strategy using AC-DC parallel tie lines and TCPS. An extensive analysis is done to study the LFC performance of the OFC for the interconnected power system models in new power system environment considering AC-DC parallel tie lines and TCPS. In the section 5.2, a TAIPS model comprising hydro, thermal with reheat-turbine and gas units in each control area with AC-DC parallel tie line as shown in Fig. 5.2 is presented. HVDC link is connected in parallel with the existing AC link for stabilizing the frequency oscillations of AC system. Further in the section 5.3.2, a TAIPS model comprising hydro, thermal with reheat-turbine and gas units in each control area as shown in Fig. 5.7 is presented. TCPS is connected in series with the AC tie line for stabilizing the control area frequency and tie line power deviations [93, 106]. The power system simulation is done using MATLAB simulink and control problem is solved using MATLAB programming. The effect of the load disturbance by varying the SLP over a wide range from 1% to 4% is examined.

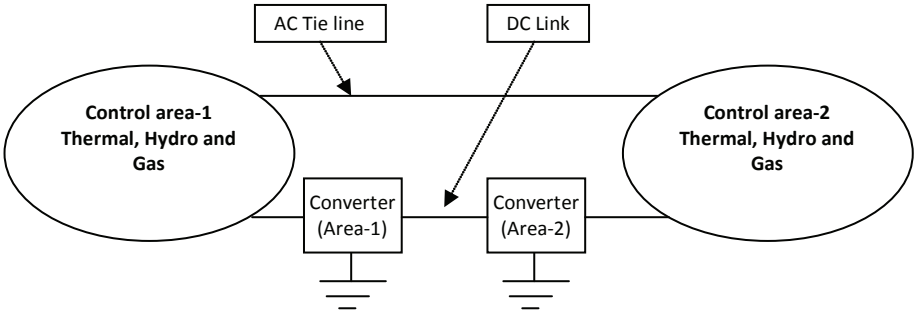

Figure 5.1: TAIPS with AC-DC parallel tie lines

5.2 Simulation of the power system with parallel AC-DC tie lines

The schematic of TAIPS model with AC-DC tie lines is shown in Fig. 5.1. The TAIPS with MSPG considering parallel AC-DC tie lines as shown in Fig. 5.2 is proposed for LFC study in this section. As shown in Fig. 5.2, each control area comprises reheat-thermal, hydro and gas generating units and the two equal areas are interconnected by AC-DC tie lines. The simulation of this interconnected power system in a new power system environment is based on the concepts of considering variety of generators with their corresponding generation contribution factors in each control area [6, 89, 117] and parallel AC-DC tie lines [77, 102]. The DC link is assumed bidirectional as most of the converters used for HVDC are intrinsically able to operate with power conversion in either direction. The system parameter values are given in Table 5.1. It is assumed that $R_{ki} = R_i$. For the TAIPS, $\Delta P_{tie,1} = \Delta P_{tie,12}$. The nominal loading of each control area is taken 1640 MW with the power generation scheduling and generation contribution factors as given in Table 5.2.

The state space form is obtained for the proposed power system model. The power system has 27 state variables. Incremental DC power flow is considered as an additional state variable in the LFC strategy. State variables x_1, x_{12}, x_{26} and x_{27} are taken as output feedback states. The state equations can be organized in the state-space form as described by the equations (2.52) and (2.38).

where, the associated vectors and matrices are as follows:

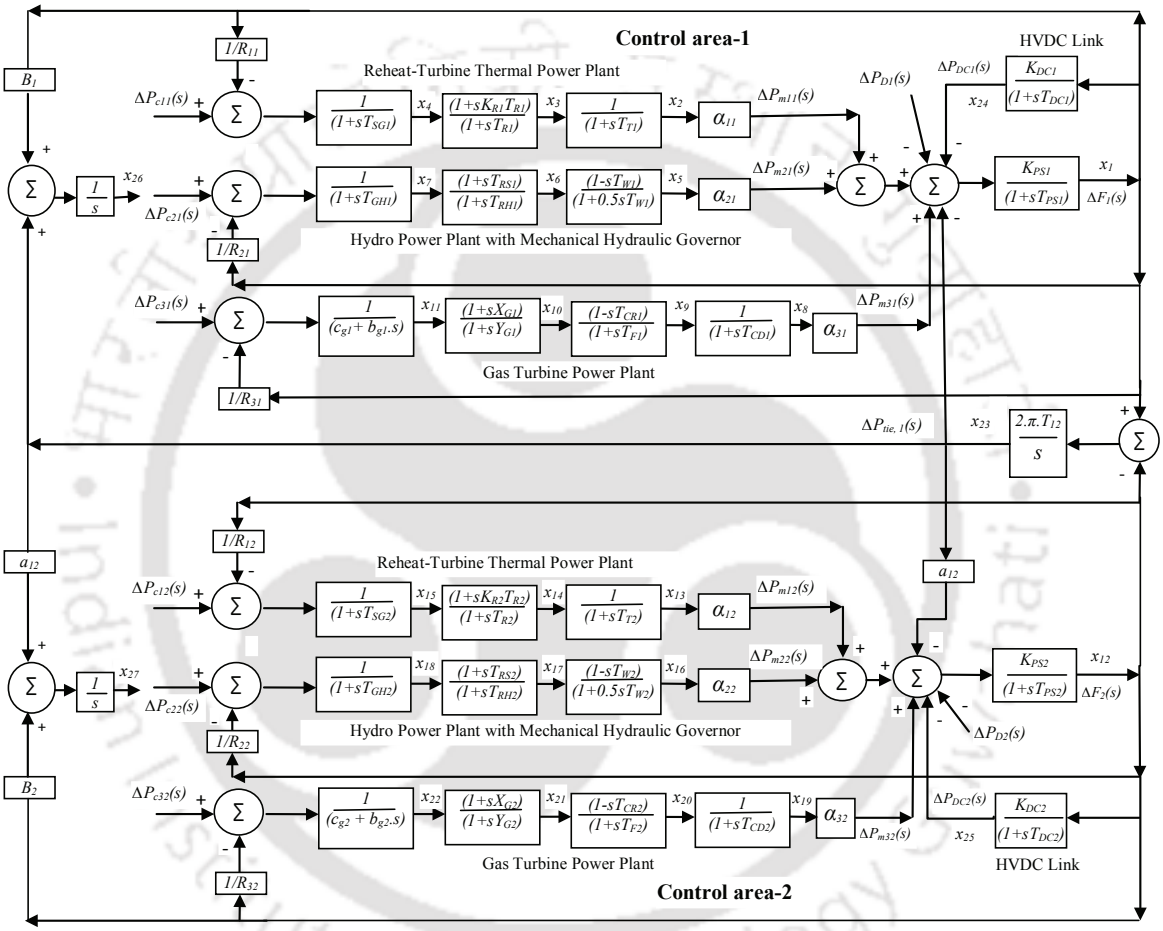

Figure 5.2: Block diagram of a TAIPS with MSPG considering AC-DC parallel tie lines

Table. 5.1: Simulation Parameters of TAIPS with MSPG considering parallel AC-DC tie lines

Parameters	Value
$P_{rt1} = P_{rt2}$	2000 MW
$P_{L1} = P_{L1}$	1640 MW
f	60 Hz
$H_1 = H_2$	5 MW-s/MVA
$D_1 = D_2$	0.0137 pu MW/Hz
$K_{PS1} = K_{PS2}$	73.1707 Hz/pu MW
T_{12}	0.0433
$T_{PS1} = T_{PS2}$	12.1951 s
$T_{SG1} = T_{SG2}$	0.08 s
$T_{T1} = T_{T2}$	0.3 s
$T_{CD1} = T_{CD2}$	0.2 s
$B_1 = B_2$	0.4303
a_{12}	- 1
$K_{R1} = K_{R2}$	0.3
$T_{R1} = T_{R2}$	10 s
$T_{W1} = T_{W2}$	1 s
$T_{RS1} = T_{RS2}$	5 s
$T_{RH1} = T_{RH2}$	28.75 s
$T_{GH1} = T_{GH2}$	0.2 s
$X_{G1} = X_{G2}$	0.6 s
$Y_{G1} = Y_{G2}$	1 s
$c_{g1} = c_{g2}$	1
$b_{g1} = c_{g1}$	0.05 s
$T_{F1} = T_{F2}$	0.23 s
$T_{CR1} = T_{CR2}$	0.01s
$R_1 = R_2$	2.4 Hz/pu MW
$\alpha_{11} = \alpha_{12}$	0.579268
$\alpha_{21} = \alpha_{22}$	0.274390
$\alpha_{31} = \alpha_{32}$	0.146342
DC link parameters	
$K_{DC1} = K_{DC2}$	1
$T_{DC1} = T_{DC2}$	0.2 s

state vector, $x = [x_1\ x_2 \ldots\ldots x_{27}]^T$

control vector, $u = [u_1\ u_2\ u_3\ u_4\ u_5\ u_6]^T = [\Delta P_{c11}\ \Delta P_{c21}\ \Delta P_{c31}\ \Delta P_{c12}\ \Delta P_{c22}\ \Delta P_{c32}]^T$

disturbance vector, $w = [w_1\ w_2]^T = [\Delta P_{D1}\ \Delta P_{D2}]^T$.

and the constant matrices $\tilde{A}$, $\tilde{B}$ and $\tilde{C}$, the disturbance matrix $\tilde{F}$ and design matrices $\tilde{Q}$ and $\tilde{R}$ are given in Appendix A.2.

The optimum gains of optimal OFC are obtained by running the MATLAB codes generated on the basis of method described in section 2.6. The computer simulations are carried out

with the optimum controller gain settings. MATLAB control system toolbox [121] is used to simulate the power system and to obtain dynamic responses of the system for 1% SLP in the control area-1.

5.2.1 Simulation results and discussion

The optimum values of the $\tilde{K}$ for the OFC by minimizing the cost function for the power system with AC tie line corresponding to nominal system parameters is

$$\tilde{K} = \begin{bmatrix} 0.4202 & -0.0936 & 0.3233 & 0.0808 \\ -0.1634 & -0.0039 & -0.0386 & -0.0522 \\ 0.1622 & -0.0597 & 0.1340 & 0.0207 \\ 0.0719 & 0.8219 & -0.1455 & 0.3840 \\ -0.0469 & -0.6530 & -0.1181 & -0.4162 \\ 0.0473 & 0.3588 & -0.0074 & 0.2008 \end{bmatrix}$$

and for the power system with AC-DC parallel tie line is

$$\tilde{K} = \begin{bmatrix} -0.1887 & 0.5428 & 0.5702 & 0.2080 \\ -0.0644 & 0.1023 & 0.0895 & 0.0568 \\ -0.1082 & 0.2338 & 0.2685 & 0.0629 \\ 0.4622 & -0.0495 & 0.2321 & 0.3059 \\ -0.2360 & 0.1406 & -0.0580 & -0.3128 \\ 0.2028 & -0.0828 & 0.0784 & 0.1894 \end{bmatrix}$$

Dynamic responses of the system are obtained for 1% SLP in the control area-1. The frequency deviation responses of control area-1 and control area-2 are shown in Figs. 5.3 and 5.4, respectively. The tie line power deviation response is shown in Fig. 5.5. It is observed that the OFC considering parallel AC-DC tie lines in power system gives better dynamic responses having relatively smaller peak overshoot and lesser settling time with zero steady state error as compared to the power system with AC tie lines only. The quantitative comparison is made in Table 5.3 where percentage reduction in the peak OS of Δf_1, Δf_2 and $\Delta P_{tie,1}$ is 60.49, 90 and 44.92, respectively with DC link. Also, system dynamic responses are obtained for the wide range of SLP varying from 1% to 4% in either control area. Further, frequency deviation and tie line power responses for different SLPs are shown in Fig. 5.6. It is apparent that for SLP varying from 1% to 4%, the first peak overshoot increases with increase in the level of SLP and settling time remains approximately same with zero steady state error. Thus, the proposed

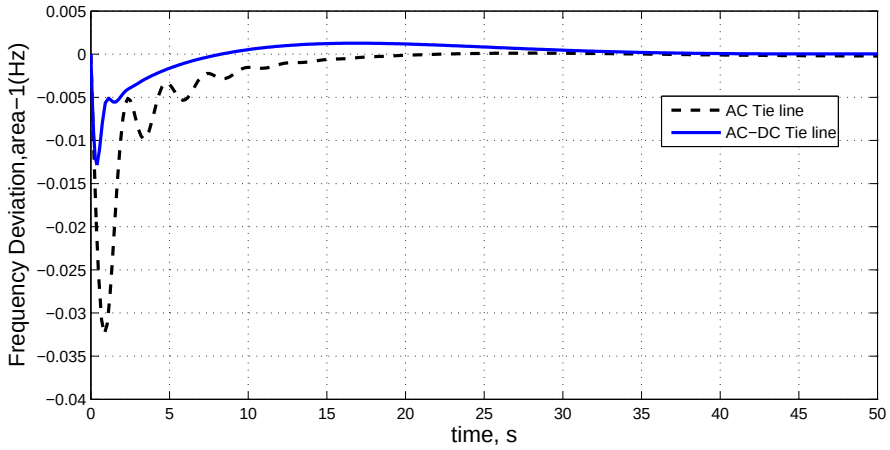

Figure 5.3: Frequency deviation response of control area-1 with AC tie line and AC-DC parallel tie line

controller satisfy the LFC problem requirement for wide variation of load disturbance.

Table. 5.2: Power Generation Scheduling to match the nominal load of the individual control area

Total control area load (MW)	Thermal contribution (MW)	Gas contribution (MW)	Hydro contribution (MW)
1640	950	240	450
Generation contribution factor	0.579268	0.146342	0.274390

Table. 5.3: Dynamic response comparison

	Peak OS of Δf_1(Hz)	Peak OS of Δf_1(Hz)	Peak OS of $\Delta P_{tie,1}$(pu MW)
With AC tie line	-0.0324	-0.0230	-0.0069
With AC-DC tie line	-0.0128	-0.0023	-0.0038
% reduction in Peak OS	60.49	90	44.92

5.3 Incremental tie line power flow considering TCPS

TCPS is a device that changes the relative phase angle between the system voltages. The tie line power flow can be regulated by controlling the phase angle (ϕ) to damp out the control area frequency deviations and improve power system stability [94, 108, 109]. The schematic of the TAIPS considering a TCPS in series with the tie line is shown in Fig. 5.8.

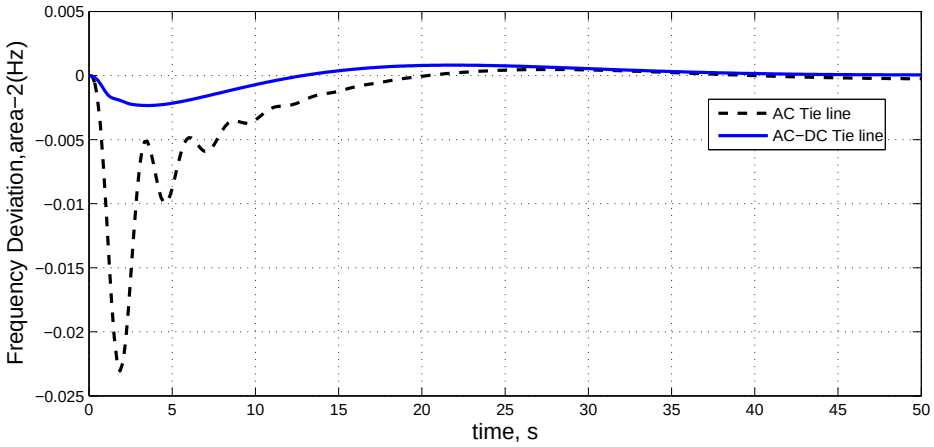

Figure 5.4: Frequency deviation response of control area-2 with AC tie line and AC-DC parallel tie line

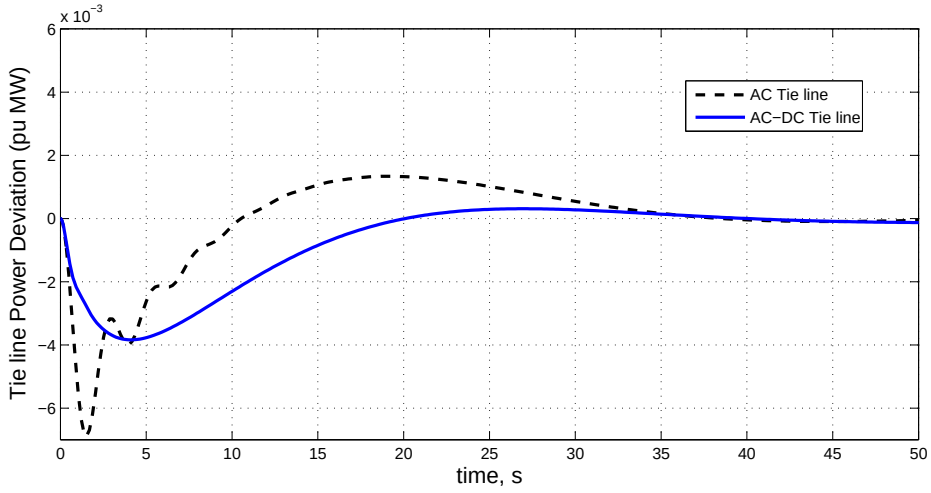

Figure 5.5: Tie line power deviation response with AC tie line and AC-DC parallel tie line

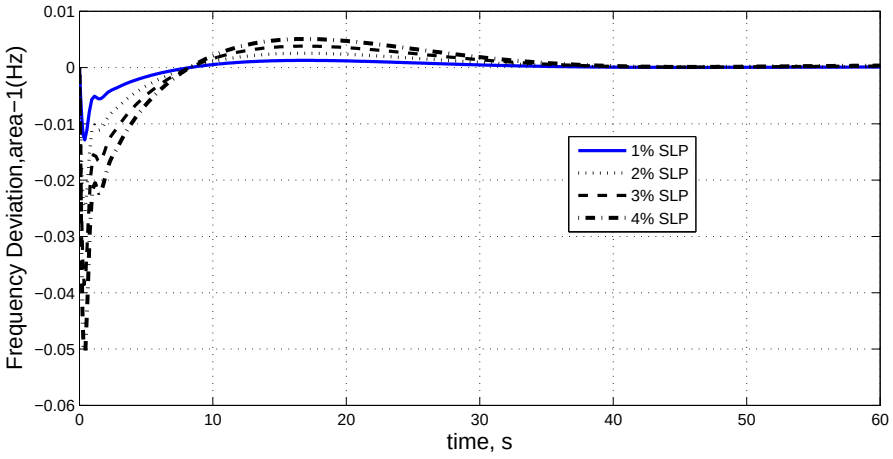

(a) Frequency deviation response of control area-1

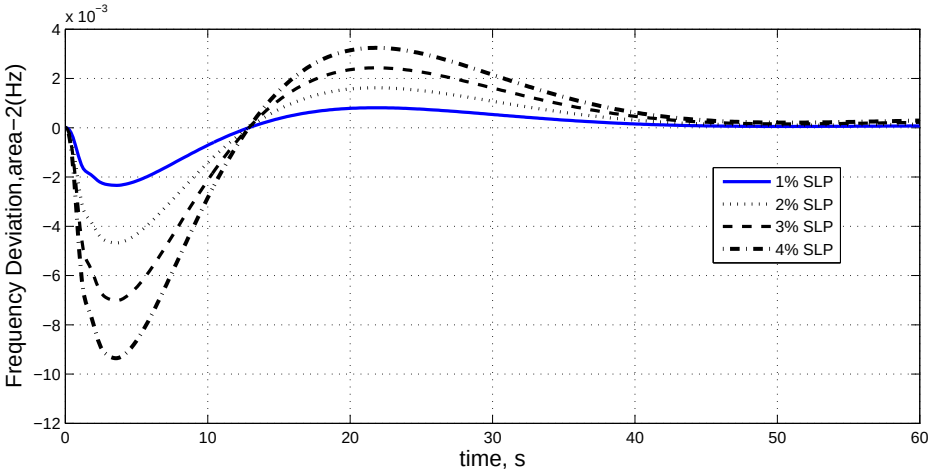

(b) Frequency deviation response of control area-2

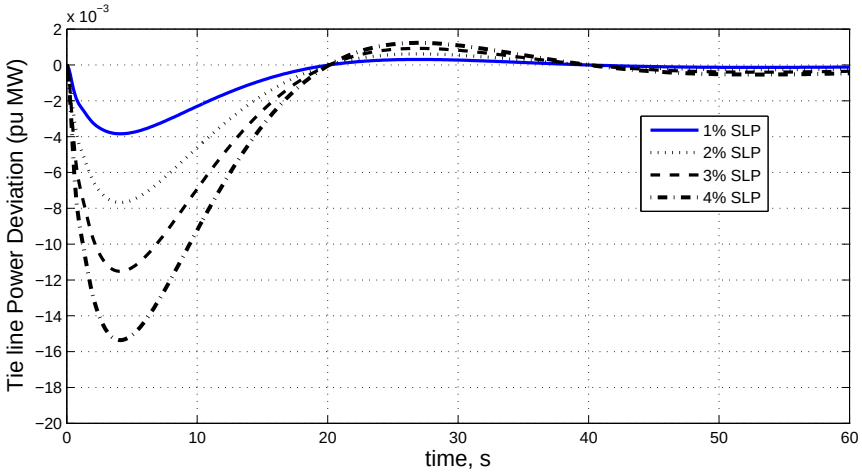

(c) Tie line power deviation response

Figure 5.6: Frequency deviation and tie line power responses for SLP varying from 1% to 4%

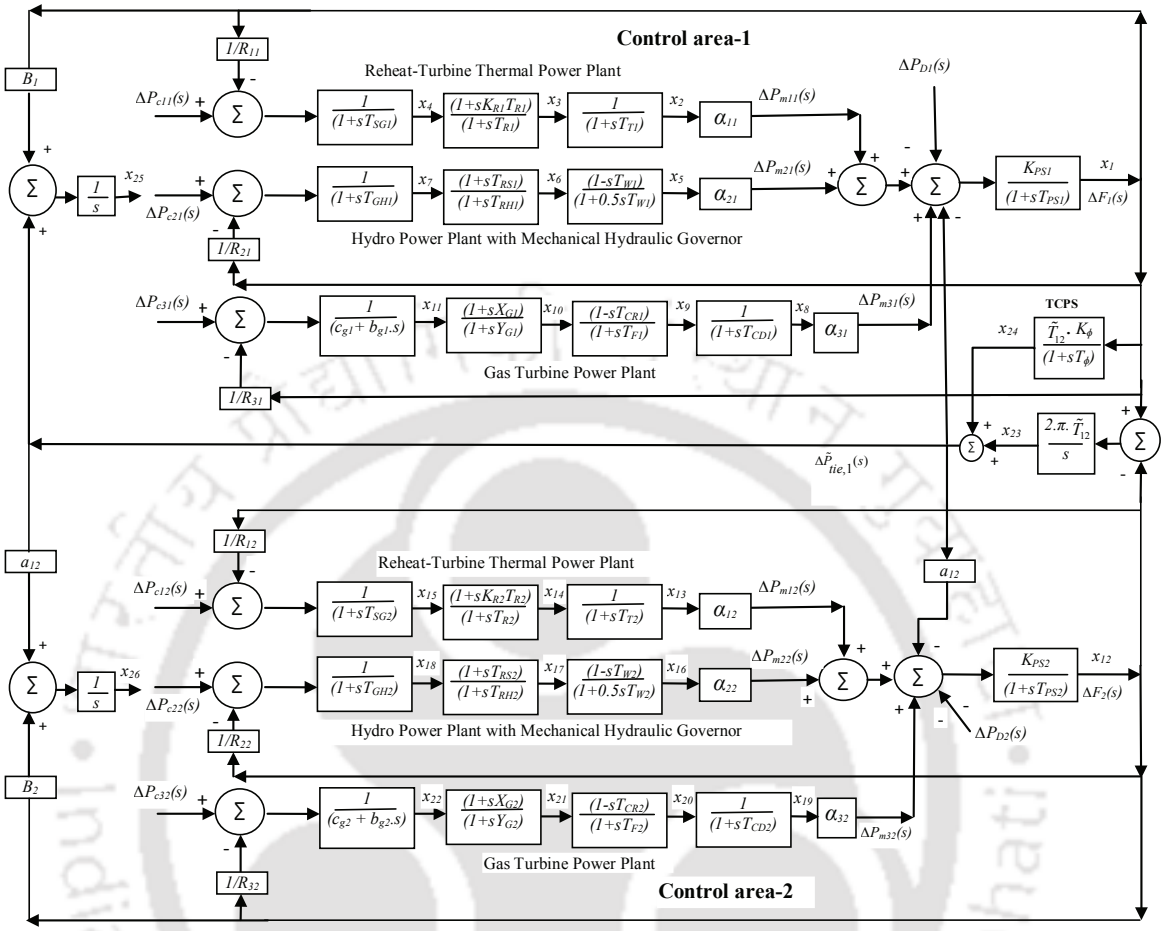

Figure 5.7: TAIPS with MSPG considering TCPS

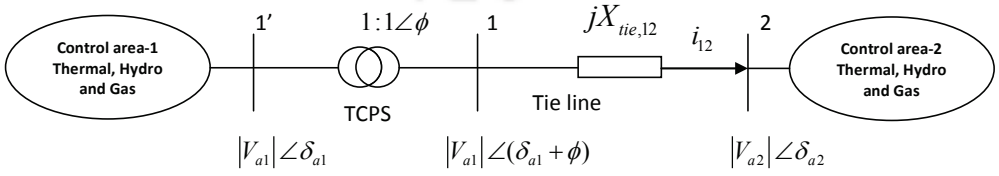

Figure 5.8: Schematic of TAIPS considering TCPS in series with tie line

In a conventional interconnected power system, the incremental tie line power flow $\Delta P_{tie,12}$ from control area-1 to control area-2 can be expressed as [2]

$$\Delta P_{tie,12}(s) = \frac{2\pi T_{12}}{s}\left(\Delta F_1(s) - \Delta F_2(s)\right) \tag{5.1}$$

When a TCPS is connected in series with the tie line as shown in Fig. 5.8, the current flowing from control area 1 to control area 2 can be expressed [109] as

$$i_{12} = \frac{|V_{a1}|\angle(\delta_{a1}+\phi) - |V_{a2}|\angle\delta_{a2}}{jX_{tie,12}} \tag{5.2}$$

Now, the tie line power becomes

$$\tilde{P}_{tie,12} - j\tilde{Q}_{tie,12} = \left[|V_{a1}|\angle -(\delta_{a1}+\phi)\right] i_{12} \tag{5.3}$$

Using equations (5.2) and (5.3) and separating the real and imaginary parts, $\tilde{P}_{tie,12}$ becomes

$$\tilde{P}_{tie,12} = \frac{|V_{a1}||V_{a2}|}{X_{tie,12}}\sin(\delta_{a1} - \delta_{a2} + \phi) \tag{5.4}$$

Perturbing δ_{a1}, δ_{a2} and ϕ from their nominal values δ_{a1}^0, δ_{a2}^0 and ϕ^0, respectively,

$$\Delta\tilde{P}_{tie,12} = \frac{|V_{a1}||V_{a2}|}{X_{tie,12}}\cos(\delta_{a1}^0 - \delta_{a2}^0 + \phi^0)\sin(\Delta\delta_{a1} - \Delta\delta_{a2} + \Delta\phi) \tag{5.5}$$

Since $(\Delta\delta_{a1} - \Delta\delta_{a2} + \Delta\phi)$ is very small, therefore

$$\sin(\Delta\delta_{a1} - \Delta\delta_{a2} + \Delta\phi) \approx (\Delta\delta_{a1} - \Delta\delta_{a2} + \Delta\phi)$$

$$\Delta\tilde{P}_{tie,12} = \frac{|V_{a1}||V_{a2}|}{X_{tie,12}}\cos(\delta_{a1}^0 - \delta_{a2}^0 + \phi^0)(\Delta\delta_{a1} - \Delta\delta_{a2} + \Delta\phi) \tag{5.6}$$

Let $\tilde{T}_{12}$ be the synchronizing coefficient with TCPS:

$$\tilde{T}_{12} = \frac{|V_{a1}||V_{a2}|}{X_{tie,12}}\cos(\delta_{a1}^0 - \delta_{a2}^0 + \phi^0) \tag{5.7}$$

$\Delta\tilde{P}_{tie,12}$ can be given as

$$\Delta\tilde{P}_{tie,12} = \tilde{T}_{12}(\Delta\delta_{a1} - \Delta\delta_{a2}) + \tilde{T}_{12}\Delta\phi \tag{5.8}$$

where,

$\Delta\delta_{a1} = 2\pi\int_0^t \Delta f_1 dt$ and $\Delta\delta_{a2} = 2\pi\int_0^t \Delta f_2 dt$

Taking the Laplace transform of equation (5.8)

$$\Delta\tilde{P}_{tie,12}(s) = \frac{2\pi\tilde{T}_{12}}{s}\left[\Delta F_1(s) - \Delta F_2(s)\right] + \tilde{T}_{12}\Delta\phi(s) \tag{5.9}$$

As given in equation (5.9) tie line power flow can be controlled by controlling the phase shifter angle $\Delta\phi$. The phase shifter angle $\Delta\phi$ can be given [107, 108] as

$$\Delta\phi(s) = \frac{K_\Phi}{(1+sT_\Phi)}\Delta Error(s) \tag{5.10}$$

where, K_Φ and T_Φ are gain constant and time constant of TCPS.

5.3.1 TCPS control strategy

Error signal to TCPS can be any signal such as the control area frequency deviation or area control error to control the TCPS phase shifter angle. If the frequency deviation of control area-1 is sensed as error signal, it can be used as the control signal to the TCPS unit to control the TCPS phase shifter angle which results in controlling the tie line power flow [107, 108]. Thus,

$$\Delta\phi(s) = \frac{K_\Phi}{(1+sT_\Phi)}\Delta F_1(s) \tag{5.11}$$

and

$$\Delta\tilde{P}_{tie,12}(s) = \frac{2\pi\tilde{T}_{12}}{s}\left[\Delta F_1(s) - \Delta F_2(s)\right] + \tilde{T}_{12}\frac{K_\Phi}{(1+sT_\Phi)}\Delta F_1(s) \tag{5.12}$$

The total incremental tie line power flow between control area-1 and other control areas, $\Delta\tilde{P}_{tie,1}(s)$ may be given as:

$$\Delta\tilde{P}_{tie,1}(s) = \Delta\tilde{P}_{tie,12}(s) \tag{5.13}$$

5.3.2 Simulation of the power system model considering TCPS

The TAIPS model with MSPG considering TCPS is shown in Fig. 5.7, where each control area comprises reheat-thermal, hydro and gas generating units and the two equal areas are interconnected. The simulation of this interconnected power system in a new power system environment is based on the concepts of considering variety of generators with their corresponding generation contribution factors in each control area [6, 89, 117] and TCPS [108, 109]. The system parameter values are given in Tabel 5.4 . It is assumed that $R_{ki} = R_i$. The nominal loading of each control area is taken 1640 MW with the power generation scheduling and generation contribution factors as given in Table 5.5.

Table. 5.4: Simulation Parameters of TAIPS model with MSPG considering TCPS

Parameters	Value
$P_{rt1} = P_{rt2}$	2000 MW
$P_{L1} = P_{L1}$	1640 MW
f	60 Hz
$H_1 = H_2$	5 MW-s/MVA
$D_1 = D_2$	0.0137 pu MW/Hz
$K_{PS1} = K_{PS2}$	73.1707 Hz/pu MW
$\tilde{T}_{12}$	0.0433
$T_{PS1} = T_{PS2}$	12.1951 s
$T_{SG1} = T_{SG2}$	0.08 s
$T_{T1} = T_{T2}$	0.3 s
$T_{CD1} = T_{CD2}$	0.2 s
$B_1 = B_2$	0.4303
a_{12}	- 1
$K_{R1} = K_{R2}$	0.3
$T_{R1} = T_{R2}$	10 s
$T_{W1} = T_{W2}$	1 s
$T_{RS1} = T_{RS2}$	5 s
$T_{RH1} = T_{RH2}$	28.75 s
$T_{GH1} = T_{GH2}$	0.2 s
$X_{G1} = X_{G2}$	0.6 s
$Y_{G1} = Y_{G2}$	1 s
$c_{g1} = c_{g2}$	1
$b_{g1} = c_{g1}$	0.05 s
$T_{F1} = T_{F2}$	0.23 s
$T_{CR1} = T_{CR2}$	0.01s
$R_1 = R_2$	2.4 Hz/pu MW
$\alpha_{11} = \alpha_{12}$	0.579268
$\alpha_{21} = \alpha_{22}$	0.274390
$\alpha_{31} = \alpha_{32}$	0.146342
TCPS parameters	
K_Φ = 1.5 rad/Hz	T_Φ = 0.1 s
$\Phi_{max} = 10^0$	$\Phi_{min} = -10^0$

The state space form is obtained for the proposed power system model. The power system has 26 state variables. State variables x_1, x_{12}, x_{25} and x_{26} are taken as output feedback states. The state equations can be organized in the state-space form as described by the equations (2.52) and 2.38.

where, the associated vectors and matrices are as follows:

state vector, $x = [x_1\ x_2 \ldots\ldots x_{26}]^T$

control vector, $u = [u_1\ u_2\ u_3\ u_4\ u_5\ u_6]^T = [\Delta P_{c11}\ \Delta P_{c21}\ \Delta P_{c31}\ \Delta P_{c12}\ \Delta P_{c22}\ \Delta P_{c32}]^T$

disturbance vector, $w = [w_1\ w_2]^T = [\Delta P_{D1}\ \Delta P_{D2}]^T$.

and the constant matrices $\tilde{A}$, $\tilde{B}$ and $\tilde{C}$, the disturbance matrix $\tilde{F}$ and design matrices $\tilde{Q}$ and $\tilde{R}$ are given in Appendix A.3.

The optimum gains of optimal OFC are obtained by running the MATLAB codes generated on the basis of method described in section 2.6. The computer simulations are carried out with the optimum controller gain settings. MATLAB control system toolbox [121] is used to simulate the power system and to obtain dynamic responses of the system for 1% SLP in the control area-1.

5.3.3 Simulation results and discussion

The optimum value of the $\tilde{K}$ for the OFC by minimizing the cost function for the power system corresponding to nominal system parameters is

$$\tilde{K} = \begin{bmatrix} 0.4202 & -0.0936 & 0.3233 & 0.0808 \\ -0.1634 & -0.0039 & -0.0386 & -0.0522 \\ 0.1622 & -0.0597 & 0.1340 & 0.0207 \\ 0.0719 & 0.8219 & -0.1455 & 0.3840 \\ -0.0469 & -0.6530 & -0.1181 & -0.4162 \\ 0.0473 & 0.3588 & -0.0074 & 0.2008 \end{bmatrix}$$

and for the power system with TCPS is

$$\tilde{K} = \begin{bmatrix} 1.4167 & -0.3404 & 5.8889 & -0.5138 \\ -0.3702 & 0.0300 & -1.1732 & 0.1551 \\ 0.4758 & -0.2213 & 2.1480 & -0.2559 \\ 0.0619 & 0.4614 & 0.5985 & 0.5440 \\ -0.3225 & -0.5033 & -1.5146 & -0.2861 \\ -0.0260 & 0.0202 & 0.1433 & 0.0902 \end{bmatrix}$$

Dynamic responses of the system are obtained for 1% SLP in the control area-1. The frequency deviation responses of control area-1 and control area-2 are shown in Figs.5.9 and 5.10, respectively. The tie line power deviation response is shown in Fig. 5.11. It is observed that the OFC considering TCPS in power system gives better dynamic responses having relatively smaller peak overshoot and lesser settling time with zero steady state error as compared to the power system without TCPS. The quantitative comparison is made in Tables 5.6 and 5.7 where percentage reduction in the peak OS of Δf_1, Δf_2 and $\Delta \tilde{P}_{tie,1}$ becoming 34.56, 50 and 39.13, respectively and the settling time of Δf_1, Δf_2 and $\Delta \tilde{P}_{tie,1}$ becoming 41.61, 54.89 and 53.10, respectively. The phase angle deviation of TCPS in response to 1% SLP in control area-1 is shown in Fig. 5.12, where maximum phase angle deviation on positive side is 1.32^0 and on negative side is 1.78^0. Further, system dynamic responses are obtained for the wide range of SLP varying from 1% to 4% in either control area and shown in Fig. 5.13. It is evident that for SLP varying from 1% to 4%, the first peak overshoot increases with increase in the level of SLP and settling time remains approximately same with zero steady state error. The dynamic responses are improved with TCPS and satisfy the LFC requirements.

Table. 5.5: Power Generation Scheduling to match the nominal load of the individual control area

Total control area load (MW)	Thermal contribution (MW)	Gas contribution (MW)	Hydro contribution (MW)
1640	950	240	450
Generation contribution factor	0.579268	0.146342	0.274390

Table. 5.6: Dynamic response comparison in terms of peak OS

	Peak OS of Δf_1(Hz)	Peak OS of Δf_1(Hz)	Peak OS of $\Delta \tilde{P}_{tie,1}$(pu MW)
Without TCPS	-0.0324	-0.0230	-0.0069
With TCPS	-0.0212	-0.0115	-0.0042
% reduction in Peak OS	34.56	50	39.13

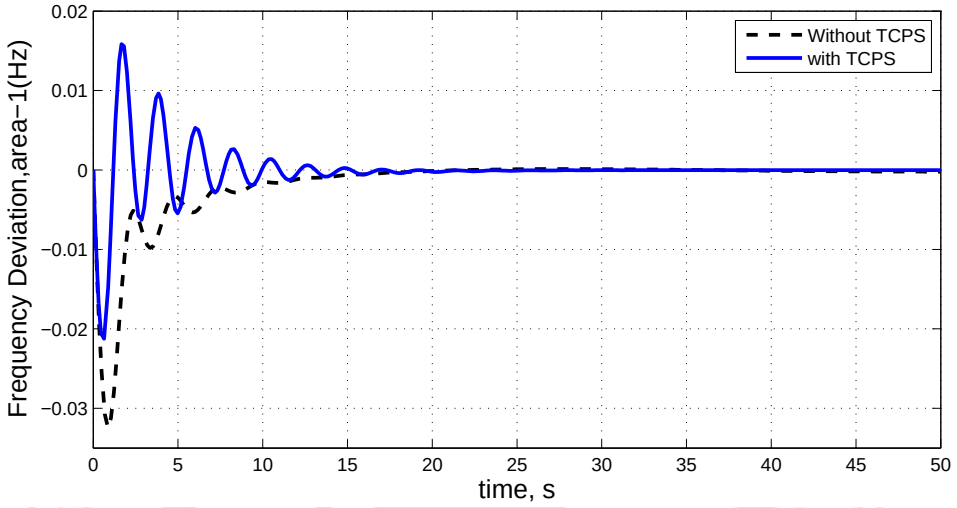

Figure 5.9: Frequency deviation response of control area-1

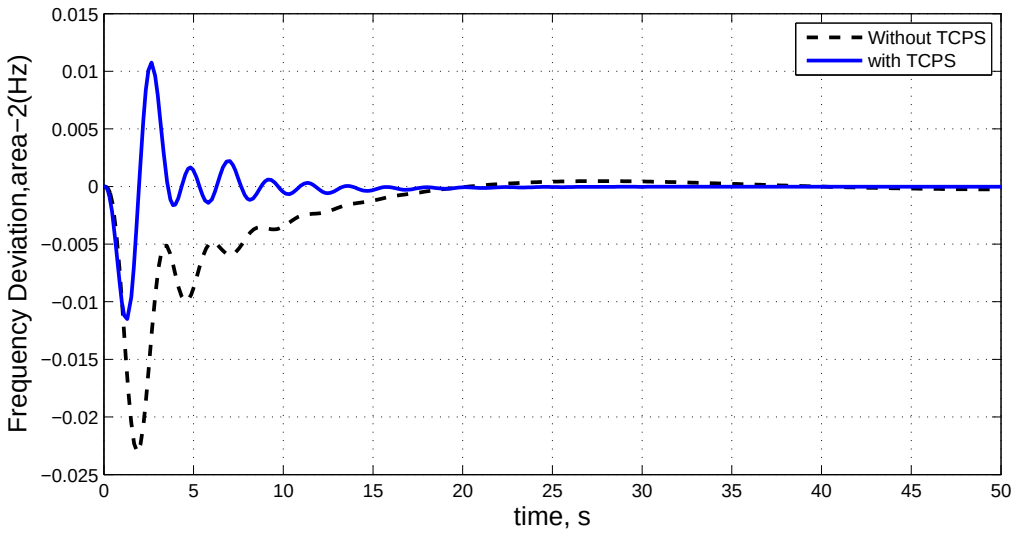

Figure 5.10: Frequency deviation response of control area-2

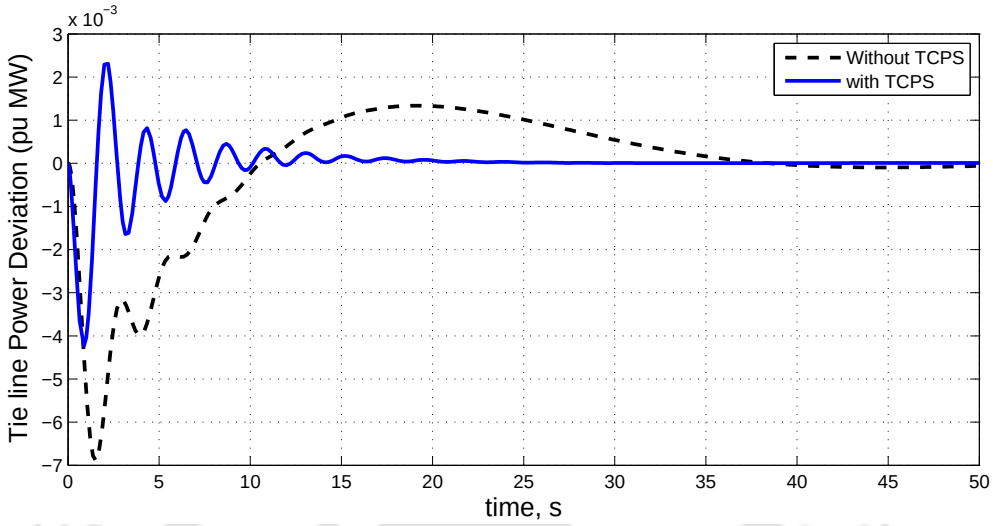

Figure 5.11: Tie line power deviation response

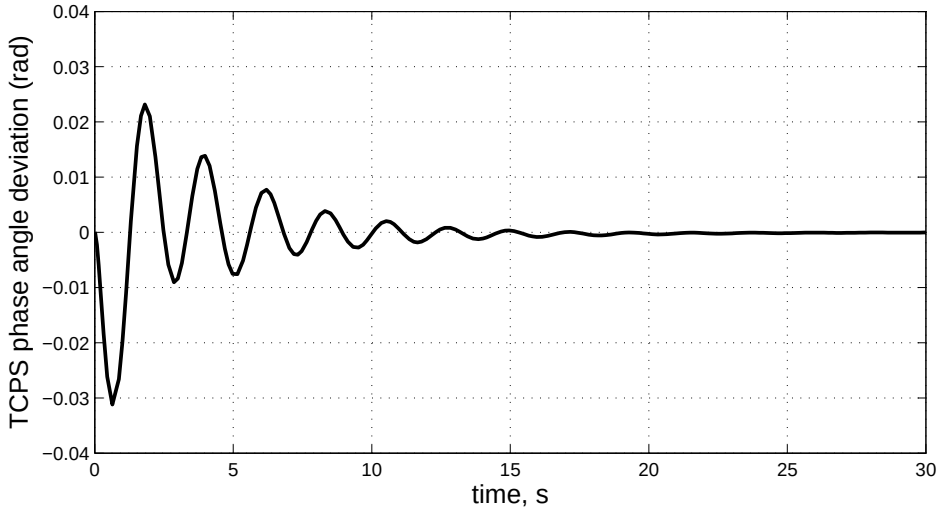

Figure 5.12: TCPS phase shift deviation response

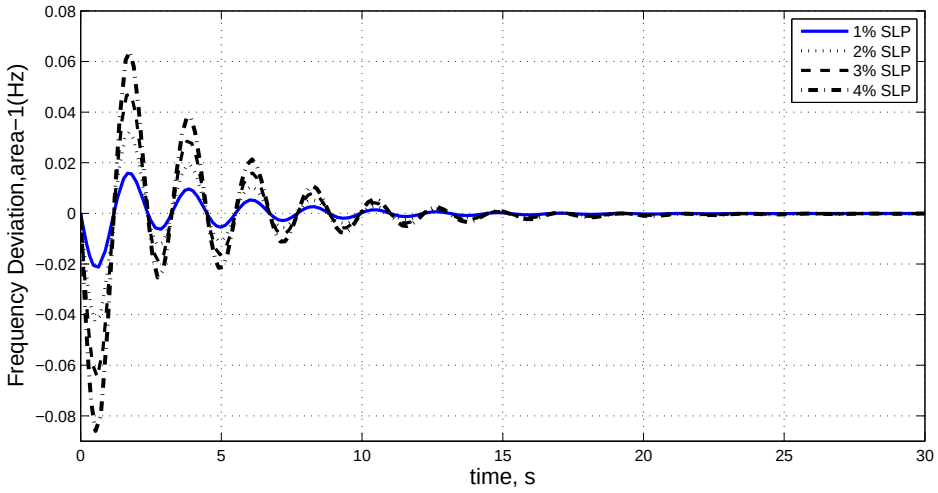

(a) Frequency deviation response of control area-1

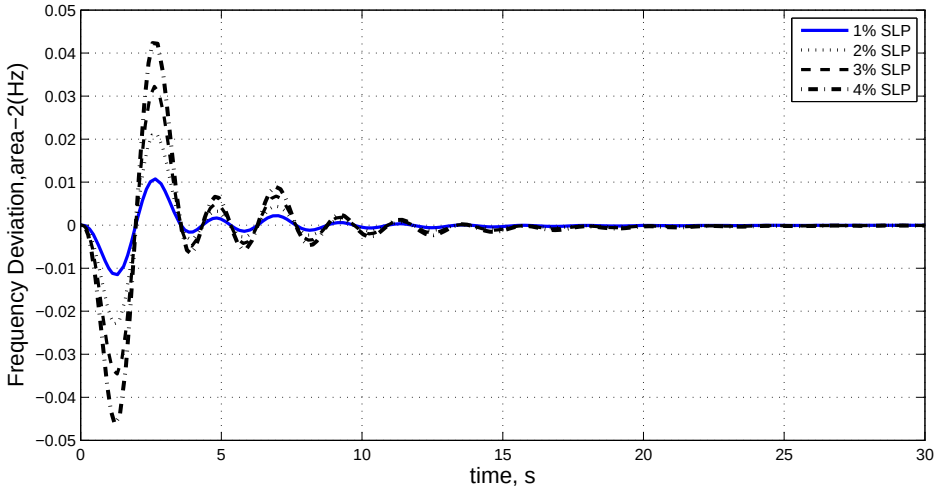

(b) Frequency deviation response of control area-2

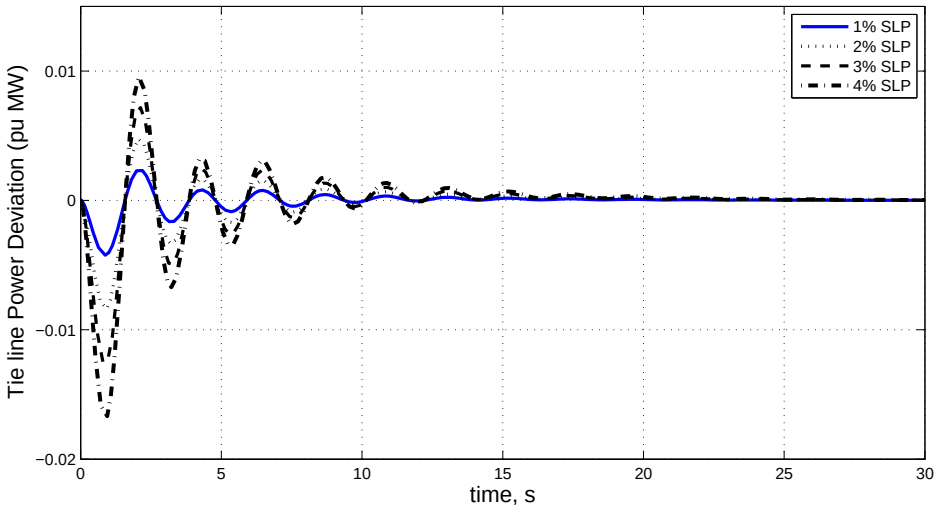

(c) Tie line power deviation response

Figure 5.13: Frequency deviation and tie line power responses for SLP varying from 1% to 4%

Table. 5.7: Dynamic response comparison in terms of ST

	ST of Δf_1(s)	ST of Δf_1(s)	ST of $\Delta\tilde{P}_{tie,1}$(s)
Without TCPS	32.27	40.26	49.37
With TCPS	18.84	18.16	23.15
% reduction in ST	41.61	54.89	53.10

5.4 Summary

An attempt is made in this chapter to study the the dynamic performance of LFC of the power systems considering AC-DC tie lines and TCPS. A simple but practical controller is used to improve the dynamic response of LFC system in the the new power system environment. The OFC performs well for the power system with DC link giving better dynamic response having relatively smaller peak overshoot and lesser settling time with zero steady state error as compared to the power system considering AC tie lines only. The dynamic response of the system with DC link is improved significantly with the percentage reduction in the peak OS of Δf_1, Δf_2 and $\Delta P_{tie,1}$ becoming 60.49, 90 and 44.92, respectively. Dynamic responses are obtained for wide range of variation in SLP from 1% to 4% which satisfy the LFC requirements. The simulation results show that proposed control strategy considering parallel AC-DC tie line is very effective and guarantees good performance. Further, the OFC is proposed to control the TCPS phase angle which in turn controls the tie line power flow. The proposed controller for the power system with TCPS gives better dynamic responses having relatively smaller peak overshoot and lesser settling time with zero steady state error as compared to the power system without TCPS. The dynamic responses of the system with TCPS are improved significantly with the percentage reduction in the peak OS of Δf_1, Δf_2 and $\Delta\tilde{P}_{tie,1}$ becoming 34.56, 50 and 39.13, respectively and the settling time of Δf_1, Δf_2 and $\Delta\tilde{P}_{tie,1}$ becoming 41.61, 54.89 and 53.10, respectively. Dynamic responses are obtained for wide range of variation in load disturbance from 1% to 4% which satisfy the LFC requirements. Simulation results show that the due to the presence of TCPS, the dynamic performance in terms of settling time and peak overshoot is greatly improved. The system with TCPS is capable of suppressing the control area frequency and tie line power deviations more effectively under the occurrence of control area load perturbations. The simulation results show that proposed control strategy considering TCPS is very effective and

guarantees good performance. Hence for all practical purposes, the controller is quite robust.

CHAPTER 6

LFC IN RESTRUCTURED POWER SYSTEM ENVIRONMENT

6.1 Introduction

LFC is one of the important control problems in electric power system design and operation. Any deviations in frequency can directly impact on power system operation and system reliability. A large frequency deviation can cause an unstable condition for the power system. Maintaining frequency and tie line power interchanges with neighboring control areas at the scheduled values are the two main primary objectives of a power system LFC [2–4, 90]. Many researchers presented the LFC scheme of conventional power system using different control strategies [1, 9, 13, 90–94, 108, 124].

In the restructured power system environment, vertically integrated system of conventional power system do not exist [20]. In a competitive electricity market, generating companies (GENCOs), distribution companies (DISCOs), transmission companies (TRANSCOs), and power system operator (PSO) [5, 6, 11, 18, 19, 84] are all market players. As there are so many GENCOs and DISCOs in the restructured power system, a DISCO has the freedom to have a contract with any GENCOs for the transaction of power. A DISCO of one control area can make contract with a GENCO in another control area [19, 20]. For stable and secure operation of a power system, the PSO has to provide a number of ancillary services. One of the ancillary services is the frequency regulation based on the concept of the LFC. The crucial role of LFC system will continue in restructured power system environment with some modifications accounting

bilateral transactions and deregulation policy [5].

An LFC system required for Poolco-based transactions described in [20, 112] utilizes an integral controller. A method to find optimal controller gains of this type of controller for a two-area system is proposed in [20]. In [115], B. Tyagi et. al proposed a general model for multi-area LFC suitable for a competitive electricity environment. LFC work in restructured power system is reported in [5, 11, 18–20, 84, 100] where they have considered either thermal or hydro system in a control area. In new power system environment, a control area may have variety of sources like hydro, thermal, gas, renewable etc., therefore representing a control area by thermal or hydro system dynamics only may not result in a good design of LFC system [5,89,90]. Recently some researchers studied the LFC of conventional power system considering hydro, thermal and gas generating units in each control area [89, 90, 116, 117], however they did not consider the LFC scheme in restructured power system environment.

Having studied the LFC scheme in conventional power systems with optimal OFC in the previous chapters, LFC scheme is presented in restructured power system environment. A TAIPS with MSPG is proposed for LFC in restructured power system environment. Each control area includes the more feasible multi-source combination of hydro, reheat thermal and gas generating units. An extensive analysis is done for LFC scheme considering Poolco-based transactions, bilateral transactions, and a combination of these two transactions. The MATLAB simulation results are authenticated by comparing with calculated(desired) values. A state space model of the proposed power system in restructured power system environment is utilized for controller design considering all the interface variables like control area frequencies, tie line power and all other possible contracts between GENCOs and DISCOs. In this chapter, it is established that the optimal OFC performs well in restructured power system environment also.

6.2 LFC in restructured power system environment

The LFC in a restructured power market should be designed to accommodate all possible transactions [20, 112], such as Poolco-based transactions, bilateral transactions, and a combination

of these two transactions. In bilateral transactions, any DISCOs have the freedom to have a contract with any GENCOs in its own and other control areas, whereas in Poolco-based transactions, GENCOs participate in LFC of their own control areas only [19,20,100]. In a competitive electricity market, Poolco and bilateral transactions may take place simultaneously. A DISCO in any of the control areas and GENCOs in the same or in a different control area may also negotiate bilateral contracts. The power market players are responsible for having a communication path to exchange contract data as well as measurements to perform the load following function [20,84]. In such contracts, a GENCO changes its power output to supply the contracted load as long as it does not exceed the contracted value. The DISCO is responsible to maintain the load demand discipline as per contractual agreement.

In order to meet the Poolco-based and bilateral transactions, a DISCO participation matrix (DPM) is used [20] for better visualization. In a DPM, number of rows and columns are equal to the number of GENCOs and DISCOs, respectively. Each entry in a DPM is defined as contract participation factor. The cpf_{kl} is contract participation factor between k^{th} GENCO and $l^{th} DISCO$. The cpf_{kl} corresponds to the fraction of the total load power contracted by a DISCO-l from a GENCO-k [20]. It is noted that $\sum_{k} cpf_{kl} = 1$. DPM shows the participation of a DISCO in contract with a GENCO.

Each control area in this study is having three GENCOs and two DISCOs as shown in Fig. 6.1. Let GENCO-1, GENCO-2, GENCO-3, DISCO-1 and DISCO-2 be in control area-1 and GENCO-4, GENCO-5, GENCO-6, DISCO-3 and DISCO-4 be in control area-2. As a particular set of GENCOs is supposed to follow the total load demanded by a DISCO, information signals must flow from the DISCO to the particular GENCO(s) specifying corresponding demands. There may be uncontracted loads also in the control areas [84].

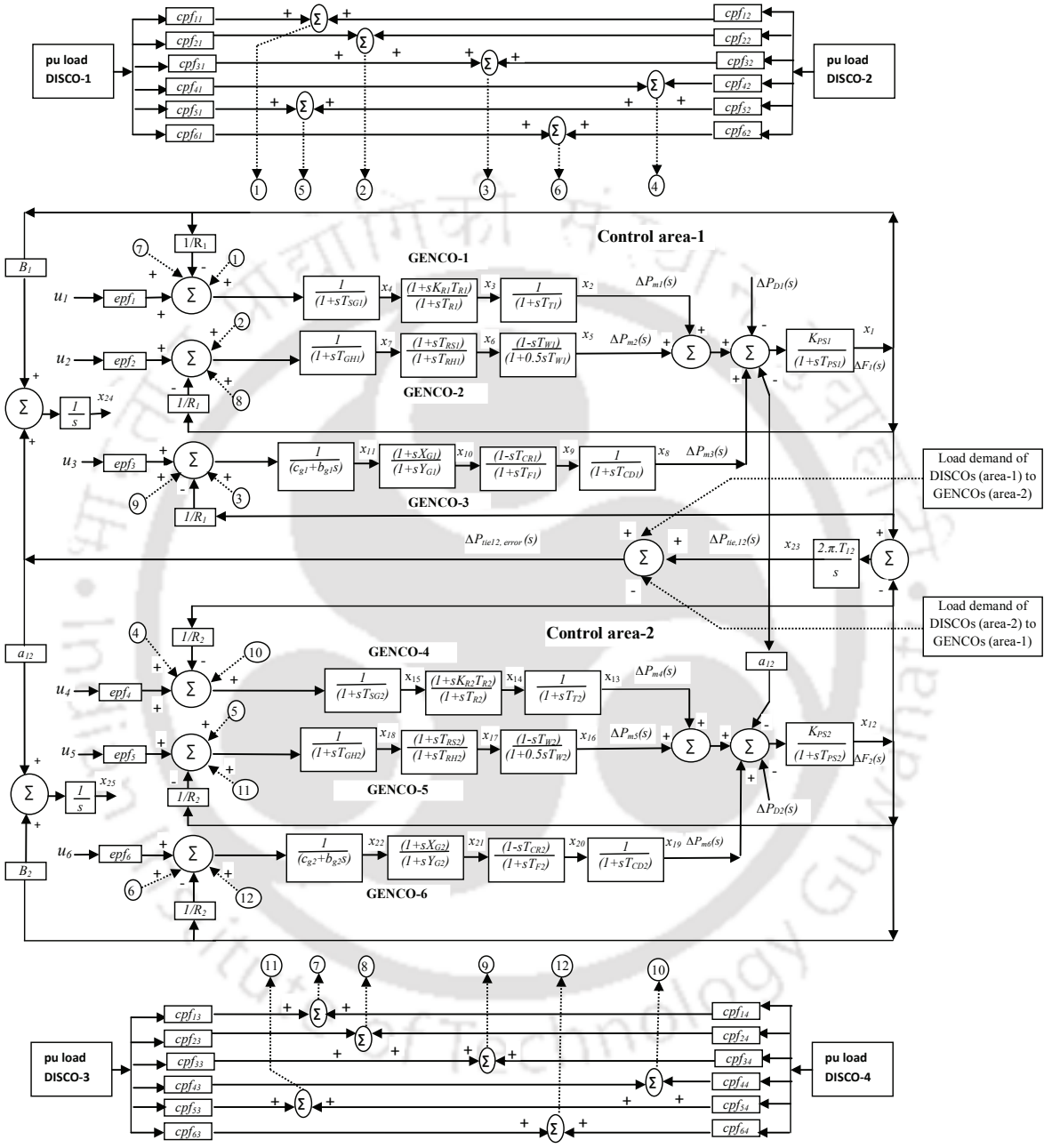

Figure 6.1: A TAIPS with MSPG in restructured power system environment

The corresponding DPM will become

$$DPM = \begin{bmatrix} cpf_{11} & cpf_{12} & cpf_{13} & cpf_{14} \\ cpf_{21} & cpf_{22} & cpf_{23} & cpf_{24} \\ cpf_{31} & cpf_{32} & cpf_{33} & cpf_{34} \\ cpf_{41} & cpf_{42} & cpf_{43} & cpf_{44} \\ cpf_{51} & cpf_{52} & cpf_{53} & cpf_{54} \\ cpf_{61} & cpf_{62} & cpf_{63} & cpf_{64} \end{bmatrix} \tag{6.1}$$

The scheduled steady state power flow on the tie line [5] is given as

$$\Delta P_{tie12,sch} = (P_{exp1}) - (P_{imp1}) \tag{6.2}$$

where;

Total power exported from control area-1 (P_{exp1}) is the demand of DISCOs in control area-2 from GENCOs in control area-1

and total power imported to control area-1 (P_{imp1}) is the demand of DISCOs in control area-1 from GENCOs in control area-2.

The error in tie line power ($\Delta P_{tie,12,error}$) may be defined as

$$\Delta P_{tie12,error} = \Delta P_{tie,12} - \Delta P_{tie,12,sch} \tag{6.3}$$

$\Delta P_{tie,12,error}$ vanishes in the steady state as the actual tie line power flow ($\Delta P_{tie,12}$) reaches the scheduled tie line power flow.

In the restructured power system, the area control errors may be defined as:

$$ACE_1 = B_1 \Delta f_1 + \Delta P_{tie,12,error} \tag{6.4}$$

$$ACE_2 = B_2 \Delta f_2 + a_{12} \Delta P_{tie,12,error} \tag{6.5}$$

where, ACE_1 and ACE_2 are the area control errors of control area-1 and 2 respectively, B_1 and B_2 are frequency bias parameters of control area-1 and 2 respectively, and a_{12} is control area capacity ratio.

6.3 Simulation and results

A TAIPS with MSPG is simulated in restructured power system environment as shown in Fig. 6.1. GENCO-1 and GENCO-4 are thermal, GENCO-2 and GENCO-5 are hydro, and GENCO-3 and GENCO-6 are gas generating units. The system parameters are given in Table 6.1. The nominal load of each control area is taken 1640 MW for all the contracts. It is assumed that $R_{ki} = R_i$. The epf_k is the economic participation factor of k^{th} GENCO. The economic participation factor of a GENCO depends on its profile, participation, bid price and capacity in the frequency regulation market [84]. The control signal (u_k) is the input to economic participation factor block of k^{th} GENCO.

The state space form is obtained for the proposed power system model. State variables x_1, x_{12}, x_{24} and x_{25} are taken as output feedback states. The state equations can be organized in the state-space form as described by the equation (6.6) given below and equation (2.38).

$$\dot{x} = \tilde{A}x + \tilde{B}u + \tilde{F}w + \bar{F}\bar{w} \tag{6.6}$$

where, the associated vectors and matrices are as follows:

state vector, $x = [x_1\ x_2 \ldots\ldots x_{25}]^T$

control vector, $u = [u_1\ u_2\ u_3\ u_4\ u_5\ u_6]^T$

disturbance vector, $w = [w_1\ w_2]^T = [\Delta P_{D1}\ \Delta P_{D2}]^T$.

and the disturbance vector ($\bar{w}$), due to contracts between GENCOs and DISCOs, is defined as:

$\bar{w} = [\Delta\tilde{P}_{L1}\ \Delta\tilde{P}_{L2}\ \Delta\tilde{P}_{L3}\ \Delta\tilde{P}_{L4}]^T$

The constant matrices $\tilde{A}$, $\tilde{B}$ and $\tilde{C}$, the disturbance matrices $\tilde{F}$ and $\bar{F}$, and design matrices $\tilde{Q}$ and $\tilde{R}$ are given in Appendix A.4.

It is assumed that all the GENCOs participate in the LFC with their corresponding economic participation factor values epf_1=0.6, epf_2=0.3, $epf_3 = 1-(epf_1+epf_2)$, epf_4=0.6, epf_5=0.3 and $epf_6 = 1-(epf_4+epf_5)$. The total local load of i^{th} control area(ΔP_{Di}) is the sum of contracted and uncontracted load demands of the DISCOs of i^{th} control area only. The optimum values of controller gains are obtained by running the MATLAB codes based on method described in the section 2.6. The computer simulations are carried out with the optimum con-

troller gains. MATLAB control system toolbox [121] is used to simulate the power system model and to obtain dynamic responses of the system for different contract scenarios (case-1, 2 and 3).

Table. 6.1: Simulation parameters of TAIPS with MSPG in restructured power environment

Parameters	Value
$P_{rt1} = P_{rt2}$	2000 MW
$P_{L1} = P_{L1}$	1640 MW
f	60 Hz
$H_1 = H_2$	5 MW-s/MVA
$D_1 = D_2$	0.0137 pu MW/Hz
$K_{PS1} = K_{PS2}$	73.1707 Hz/pu MW
T_{12}	0.0433
$T_{PS1} = T_{PS2}$	12.1951 s
$T_{SG1} = T_{SG2}$	0.08 s
$T_{T1} = T_{T2}$	0.3 s
$T_{CD1} = T_{CD2}$	0.2 s
$B_1 = B_2$	0.4303
a_{12}	- 1
$K_{R1} = K_{R2}$	0.3
$T_{R1} = T_{R2}$	10 s
$T_{W1} = T_{W2}$	1 s
$T_{RS1} = T_{RS2}$	5 s
$T_{RH1} = T_{RH2}$	28.75 s
$T_{GH1} = T_{GH2}$	0.2 s
$X_{G1} = X_{G2}$	0.6 s
$Y_{G1} = Y_{G2}$	1 s
$c_{g1} = c_{g2}$	1
$b_{g1} = c_{g2}$	0.05 s
$T_{F1} = T_{F2}$	0.23 s
$T_{CR1} = T_{CR2}$	0.01s
$R_1 = R_2$	2.4 Hz/pu MW

Case-1: Poolco based transactions

In this kind of transactions, GENCOs participate in LFC of their own control areas only [19,20]. It is assumed that the load change occurs only in control area-1. Thus, the load is demanded only by DISCO-1 and DISCO-2. Let the value of this load demand be 0.05 pu MW for each of them. DISCO-1 and DISCO-2 demand equally from GENCO-1, GENCO-2 and GENCO-3. A case of Poolco based contracts between DISCOs and available GENCOs is simulated based on

the following DPM-

$$DPM = \begin{bmatrix} 0.3333 & 0.3333 & 0 & 0 \\ 0.3333 & 0.3333 & 0 & 0 \\ 0.3333 & 0.3333 & 0 & 0 \\ 0 & 0 & 0 & 0 \\ 0 & 0 & 0 & 0 \\ 0 & 0 & 0 & 0 \end{bmatrix}$$

DISCO-3 and DISCO-4 do not demand power from any GENCOs, and hence the corresponding contract participation factors are zero. Fig. 6.2 shows control area frequency deviations and actual tie line power deviation, following a step change in the load demands of DISCO-1 and DISCO-2. The scheduled steady state tie line power flow is zero. The actual power on the tie line settles to zero. The frequency and tie line power deviation in each control area settles to zero in the steady state. In the steady state, generation of a GENCO must match the demand of DISCOs in contract with it. The desired generation of the k^{th} GENCO in pu MW can be expressed [20] in terms of contract participation factors and the total contracted demand of DISCOs as-

$$\Delta P_{mk} = cpf_{k1}\Delta\tilde{P}_{L1} + cpf_{k2}\Delta\tilde{P}_{L2} + cpf_{k3}\Delta\tilde{P}_{L3} + cpf_{k4}\Delta\tilde{P}_{L4} \tag{6.7}$$

Where $\Delta\tilde{P}_{L1}$, $\Delta\tilde{P}_{L2}$, $\Delta\tilde{P}_{L3}$ and $\Delta\tilde{P}_{L4}$ are the total contracted demands of DISCO-1, 2, 3 and 4 respectively.

In this case $\Delta\tilde{P}_{L1}$=0.05 pu MW, $\Delta\tilde{P}_{L2}$=0.05 pu MW, $\Delta\tilde{P}_{L3}$=0 and $\Delta\tilde{P}_{L4}$=0 and contract participation factors are as given in DPM. From the equation (6.7), the calculated values (desired values) of generations of GENCOs are ΔP_{m1}=0.0333 pu MW, ΔP_{m2}=0.0333 pu MW, ΔP_{m3}= 0.0333 pu MW, ΔP_{m4}=0, ΔP_{m5}=0 and ΔP_{m6}=0 at steady state. The generated powers (actual powers) of various GENCOs in response to contract with DISCOs are given in Fig. 6.3. The actual generated powers of the GENCOs reach the desired values in the steady state. GENCOs of control area-2 do not transact the power; hence, their change in generated power is zero at steady state.

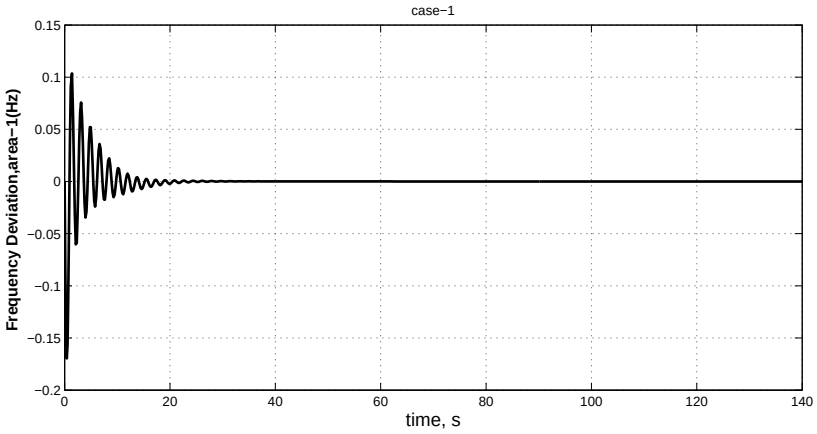

(a) Frequency deviation response of control area-1

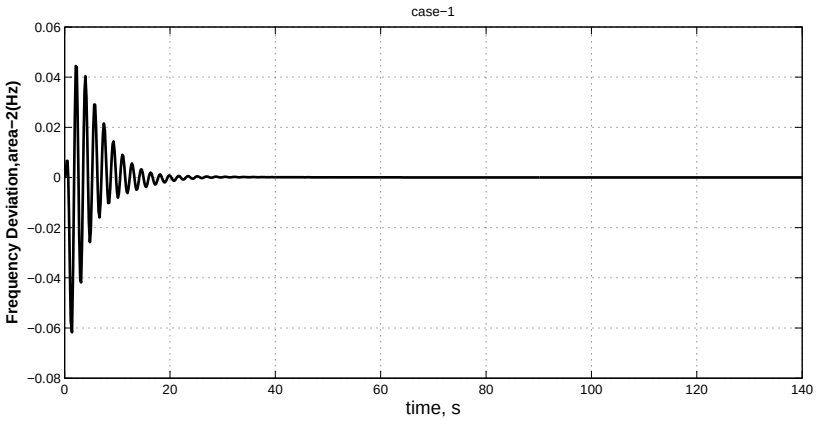

(b) Frequency deviation response of control area-2

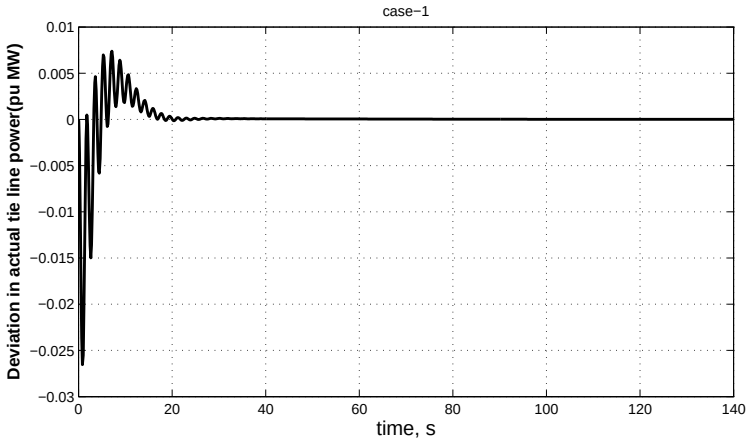

(c) Tie line power deviation response

Figure 6.2: Frequency and tie line power deviation responses for case-1

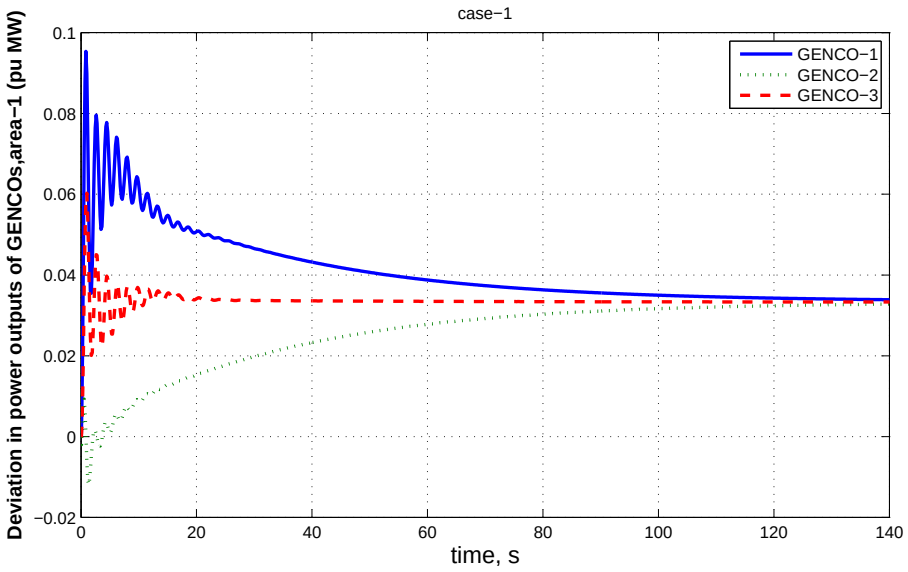

(a) Generator power output response of control area-1

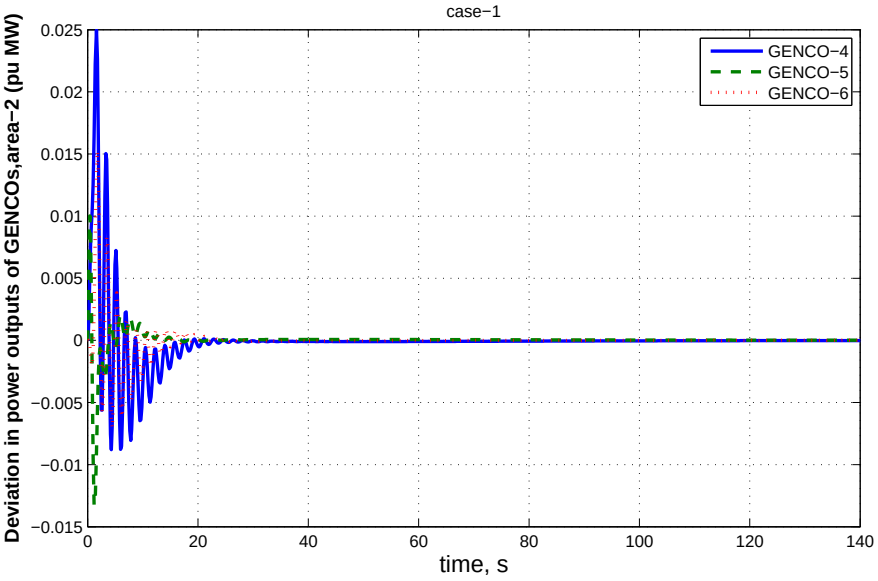

(b) Generator power output response of control area-2

Figure 6.3: Generator power output response for case-1

Case-2: Poolco and bilateral transactions

In this kind of transactions, a DISCO has the freedom to have a contract with any GENCOs in its own and other control areas [20] [19]. A case of combinations of Poolco and bilateral based contracts between DISCOs and available GENCOs is simulated based on the following DPM-

$$DPM = \begin{bmatrix} 0.2 & 0.1 & 0.3 & 0 \\ 0.2 & 0.2 & 0.1 & 0.1666 \\ 0.1 & 0.3 & 0.1 & 0.1666 \\ 0.2 & 0.1 & 0.1 & 0.3336 \\ 0.2 & 0.2 & 0.2 & 0.1666 \\ 0.1 & 0.1 & 0.2 & 0.1666 \end{bmatrix}$$

It is assumed that each DISCO demands 0.05 pu MW power from GENCOs as defined by contract participation factors in DPM matrix. The power system in Fig. 6.1 is simulated using this data and the results are shown in Figs.6.4 and 6.5. In this case $\Delta\tilde{P}_{L1}$=0.05 pu MW, $\Delta\tilde{P}_{L2}$=0.05 pu MW, $\Delta\tilde{P}_{L3}$=0.05 pu MW and $\Delta\tilde{P}_{L4}$=0.05 pu MW and contract participation factors are as given in DPM. The calculated values(desired values) of generations of GENCOs are ΔP_{m1}= 0.0300 pu MW, ΔP_{m2}=0.0333 pu MW, ΔP_{m3}=0.0333 pu MW, ΔP_{m4}=0.0367 pu MW, ΔP_{m5}=0.0383 pu MW and ΔP_{m6}= 0.0283 pu MW at steady state. The generated powers (actual powers) of various GENCOs in response to contract with DISCOs are shown in Fig. 6.5. As shown in Fig. 6.4(a-b), the control area frequency deviations settle to zero value. The tie line power deviation settles to scheduled value -0.0033 pu MW at steady state as shown in Fig. 6.4(c) which matches with the calculated (desired) value -0.0033 pu MW.

Case-3: contract violation

In some situations, DISCOs may violate a contract by demanding excess power. This excess power (uncontracted power) must be supplied by the GENCOs in the same control area as the DISCO [19, 20]. This kind of demand is reflected as a local load of the control area. Consider case-1 again with a modification that DISCO-1 demands 0.01 pu MW of excess power. The

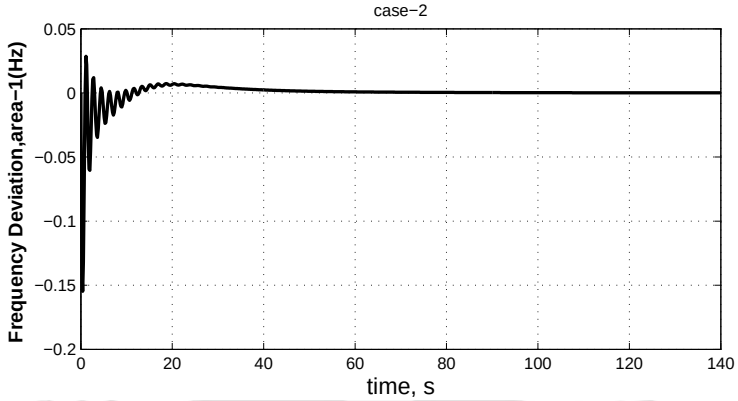

(a) Frequency deviation response of control area-1

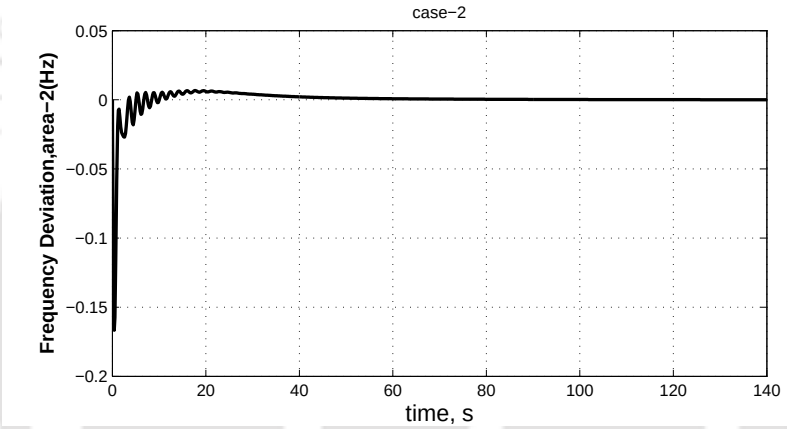

(b) Frequency deviation response of control area-2

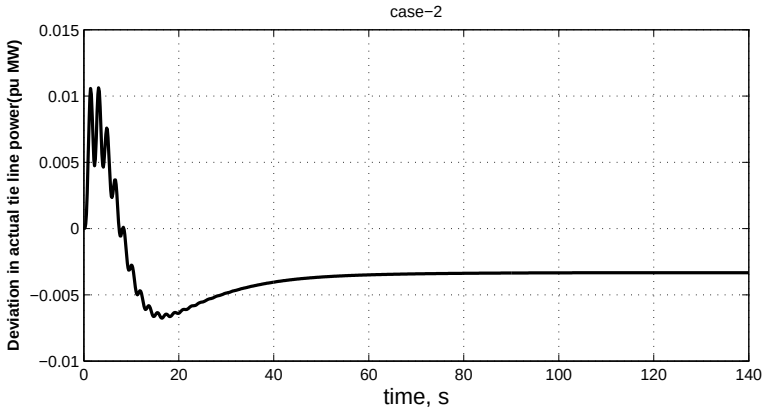

(c) Tie line power deviation response

Figure 6.4: Frequency and tie line power deviation responses for case-2

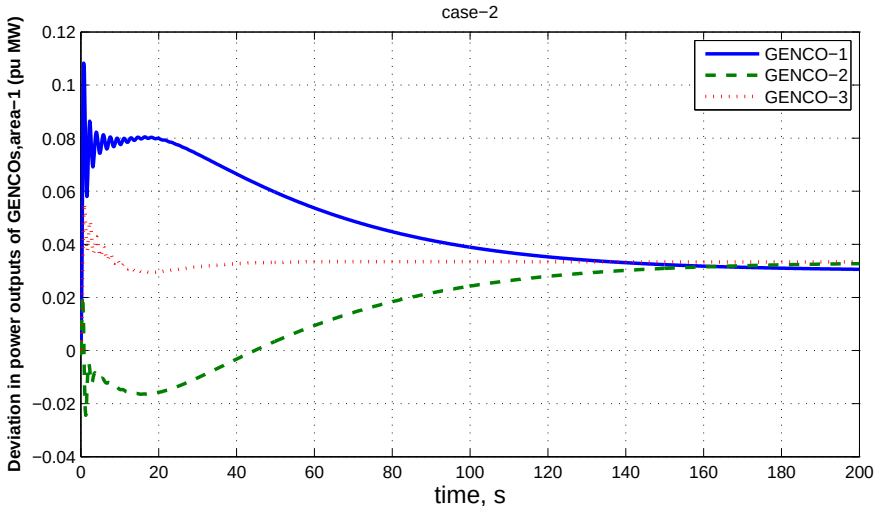

(a) Generator power output response of control area-1

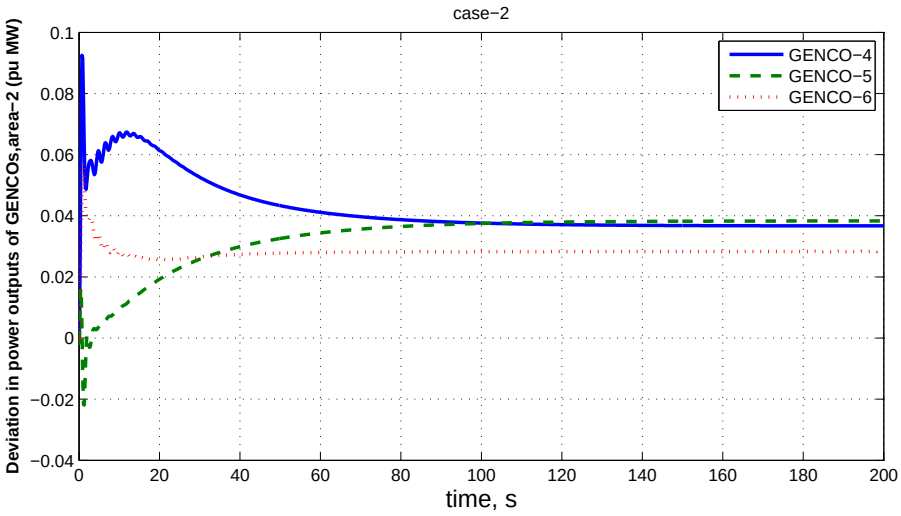

(b) Generator power output response of control area-2

Figure 6.5: Generator power output response for case-2

total local load in control area-1 becomes

ΔP_{D1}=(Load of DISCO-1)+(Load of DISCO-2) =(0.05+0.01)+(0.05)=0.11 pu MW

Similarly, the total local load in control area-2 becomes

ΔP_{D2}=(Load of DISCO-3)+(Load of DISCO-4) =(0)+(0)=0 pu MW

The frequency and tie line power deviations vanish in the steady state, shown in Fig. 6.6. As DPM is the same as in case-1 and the excess load is taken up by GENCOs in the same control area, the tie line power is the same as in case-1 in steady state. As shown in Fig.6.7, the generation of GENCOs-4, 5 and 6 is not affected by the excess load of DISCO-1. The uncontracted load of DISCO-1 is reflected in the generations of GENCO-1, 2 and 3. Sum of power generations of GENCOs in control area-1 as shown in Fig.6.7 matches with calculated (desired) value, 0.11 pu MW.

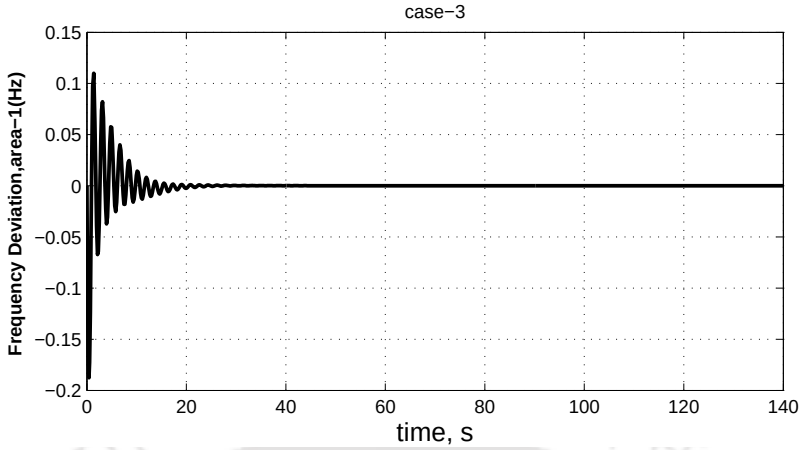

(a) Frequency deviation response of control area-1

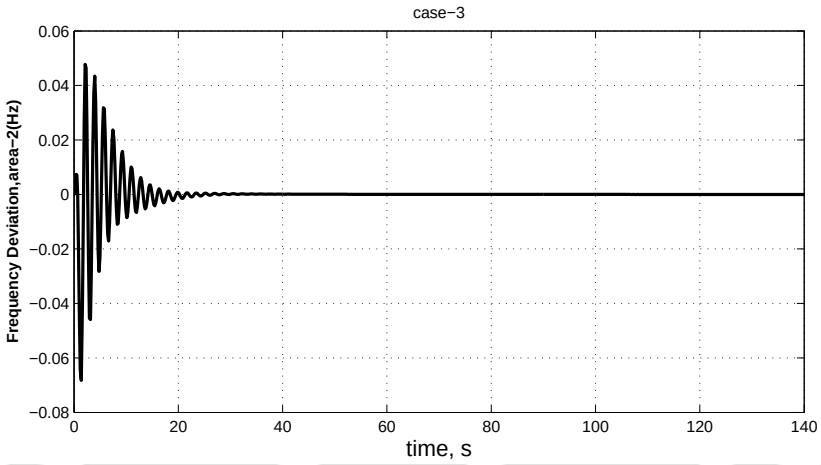

(b) Frequency deviation response of control area-2

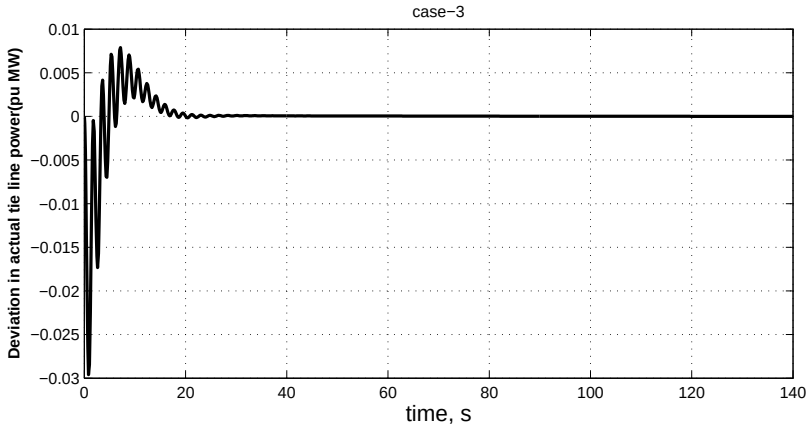

(c) Tie line power deviation response

Figure 6.6: Frequency and tie line power deviation responses for case-3

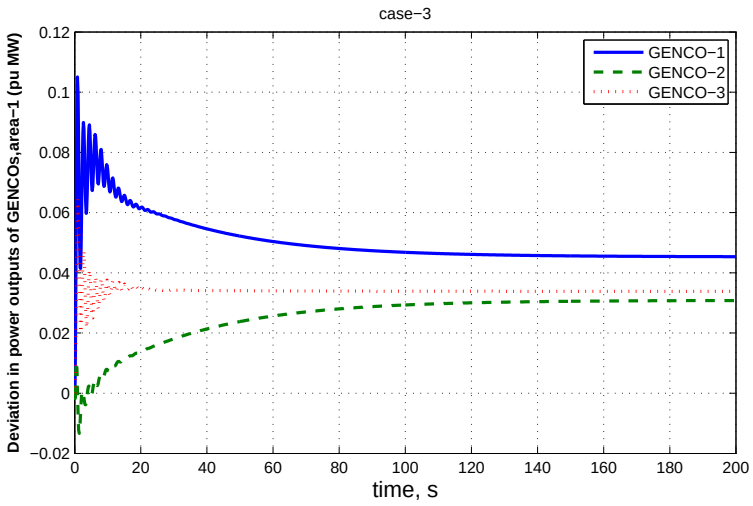

(a) Generator power output response of control area-1

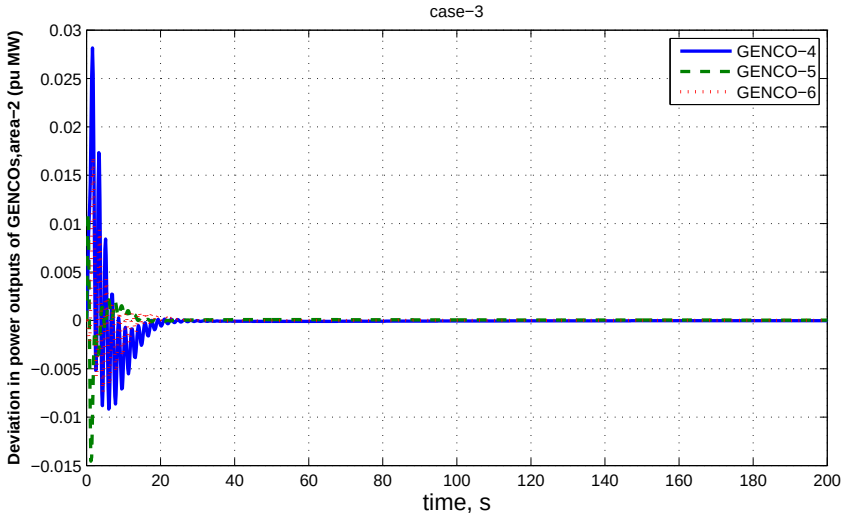

(b) Generator power output response of control area-2

Figure 6.7: Generator power output response for case-3

6.4 Summary

A new model of TAIPS with MSPG in restructured power system environment is proposed. Modified LFC scheme is presented in restructured power system environment. A state space model of the proposed power system in restructured power system environment is utilized for controller design considering all the interface variables like control area frequencies, tie line power and all other possible contracts between GENCOs and DISCOs. An extensive analysis is done for LFC scheme considering Poolco-based transactions, bilateral transactions, and a combination of these two transactions. It is found that in all the cases, the area frequency error becomes zero in the steady state which satisfy the LFC requirements. It is found that actual values of generations and tie-line power exchanges of GENCOs obtained by MATLAB Simulink model of the power system are matching with the corresponding calculated (desired) values.

CHAPTER 7

CONCLUSIONS AND FUTURE WORK

7.1 Concluding remarks

Many research work on LFC have been reported in recent years. Still there is much room for further improvement and extensions of LFC strategies. This thesis presents some improved results on LFC study of conventional and restructured power systems emphasizing on MSPG. New LFC models of the power systems with MSPG have been proposed. OFC is presented with pragmatic point of view. Briefly the results are summarized as follows:

A. Mathematical modeling and LFC of power systems

Mathematical modeling of the SAPS, MAIPS and MAIPS with MSPG are presented for LFC study. Keeping in view the new power system environment, the concept of MSPG in a control area is introduced. In addition to LFC models of SAPS and MAIPS, a new model of MAIPS with MSPG is presented for LFC study. The OFC is introduced. The control system design equations and algorithms have been presented.

B. LFC of conventional power systems

The LFC of various conventional TAIPSs has been studied using OFC. The combinations of non-reheat, reheat and hydro turbines are taken to demonstrate the suitability of OFC for LFC of interconnected power systems. The dynamic responses are obtained for TAIPSs considering (i) thermal-thermal with non-reheat turbine, (ii) thermal-thermal with reheat turbine and (iii) hydro-thermal generating units. The Dynamic responses obtained with OFC have been compared with that of FSFC. It has been found that dynamic responses obtained with proposed OFC are comparatively better and competes well with FSFC, satisfying the LFC requirements. The

OFC is presented from pragmatic point of view which uses less number of states as feedback, thereby reducing the controller cost and complexities.

C. LFC of power systems with multi-source power generation

LFC scheme is presented for power systems with MSPG. The performance of the proposed controller is demonstrated on the multi-source power systems and its dynamic responses are compared with that of FSFC. The OFC gives better dynamic response having relatively smaller peak overshoot and lesser settling time with zero steady state error as compared to that of FSFC. The effect of GRC on dynamic response is discussed. The critical examination of dynamic responses reveals that GRC results in increased peak overshoot, however settling time remains same for this particular power system model. The controller gives satisfactory dynamic responses for turbines considering GRC. It shows that OFC is able to accommodate the effect of GRC also. Investigations reveal that it is better to prefer the medium value of R i.e. 4% with corresponding optimum controller gains to provide better dynamic response of LFC for the proposed system. The dynamic responses are obtained for 1% to 5% SLPs. It is observed that for SLPs varying from 1% to 5%, the first peak overshoot increases with increase in the level of SLP and settling time remains approximately same with zero steady state error. The sensitivity analysis reveals that the optimum values of controller gains obtained for nominal system parameters and load condition are quite insensitive to wide parameter variation $\pm 25\%$. Hence for all practical purposes, the controller is quite robust. The LFC of hydro power plants operational in Iran has also been studied. The proposed controller performs well on this system and improves the frequency deviation responses remarkably. The simulation results show that proposed control strategy is very effective and guarantees good performance. In fact, this method provides a control system that satisfies the load frequency control requirements with a credible dynamic response.

D. LFC of power systems considering AC-DC tie lines and TCPS

An attempt is made to study the the dynamic performance of LFC of the power systems considering AC-DC tie lines and TCPS. A simple but practical controller is used to improve the dynamic response of LFC system in the the new power system environment. The OFC performs

well for the power system with DC link, giving better dynamic responses having relatively smaller peak overshoot and lesser settling time with zero steady state error as compared to the power system considering AC tie lines only. The dynamic response of the system with DC link is improved significantly with the percentage reduction in the peak overshoot of Δf_1, Δf_2 and $\Delta P_{tie,1}$ becoming 60.49, 90 and 44.92, respectively. Dynamic responses are obtained for wide range of variation in SLP from 1% to 4% which satisfy the LFC requirements. The simulation results show that proposed control strategy considering parallel AC-DC tie line is very effective and guarantees good performance. Further, the OFC is proposed to control the TCPS phase angle which in turn controls the tie line power flow. The proposed controller for the power system with TCPS gives better dynamic responses having relatively smaller peak overshoot and lesser settling time with zero steady state error as compared to the power system without TCPS. The dynamic response of the system with TCPS is improved significantly with the percentage reduction in the peak OS of Δf_1, Δf_2 and $\Delta \tilde{P}_{tie,1}$ becoming 34.56, 50 and 39.13, respectively and the settling time of Δf_1, Δf_2 and $\Delta \tilde{P}_{tie,1}$ becoming 41.61, 54.89 and 53.10, respectively. Dynamic responses are obtained for wide range of variation in load disturbance from 1% to 4% which satisfy the LFC requirements. Simulation results show that the due to the presence of TCPS, the dynamic performance in terms of settling time and peak overshoot is greatly improved. The system with TCPS is capable of suppressing the control area frequency and tie line power deviations more effectively under the occurrence of control area load perturbations. The simulation results show that proposed control strategy considering TCPS is very effective and guarantees good performance. Hence for all practical purposes, the controller is quite robust.

E. LFC in restructured power system environment

A new model of TAIPS with MSPG in restructured power system environment is proposed. Modified LFC scheme is presented in restructured power system environment. A state space model of the proposed power system in restructured power system environment is utilized for controller design considering all the interface variables like control area frequencies, tie line power and all other possible contracts between GENCOs and DISCOs. An extensive analysis

is done for LFC scheme considering Poolco-based transactions, bilateral transactions, and a combination of these two transactions. It is found that in all the cases, the area frequency error becomes zero in the steady state which satisfy the LFC requirements. It is found that actual values of generations and tie-line power exchanges of GENCOs obtained by MATLAB Simulink model of the power system are matching with the corresponding calculated (desired) values. Thus, the proposed LFC scheme is suitable in restructured power system environment.

7.2 Suggestions for further work

Following the LFC described in this thesis, a number of possible directions for extensions to this work are discussed below:

- Research work may be extended to renewable energy sources integration in the control area.
- Method may be extended to LFC study of the Micro-grids.
- Some energy storage devices may be included.
- Some evolutionary algorithms may be incorporated with proposed method and power system models.
- LFC study may be extended for combined cycle gas turbine and pumped storage hydro power plants.
- Price based LFC mechanism can be extended to improve frequency profile of the power system.

APPENDIX A

MATRICES OF POWER SYSTEMS

A.1 Matrices of TAIPS with MSPG

The matrix $\tilde{A}$ is of the dimension 25×25, where $\tilde{A}_{i,j}$ is the element of i^{th} row and j^{th} column of the matrix $\tilde{A}$. The non-zero elements are given below:

$\tilde{A}_{1,1} = -1/T_{PS1}$

$\tilde{A}_{1,2} = K_{PS1}\alpha_{11}/T_{PS1}$

$\tilde{A}_{1,5} = K_{PS1}\alpha_{21}/T_{PS1}$

$\tilde{A}_{1,8} = K_{PS1}\alpha_{31}/T_{PS1}$

$\tilde{A}_{1,23} = -K_{PS1}/T_{PS1}$

$\tilde{A}_{2,2} = -1/T_{T1}$

$\tilde{A}_{2,3} = 1/T_{T1}$

$\tilde{A}_{3,1} = -K_{R1}/(T_{SG1}R_{11})$

$\tilde{A}_{3,3} = -1/T_{R1}$

$\tilde{A}_{3,4} = 1/T_{R1} - K_{R1}/T_{SG1}$

$\tilde{A}_{4,1} = -1/(T_{SG1}R_{11})$

$\tilde{A}_{4,4} = -1/T_{SG1}$

$\tilde{A}_{5,1} = 2T_{RS1}/(T_{RH1}T_{GH1}R_{21})$

$\tilde{A}_{5,5} = -2/T_{W1}$

$\tilde{A}_{5,6} = 2/T_{W1} + 2/T_{RH1}$

$\tilde{A}_{5,7} = 2T_{RS1}/(T_{RH1}T_{GH1}) - 2/T_{RH1}$

$\tilde{A}_{6,1} = -T_{RS1}/(T_{RH1}T_{GH1}R_{21})$

$\tilde{A}_{6,6} = -1/T_{RH1}$

$\tilde{A}_{6,7} = 1/T_{RH1} - T_{RS1}/(T_{RH1}T_{GH1})$

$\tilde{A}_{7,1} = -1/(T_{GH1}R_{21})$

$\tilde{A}_{7,7} = -1/T_{GH1}$

$\tilde{A}_{8,8} = -1/T_{CD1}$

$\tilde{A}_{8,9} = 1/T_{CD1}$

$\tilde{A}_{9,1} = T_{CR1}X_{G1}/(T_{F1}R_{31}Y_{G1}b_{g1})$

$\tilde{A}_{9,9} = -1/T_{F1}$

$\tilde{A}_{9,10} = 1/T_{F1} + T_{CR1}/(T_{F1}Y_{G1})$

$\tilde{A}_{9,11} = T_{CR1}X_{G1}c_{g1}/(T_{F1}Y_{G1}b_{g1}) - T_{CR1}/(T_{F1}Y_{G1})$

$\tilde{A}_{10,1} = -X_{G1}/(R_{31}Y_{G1}b_{g1})$

$\tilde{A}_{10,10} = -1/Y_{G1}$

$\tilde{A}_{10,11} = 1/Y_{G1} - X_{G1}c_{g1}/(Y_{G1}b_{g1})$

$\tilde{A}_{11,1} = -1/(R_{31}b_{g1})$

$\tilde{A}_{11,11} = -c_{g1}/b_{g1}$

$\tilde{A}_{12,12} = -1/T_{PS2}$

$\tilde{A}_{12,13} = K_{PS2}\alpha_{12}/T_{PS2}$

$\tilde{A}_{12,16} = K_{PS2}\alpha_{22}/T_{PS2}$

$\tilde{A}_{12,19} = K_{PS2}\alpha_{32}/T_{PS2}$

$\tilde{A}_{12,23} = -a_{12}K_{PS2}/T_{PS2}$

$\tilde{A}_{13,13} = -1/T_{T2}$

$\tilde{A}_{13,14} = 1/T_{T2}$

$\tilde{A}_{14,12} = -K_{R2}/(T_{SG2}R_{12})$

$\tilde{A}_{14,14} = -1/T_{R2}$

$\tilde{A}_{14,15} = 1/T_{R2} - K_{R2}/T_{SG2}$

$\tilde{A}_{15,12} = -1/(T_{SG2}R_{12})$

$\tilde{A}_{15,15} = -1/T_{SG2}$

$\tilde{A}_{16,12} = 2T_{RS2}/(T_{RH2}T_{GH2}R_{22})$

$\tilde{A}_{16,16} = -2/T_{W2}$

$\tilde{A}_{16,17} = 2/T_{W2} + 2/T_{RH2}$

$\tilde{A}_{16,18} = 2T_{RS2}/(T_{RH2}T_{GH2}) - 2/T_{RH2}$

$\tilde{A}_{17,12} = -T_{RS2}/(T_{RH2}T_{GH2}R_{22})$

$\tilde{A}_{17,17} = -1/T_{RH2}$

$\tilde{A}_{17,18} = 1/T_{RH2} - T_{RS2}/(T_{RH2}T_{GH2})$

$\tilde{A}_{18,12} = -1/(T_{GH2}R_{22})$

$\tilde{A}_{18,18} = -1/T_{GH2}$

$\tilde{A}_{19,19} = -1/T_{CD2}$

$\tilde{A}_{19,20} = 1/T_{CD2}$

$\tilde{A}_{20,12} = T_{CR2}X_{G2}/(T_{F2}R_{32}Y_{G2}b_{g2})$

$\tilde{A}_{20,20} = -1/T_{F2}$

$\tilde{A}_{20,21} = 1/T_{F2} + T_{CR2}/(T_{F2}Y_{G2})$

$\tilde{A}_{20,22} = T_{CR2}X_{G2}c_{g2}/(T_{F2}Y_{G2}b_{g2}) - T_{CR2}/(T_{F2}Y_{G2})$

$\tilde{A}_{21,12} = -X_{G2}/(R_{32}Y_{G2}b_{g2})$

$\tilde{A}_{21,21} = -1/Y_{G2}$

$\tilde{A}_{21,22} = 1/Y_{G2} - X_{G2}c_{g2}/(Y_{G2}b_{g2})$

$\tilde{A}_{22,12} = -1/(R_{32}b_{g2})$

$\tilde{A}_{22,22} = -c_{g2}/b_{g2}$

$\tilde{A}_{23,1} = 2\pi T_{12}$

$\tilde{A}_{23,12} = -2\pi T_{12}$

$\tilde{A}_{24,1} = B_1$

$\tilde{A}_{24,23} = 1$

$\tilde{A}_{25,12} = B_2$

$\tilde{A}_{25,23} = a_{12}$

The matrix $\tilde{B}$ is of the dimension 25×6, where $\tilde{B}_{i,j}$ is the element of i^{th} row and j^{th} column of the matrix $\tilde{B}$. The non-zero elements are given below:

$\tilde{B}_{3,1} = K_{R1}/T_{SG1}$

$\tilde{B}_{4,1} = 1/T_{SG1}$

$\tilde{B}_{5,2} = -2T_{RS1}/(T_{RH1}T_{GH1})$

$\tilde{B}_{6,2} = T_{RS1}/(T_{RH1}T_{GH1})$

$\tilde{B}_{7,2} = 1/T_{GH1}$

$\tilde{B}_{9,3} = -X_{G1}T_{CR1}/(T_{F1}Y_{G1}b_{g1})$

$\tilde{B}_{10,3} = X_{G1}/(Y_{G1}b_{g1})$

$\tilde{B}_{11,3} = 1/b_{g1}$

$\tilde{B}_{14,4} = K_{R2}/T_{SG2}$

$\tilde{B}_{15,4} = 1/T_{SG2}$

$\tilde{B}_{16,5} = -2T_{RS2}/(T_{RH2}T_{GH2})$

$\tilde{B}_{17,5} = T_{RS2}/(T_{RH2}T_{GH2})$

$\tilde{B}_{18,5} = 1/T_{GH2}$

$\tilde{B}_{20,6} = -X_{G2}T_{CR2}/(T_{F2}Y_{G2}b_{g2})$

$\tilde{B}_{21,6} = X_{G2}/(Y_{G2}b_{g2})$

$\tilde{B}_{22,6} = 1/b_{g2}$

The matrix $\tilde{F}$ is of the dimension 25×2, where $\tilde{F}_{i,j}$ is the element of i^{th} row and j^{th} column of the matrix $\tilde{F}$. The non-zero elements are given below:

$\tilde{F}_{1,1} = -K_{PS1}/T_{PS1}$

$\tilde{F}_{12,2} = -K_{PS2}/T_{PS2}$

The matrix $\tilde{C}$ is defined as

$$\tilde{C} = \begin{bmatrix} 1 & 0 & 0 & 0 & 0 & 0 & 0 & 0 & 0 & 0 & 0 & 0 & 0 & 0 & 0 & 0 & 0 & 0 & 0 & 0 & 0 & 0 & 0 & 0 & 0 \\ 0 & 0 & 0 & 0 & 0 & 0 & 0 & 0 & 0 & 0 & 0 & 1 & 0 & 0 & 0 & 0 & 0 & 0 & 0 & 0 & 0 & 0 & 0 & 0 & 0 \\ 0 & 0 & 0 & 0 & 0 & 0 & 0 & 0 & 0 & 0 & 0 & 0 & 0 & 0 & 0 & 0 & 0 & 0 & 0 & 0 & 0 & 0 & 1 & 0 & 0 \\ 0 & 0 & 0 & 0 & 0 & 0 & 0 & 0 & 0 & 0 & 0 & 0 & 0 & 0 & 0 & 0 & 0 & 0 & 0 & 0 & 0 & 0 & 0 & 1 & 0 \end{bmatrix}$$

The matrix $\tilde{Q}$ is of the dimension 25×25, where $\tilde{Q}_{i,j}$ is the element of i^{th} row and j^{th} column of the matrix $\tilde{Q}$. The non-zero elements are given below:

$\tilde{Q}_{1,1} = 1 + B_1^2$

$\tilde{Q}_{1,23} = B_1$

$\tilde{Q}_{12,12} = 1 + B_2^2$

$\tilde{Q}_{12,23} = B_2 a_{12}$

$\tilde{Q}_{23,1} = B_1$

$\tilde{Q}_{23,12} = B_2 a_{12}$

$\tilde{Q}_{23,23} = 1 + a_{12}^2$

$\tilde{Q}_{24,24} = 1$

$\tilde{Q}_{25,25} = 1$

and the matrix $\tilde{R}$ is an identity matrix of the dimension 6×6.

A.2 Matrices of TAIPS with MSPG considering AC-DC tie lines

The matrix $\tilde{A}$ is of the dimension 27×27, where $\tilde{A}_{i,j}$ is the element of i^{th} row and j^{th} column of the matrix $\tilde{A}$. The non-zero elements are given below:

$\tilde{A}_{1,1} = -1/T_{PS1}$

$\tilde{A}_{1,2} = K_{PS1}\alpha_{11}/T_{PS1}$

$\tilde{A}_{1,5} = K_{PS1}\alpha_{21}/T_{PS1}$

$\tilde{A}_{1,8} = K_{PS1}\alpha_{31}/T_{PS1}$

$\tilde{A}_{1,23} = -K_{PS1}/T_{PS1}$

$\tilde{A}_{1,24} = -K_{PS1}/T_{PS1}$

$\tilde{A}_{2,2} = -1/T_{T1}$

$\tilde{A}_{2,3} = 1/T_{T1}$

$\tilde{A}_{3,1} = -K_{R1}/(T_{SG1}R_{11})$

$\tilde{A}_{3,3} = -1/T_{R1}$

$\tilde{A}_{3,4} = 1/T_{R1} - K_{R1}/T_{SG1}$

$\tilde{A}_{4,1} = -1/(T_{SG1}R_{11})$

$\tilde{A}_{4,4} = -1/T_{SG1}$

$\tilde{A}_{5,1} = 2T_{RS1}/(T_{RH1}T_{GH1}R_{21})$

$\tilde{A}_{5,5} = -2/T_{W1}$

$\tilde{A}_{5,6} = 2/T_{W1} + 2/T_{RH1}$

$\tilde{A}_{5,7} = 2T_{RS1}/(T_{RH1}T_{GH1}) - 2/T_{RH1}$

$\tilde{A}_{6,1} = -T_{RS1}/(T_{RH1}T_{GH1}R_{21})$

$\tilde{A}_{6,6} = -1/T_{RH1}$

$\tilde{A}_{6,7} = 1/T_{RH1} - T_{RS1}/(T_{RH1}T_{GH1})$

$\tilde{A}_{7,1} = -1/(T_{GH1}R_{21})$

$\tilde{A}_{7,7} = -1/T_{GH1}$

$\tilde{A}_{8,8} = -1/T_{CD1}$

$\tilde{A}_{8,9} = 1/T_{CD1}$

$\tilde{A}_{9,1} = T_{CR1}X_{G1}/(T_{F1}R_{31}Y_{G1}b_{g1})$

$\tilde{A}_{9,9} = -1/T_{F1}$

$\tilde{A}_{9,10} = 1/T_{F1} + T_{CR1}/(T_{F1}Y_{G1})$

$\tilde{A}_{9,11} = T_{CR1}X_{G1}c_{g1}/(T_{F1}Y_{G1}b_{g1}) - T_{CR1}/(T_{F1}Y_{G1})$

$\tilde{A}_{10,1} = -X_{G1}/(R_{31}Y_{G1}b_{g1})$

$\tilde{A}_{10,10} = -1/Y_{G1}$

$\tilde{A}_{10,11} = 1/Y_{G1} - X_{G1}c_{g1}/(Y_{G1}b_{g1})$

$\tilde{A}_{11,1} = -1/(R_{31}b_{g1})$

$\tilde{A}_{11,11} = -c_{g1}/b_{g1}$

$\tilde{A}_{12,12} = -1/T_{PS2}$

$\tilde{A}_{12,13} = K_{PS2}\alpha_{12}/T_{PS2}$

$\tilde{A}_{12,16} = K_{PS2}\alpha_{22}/T_{PS2}$

$\tilde{A}_{12,19} = K_{PS2}\alpha_{32}/T_{PS2}$

$\tilde{A}_{12,23} = -a_{12}K_{PS2}/T_{PS2}$

$\tilde{A}_{12,25} = -K_{PS2}/T_{PS2}$

$\tilde{A}_{13,13} = -1/T_{T2}$

$\tilde{A}_{13,14} = 1/T_{T2}$

$\tilde{A}_{14,12} = -K_{R2}/(T_{SG2}R_{12})$

$\tilde{A}_{14,14} = -1/T_{R2}$

$\tilde{A}_{14,15} = 1/T_{R2} - K_{R2}/T_{SG2}$

$\tilde{A}_{15,12} = -1/(T_{SG2}R_{12})$

$\tilde{A}_{15,15} = -1/T_{SG2}$

$\tilde{A}_{16,12} = 2T_{RS2}/(T_{RH2}T_{GH2}R_{22})$

$\tilde{A}_{16,16} = -2/T_{W2}$

$\tilde{A}_{16,17} = 2/T_{W2} + 2/T_{RH2}$

$\tilde{A}_{16,18} = 2T_{RS2}/(T_{RH2}T_{GH2}) - 2/T_{RH2}$

$\tilde{A}_{17,12} = -T_{RS2}/(T_{RH2}T_{GH2}R_{22})$

$\tilde{A}_{17,17} = -1/T_{RH2}$

$\tilde{A}_{17,18} = 1/T_{RH2} - T_{RS2}/(T_{RH2}T_{GH2})$

$\tilde{A}_{18,12} = -1/(T_{GH2}R_{22})$

$\tilde{A}_{18,18} = -1/T_{GH2}$

$\tilde{A}_{19,19} = -1/T_{CD2}$

$\tilde{A}_{19,20} = 1/T_{CD2}$

$\tilde{A}_{20,12} = T_{CR2}X_{G2}/(T_{F2}R_{32}Y_{G2}b_{g2})$

$\tilde{A}_{20,20} = -1/T_{F2}$

$\tilde{A}_{20,21} = 1/T_{F2} + T_{CR2}/(T_{F2}Y_{G2})$

$\tilde{A}_{20,22} = T_{CR2}X_{G2}c_{g2}/(T_{F2}Y_{G2}b_{g2}) - T_{CR2}/(T_{F2}Y_{G2})$

$\tilde{A}_{21,12} = -X_{G2}/(R_{32}Y_{G2}b_{g2})$

$\tilde{A}_{21,21} = -1/Y_{G2}$

$\tilde{A}_{21,22} = 1/Y_{G2} - X_{G2}c_{g2}/(Y_{G2}b_{g2})$

$\tilde{A}_{22,12} = -1/(R_{32}b_{g2})$

$\tilde{A}_{22,22} = -c_{g2}/b_{g2}$

$\tilde{A}_{23,1} = 2\pi T_{12}$

$\tilde{A}_{23,12} = -2\pi T_{12}$

$\tilde{A}_{24,1} = K_{DC1}/T_{DC1}$

$\tilde{A}_{24,24} = -1/T_{DC1}$

$\tilde{A}_{25,12} = K_{DC2}/T_{DC2}$

$\tilde{A}_{25,25} = -1/T_{DC2}$

$\tilde{A}_{26,1} = B_1$

$\tilde{A}_{26,23} = 1$

$\tilde{A}_{27,12} = B_2$

$\tilde{A}_{27,23} = a_{12}$

The matrix $\tilde{B}$ is of the dimension 27×6, where $\tilde{B}_{i,j}$ is the element of i^{th} row and j^{th} column of the matrix $\tilde{B}$. The non-zero elements are given below:

$\tilde{B}_{3,1} = K_{R1}/T_{SG1}$

$\tilde{B}_{4,1} = 1/T_{SG1}$

$\tilde{B}_{5,2} = -2T_{RS1}/(T_{RH1}T_{GH1})$

$\tilde{B}_{6,2} = T_{RS1}/(T_{RH1}T_{GH1})$

$\tilde{B}_{7,2} = 1/T_{GH1}$

$\tilde{B}_{9,3} = -X_{G1}T_{CR1}/(T_{F1}Y_{G1}b_{g1})$

$\tilde{B}_{10,3} = X_{G1}/(Y_{G1}b_{g1})$

$\tilde{B}_{11,3} = 1/b_{g1}$

$\tilde{B}_{14,4} = K_{R2}/T_{SG2}$

$\tilde{B}_{15,4} = 1/T_{SG2}$

$\tilde{B}_{16,5} = -2T_{RS2}/(T_{RH2}T_{GH2})$

$\tilde{B}_{17,5} = T_{RS2}/(T_{RH2}T_{GH2})$

$\tilde{B}_{18,5} = 1/T_{GH2}$

$\tilde{B}_{20,6} = -X_{G2}T_{CR2}/(T_{F2}Y_{G2}b_{g2})$

$\tilde{B}_{21,6} = X_{G2}/(Y_{G2}b_{g2})$

$\tilde{B}_{22,6} = 1/b_{g2}$

The matrix $\tilde{F}$ is of the dimension 27×2, where $\tilde{F}_{i,j}$ is the element of i^{th} row and j^{th} column of the matrix $\tilde{F}$. The non-zero elements are given below:

$\tilde{F}_{1,1} = -K_{PS1}/T_{PS1}$

$\tilde{F}_{12,2} = -K_{PS2}/T_{PS2}$

The matrix $\tilde{C}$ is defined as

$$\tilde{C} = \begin{bmatrix} 1 & 0 & 0 & 0 & 0 & 0 & 0 & 0 & 0 & 0 & 0 & 0 & 0 & 0 & 0 & 0 & 0 & 0 & 0 & 0 & 0 & 0 & 0 & 0 & 0 & 0 \\ 0 & 0 & 0 & 0 & 0 & 0 & 0 & 0 & 0 & 0 & 0 & 1 & 0 & 0 & 0 & 0 & 0 & 0 & 0 & 0 & 0 & 0 & 0 & 0 & 0 & 0 \\ 0 & 0 & 0 & 0 & 0 & 0 & 0 & 0 & 0 & 0 & 0 & 0 & 0 & 0 & 0 & 0 & 0 & 0 & 0 & 0 & 0 & 0 & 0 & 0 & 1 & 0 \\ 0 & 0 & 0 & 0 & 0 & 0 & 0 & 0 & 0 & 0 & 0 & 0 & 0 & 0 & 0 & 0 & 0 & 0 & 0 & 0 & 0 & 0 & 0 & 0 & 0 & 1 \end{bmatrix}$$

The matrix $\tilde{Q}$ is of the dimension 27×27, where $\tilde{Q}_{i,j}$ is the element of i^{th} row and j^{th} column of the matrix $\tilde{Q}$. The non-zero elements are given below:

$\tilde{Q}_{1,1} = 1 + B_1^2$

$\tilde{Q}_{1,23} = B_1$

$\tilde{Q}_{12,12} = 1 + B_2^2$

$\tilde{Q}_{12,23} = B_2 a_{12}$

$\tilde{Q}_{23,1} = B_1$

$\tilde{Q}_{23,12} = B_2 a_{12}$

$\tilde{Q}_{23,23} = 1 + a_{12}^2$

$\tilde{Q}_{26,26} = 1$

$\tilde{Q}_{27,27} = 1$

and the matrix $\tilde{R}$ is an identity matrix of the dimension 6×6.

A.3 Matrices of TAIPS with MSPG considering TCPS

The matrix $\tilde{A}$ is of the dimension 26×26, where $\tilde{A}_{i,j}$ is the element of i^{th} row and j^{th} column of the matrix $\tilde{A}$. The non-zero elements are given below:

$\tilde{A}_{1,1} = -1/T_{PS1}$

$\tilde{A}_{1,2} = K_{PS1}\alpha_{11}/T_{PS1}$

$\tilde{A}_{1,5} = K_{PS1}\alpha_{21}/T_{PS1}$

$\tilde{A}_{1,8} = K_{PS1}\alpha_{31}/T_{PS1}$

$\tilde{A}_{1,23} = -K_{PS1}/T_{PS1}$

$\tilde{A}_{1,24} = -K_{PS1}/T_{PS1}$

$\tilde{A}_{2,2} = -1/T_{T1}$

$\tilde{A}_{2,3} = 1/T_{T1}$

$\tilde{A}_{3,1} = -K_{R1}/(T_{SG1}R_{11})$

$\tilde{A}_{3,3} = -1/T_{R1}$

$\tilde{A}_{3,4} = 1/T_{R1} - K_{R1}/T_{SG1}$

$\tilde{A}_{4,1} = -1/(T_{SG1}R_{11})$

$\tilde{A}_{4,4} = -1/T_{SG1}$

$\tilde{A}_{5,1} = 2T_{RS1}/(T_{RH1}T_{GH1}R_{21})$

$\tilde{A}_{5,5} = -2/T_{W1}$

$\tilde{A}_{5,6} = 2/T_{W1} + 2/T_{RH1}$

$\tilde{A}_{5,7} = 2T_{RS1}/(T_{RH1}T_{GH1}) - 2/T_{RH1}$

$\tilde{A}_{6,1} = -T_{RS1}/(T_{RH1}T_{GH1}R_{21})$

$\tilde{A}_{6,6} = -1/T_{RH1}$

$\tilde{A}_{6,7} = 1/T_{RH1} - T_{RS1}/(T_{RH1}T_{GH1})$

$\tilde{A}_{7,1} = -1/(T_{GH1}R_{21})$

$\tilde{A}_{7,7} = -1/T_{GH1}$

$\tilde{A}_{8,8} = -1/T_{CD1}$

$\tilde{A}_{8,9} = 1/T_{CD1}$

$\tilde{A}_{9,1} = T_{CR1}X_{G1}/(T_{F1}R_{31}Y_{G1}b_{g1})$

$\tilde{A}_{9,9} = -1/T_{F1}$

$\tilde{A}_{9,10} = 1/T_{F1} + T_{CR1}/(T_{F1}Y_{G1})$

$\tilde{A}_{9,11} = T_{CR1}X_{G1}c_{g1}/(T_{F1}Y_{G1}b_{g1}) - T_{CR1}/(T_{F1}Y_{G1})$

$\tilde{A}_{10,1} = -X_{G1}/(R_{31}Y_{G1}b_{g1})$

$\tilde{A}_{10,10} = -1/Y_{G1}$

$\tilde{A}_{10,11} = 1/Y_{G1} - X_{G1}c_{g1}/(Y_{G1}b_{g1})$

$\tilde{A}_{11,1} = -1/(R_{31}b_{g1})$

$\tilde{A}_{11,11} = -c_{g1}/b_{g1}$

$\tilde{A}_{12,12} = -1/T_{PS2}$

$\tilde{A}_{12,13} = K_{PS2}\alpha_{12}/T_{PS2}$

$\tilde{A}_{12,16} = K_{PS2}\alpha_{22}/T_{PS2}$

$\tilde{A}_{12,19} = K_{PS2}\alpha_{32}/T_{PS2}$

$\tilde{A}_{12,23} = -a_{12}K_{PS2}/T_{PS2}$

$\tilde{A}_{12,24} = -a_{12}K_{PS2}/T_{PS2}$

$\tilde{A}_{13,13} = -1/T_{T2}$

$\tilde{A}_{13,14} = 1/T_{T2}$

$\tilde{A}_{14,12} = -K_{R2}/(T_{SG2}R_{12})$

$\tilde{A}_{14,14} = -1/T_{R2}$

$\tilde{A}_{14,15} = 1/T_{R2} - K_{R2}/T_{SG2}$

$\tilde{A}_{15,12} = -1/(T_{SG2}R_{12})$

$\tilde{A}_{15,15} = -1/T_{SG2}$

$\tilde{A}_{16,12} = 2T_{RS2}/(T_{RH2}T_{GH2}R_{22})$

$\tilde{A}_{16,16} = -2/T_{W2}$

$\tilde{A}_{16,17} = 2/T_{W2} + 2/T_{RH2}$

$\tilde{A}_{16,18} = 2T_{RS2}/(T_{RH2}T_{GH2}) - 2/T_{RH2}$

$\tilde{A}_{17,12} = -T_{RS2}/(T_{RH2}T_{GH2}R_{22})$

$\tilde{A}_{17,17} = -1/T_{RH2}$

$\tilde{A}_{17,18} = 1/T_{RH2} - T_{RS2}/(T_{RH2}T_{GH2})$

$\tilde{A}_{18,12} = -1/(T_{GH2}R_{22})$

$\tilde{A}_{18,18} = -1/T_{GH2}$

$\tilde{A}_{19,19} = -1/T_{CD2}$

$\tilde{A}_{19,20} = 1/T_{CD2}$

$\tilde{A}_{20,12} = T_{CR2}X_{G2}/(T_{F2}R_{32}Y_{G2}b_{g2})$

$\tilde{A}_{20,20} = -1/T_{F2}$

$\tilde{A}_{20,21} = 1/T_{F2} + T_{CR2}/(T_{F2}Y_{G2})$

$\tilde{A}_{20,22} = T_{CR2}X_{G2}c_{g2}/(T_{F2}Y_{G2}b_{g2}) - T_{CR2}/(T_{F2}Y_{G2})$

$\tilde{A}_{21,12} = -X_{G2}/(R_{32}Y_{G2}b_{g2})$

$\tilde{A}_{21,21} = -1/Y_{G2}$

$\tilde{A}_{21,22} = 1/Y_{G2} - X_{G2}c_{g2}/(Y_{G2}b_{g2})$

$\tilde{A}_{22,12} = -1/(R_{32}b_{g2})$

$\tilde{A}_{22,22} = -c_{g2}/b_{g2}$

$\tilde{A}_{23,1} = 2\pi\tilde{T}_{12}$

$\tilde{A}_{23,12} = -2\pi\tilde{T}_{12}$

$\tilde{A}_{24,1} = \tilde{T}_{12}K_{\phi}/T_{\phi}$

$\tilde{A}_{24,24} = -1/T_{\phi}$

$\tilde{A}_{25,1} = B_1$

$\tilde{A}_{25,23} = 1$

$\tilde{A}_{25,24} = 1$

$\tilde{A}_{26,12} = B_2$

$\tilde{A}_{26,23} = a_{12}$

$\tilde{A}_{26,24} = a_{12}$

The matrix $\tilde{B}$ is of the dimension 26×6, where $\tilde{B}_{i,j}$ is the element of i^{th} row and j^{th} column of the matrix $\tilde{B}$. The non-zero elements are given below:

$\tilde{B}_{3,1} = K_{R1}/T_{SG1}$

$\tilde{B}_{4,1} = 1/T_{SG1}$

$\tilde{B}_{5,2} = -2T_{RS1}/(T_{RH1}T_{GH1})$

$\tilde{B}_{6,2} = T_{RS1}/(T_{RH1}T_{GH1})$

$\tilde{B}_{7,2} = 1/T_{GH1}$

$\tilde{B}_{9,3} = -X_{G1}T_{CR1}/(T_{F1}Y_{G1}b_{g1})$

$\tilde{B}_{10,3} = X_{G1}/(Y_{G1}b_{g1})$

$\tilde{B}_{11,3} = 1/b_{g1}$

$\tilde{B}_{14,4} = K_{R2}/T_{SG2}$

$\tilde{B}_{15,4} = 1/T_{SG2}$

$\tilde{B}_{16,5} = -2T_{RS2}/(T_{RH2}T_{GH2})$

$\tilde{B}_{17,5} = T_{RS2}/(T_{RH2}T_{GH2})$

$\tilde{B}_{18,5} = 1/T_{GH2}$

$\tilde{B}_{20,6} = -X_{G2}T_{CR2}/(T_{F2}Y_{G2}b_{g2})$

$\tilde{B}_{21,6} = X_{G2}/(Y_{G2}b_{g2})$

$\tilde{B}_{22,6} = 1/b_{g2}$

The matrix $\tilde{F}$ is of the dimension 26×2, where $\tilde{F}_{i,j}$ is the element of i^{th} row and j^{th} column of the matrix $\tilde{F}$. The non-zero elements are given below:

$\tilde{F}_{1,1} = -K_{PS1}/T_{PS1}$

$\tilde{F}_{12,2} = -K_{PS2}/T_{PS2}$

The matrix $\tilde{C}$ is defined as

$$\tilde{C} = \begin{bmatrix} 1 & 0 & 0 & 0 & 0 & 0 & 0 & 0 & 0 & 0 & 0 & 0 & 0 & 0 & 0 & 0 & 0 & 0 & 0 & 0 & 0 & 0 & 0 & 0 & 0 & 0 \\ 0 & 0 & 0 & 0 & 0 & 0 & 0 & 0 & 0 & 0 & 0 & 1 & 0 & 0 & 0 & 0 & 0 & 0 & 0 & 0 & 0 & 0 & 0 & 0 & 0 & 0 \\ 0 & 0 & 0 & 0 & 0 & 0 & 0 & 0 & 0 & 0 & 0 & 0 & 0 & 0 & 0 & 0 & 0 & 0 & 0 & 0 & 0 & 0 & 0 & 0 & 1 & 0 \\ 0 & 0 & 0 & 0 & 0 & 0 & 0 & 0 & 0 & 0 & 0 & 0 & 0 & 0 & 0 & 0 & 0 & 0 & 0 & 0 & 0 & 0 & 0 & 0 & 0 & 1 \end{bmatrix}$$

The matrix $\tilde{Q}$ is of the dimension 26×26, where $\tilde{Q}_{i,j}$ is the element of i^{th} row and j^{th} column of the matrix $\tilde{Q}$. The non-zero elements are given below:

$\tilde{Q}_{1,1} = 1 + B_1^2$

$\tilde{Q}_{1,23} = B_1$

$\tilde{Q}_{1,24} = B_1$

$\tilde{Q}_{12,12} = 1 + B_2^2$

$\tilde{Q}_{12,23} = B_2 a_{12}$

$\tilde{Q}_{12,24} = B_2 a_{12}$

$\tilde{Q}_{23,1} = B_1$

$\tilde{Q}_{23,12} = B_2 a_{12}$

$\tilde{Q}_{23,23} = 1 + a_{12}^2$

$\tilde{Q}_{23,24} = 1 + a_{12}$

$\tilde{Q}_{24,1} = B_1$

$\tilde{Q}_{24,12} = B_2 a_{12}$

$\tilde{Q}_{24,23} = 1 + a_{12}$

$\tilde{Q}_{25,25} = 1$

$\tilde{Q}_{26,26} = 1$

and the matrix $\tilde{R}$ is an identity matrix of the dimension 6×6.

A.4 Matrices of TAIPS with MSPG in restructured power system

The matrix $\tilde{A}$ is of the dimension 25×25, where $\tilde{A}_{i,j}$ is the element of i^{th} row and j^{th} column of the matrix $\tilde{A}$. The non-zero elements are given below:

$\tilde{A}_{1,1} = -1/T_{PS1}$

$\tilde{A}_{1,2} = K_{PS1}/T_{PS1}$

$\tilde{A}_{1,5} = K_{PS1}/T_{PS1}$

$\tilde{A}_{1,8} = K_{PS1}/T_{PS1}$

$\tilde{A}_{1,23} = -K_{PS1}/T_{PS1}$

$\tilde{A}_{2,2} = -1/T_{T1}$

$\tilde{A}_{2,3} = 1/T_{T1}$

$\tilde{A}_{3,1} = -K_{R1}/(T_{SG1}R_{11})$

$\tilde{A}_{3,3} = -1/T_{R1}$

$\tilde{A}_{3,4} = 1/T_{R1} - K_{R1}/T_{SG1}$

$\tilde{A}_{4,1} = -1/(T_{SG1}R_{11})$

$\tilde{A}_{4,4} = -1/T_{SG1}$

$\tilde{A}_{5,1} = 2T_{RS1}/(T_{RH1}T_{GH1}R_{21})$

$\tilde{A}_{5,5} = -2/T_{W1}$

$\tilde{A}_{5,6} = 2/T_{W1} + 2/T_{RH1}$

$\tilde{A}_{5,7} = 2T_{RS1}/(T_{RH1}T_{GH1}) - 2/T_{RH1}$

$\tilde{A}_{6,1} = -T_{RS1}/(T_{RH1}T_{GH1}R_{21})$

$\tilde{A}_{6,6} = -1/T_{RH1}$

$\tilde{A}_{6,7} = 1/T_{RH1} - T_{RS1}/(T_{RH1}T_{GH1})$

$\tilde{A}_{7,1} = -1/(T_{GH1}R_{21})$

$\tilde{A}_{7,7} = -1/T_{GH1}$

$\tilde{A}_{8,8} = -1/T_{CD1}$

$\tilde{A}_{8,9} = 1/T_{CD1}$

$\tilde{A}_{9,1} = T_{CR1}X_{G1}/(T_{F1}R_{31}Y_{G1}b_{g1})$

$\tilde{A}_{9,9} = -1/T_{F1}$

$\tilde{A}_{9,10} = 1/T_{F1} + T_{CR1}/(T_{F1}Y_{G1})$

$\tilde{A}_{9,11} = T_{CR1}X_{G1}c_{g1}/(T_{F1}Y_{G1}b_{g1}) - T_{CR1}/(T_{F1}Y_{G1})$

$\tilde{A}_{10,1} = -X_{G1}/(R_{31}Y_{G1}b_{g1})$

$\tilde{A}_{10,10} = -1/Y_{G1}$

$\tilde{A}_{10,11} = 1/Y_{G1} - X_{G1}c_{g1}/(Y_{G1}b_{g1})$

$\tilde{A}_{11,1} = -1/(R_{31}b_{g1})$

$\tilde{A}_{11,11} = -c_{g1}/b_{g1}$

$\tilde{A}_{12,12} = -1/T_{PS2}$

$\tilde{A}_{12,13} = K_{PS2}/T_{PS2}$

$\tilde{A}_{12,16} = K_{PS2}/T_{PS2}$

$\tilde{A}_{12,19} = K_{PS2}/T_{PS2}$

$\tilde{A}_{12,23} = -a_{12}K_{PS2}/T_{PS2}$

$\tilde{A}_{13,13} = -1/T_{T2}$

$\tilde{A}_{13,14} = 1/T_{T2}$

$\tilde{A}_{14,12} = -K_{R2}/(T_{SG2}R_{12})$

$\tilde{A}_{14,14} = -1/T_{R2}$

$\tilde{A}_{14,15} = 1/T_{R2} - K_{R2}/T_{SG2}$

$\tilde{A}_{15,12} = -1/(T_{SG2}R_{12})$

$\tilde{A}_{15,15} = -1/T_{SG2}$

$\tilde{A}_{16,12} = 2T_{RS2}/(T_{RH2}T_{GH2}R_{22})$

$\tilde{A}_{16,16} = -2/T_{W2}$

$\tilde{A}_{16,17} = 2/T_{W2} + 2/T_{RH2}$

$\tilde{A}_{16,18} = 2T_{RS2}/(T_{RH2}T_{GH2}) - 2/T_{RH2}$

$\tilde{A}_{17,12} = -T_{RS2}/(T_{RH2}T_{GH2}R_{22})$

$\tilde{A}_{17,17} = -1/T_{RH2}$

$\tilde{A}_{17,18} = 1/T_{RH2} - T_{RS2}/(T_{RH2}T_{GH2})$

$\tilde{A}_{18,12} = -1/(T_{GH2}R_{22})$

$\tilde{A}_{18,18} = -1/T_{GH2}$

$\tilde{A}_{19,19} = -1/T_{CD2}$

$\tilde{A}_{19,20} = 1/T_{CD2}$

$\tilde{A}_{20,12} = T_{CR2}X_{G2}/(T_{F2}R_{32}Y_{G2}b_{g2})$

$\tilde{A}_{20,20} = -1/T_{F2}$

$\tilde{A}_{20,21} = 1/T_{F2} + T_{CR2}/(T_{F2}Y_{G2})$

$\tilde{A}_{20,22} = T_{CR2}X_{G2}c_{g2}/(T_{F2}Y_{G2}b_{g2}) - T_{CR2}/(T_{F2}Y_{G2})$

$\tilde{A}_{21,12} = -X_{G2}/(R_{32}Y_{G2}b_{g2})$

$\tilde{A}_{21,21} = -1/Y_{G2}$

$\tilde{A}_{21,22} = 1/Y_{G2} - X_{G2}c_{g2}/(Y_{G2}b_{g2})$

$\tilde{A}_{22,12} = -1/(R_{32}b_{g2})$

$\tilde{A}_{22,22} = -c_{g2}/b_{g2}$

$\tilde{A}_{23,1} = 2\pi T_{12}$

$\tilde{A}_{23,12} = -2\pi T_{12}$

$\tilde{A}_{24,1} = B_1$

$\tilde{A}_{24,23} = 1$

$\tilde{A}_{25,12} = B_2$

$\tilde{A}_{25,23} = a_{12}$

The matrix $\tilde{B}$ is of the dimension 25×6, where $\tilde{B}_{i,j}$ is the element of i^{th} row and j^{th} column of the matrix $\tilde{B}$. The non-zero elements are given below:

$\tilde{B}_{3,1} = K_{R1}epf_1/T_{SG1}$

$\tilde{B}_{4,1} = epf_1/T_{SG1}$

$\tilde{B}_{5,2} = -2T_{RS1}epf_2/(T_{RH1}T_{GH1})$

$\tilde{B}_{6,2} = T_{RS1}epf_2/(T_{RH1}T_{GH1})$

$\tilde{B}_{7,2} = epf_2/T_{GH1}$

$\tilde{B}_{9,3} = -X_{G1}T_{CR1}epf_3/(T_{F1}Y_{G1}b_{g1})$

$\tilde{B}_{10,3} = X_{G1}epf_3/(Y_{G1}b_{g1})$

$\tilde{B}_{11,3} = epf_3/b_{g1}$

$\tilde{B}_{14,4} = K_{R2} epf_4 / T_{SG2}$

$\tilde{B}_{15,4} = epf_4 / T_{SG2}$

$\tilde{B}_{16,5} = -2T_{RS2} epf_5 / (T_{RH2} T_{GH2})$

$\tilde{B}_{17,5} = T_{RS2} epf_5 / (T_{RH2} T_{GH2})$

$\tilde{B}_{18,5} = epf_5 / T_{GH2}$

$\tilde{B}_{20,6} = -X_{G2} T_{CR2} epf_6 / (T_{F2} Y_{G2} b_{g2})$

$\tilde{B}_{21,6} = X_{G2} epf_6 / (Y_{G2} b_{g2})$

$\tilde{B}_{22,6} = epf_6 / b_{g2}$

The matrix $\tilde{F}$ is of the dimension 25×2, where $\tilde{F}_{i,j}$ is the element of i^{th} row and j^{th} column of the matrix $\tilde{F}$. The non-zero elements are given below:

$\tilde{F}_{1,1} = -K_{PS1} / T_{PS1}$

$\tilde{F}_{12,2} = -K_{PS2} / T_{PS2}$

The matrix $\bar{F}$ is of the dimension 25×4, where $\bar{F}_{i,j}$ is the element of i^{th} row and j^{th} column of the matrix $\bar{F}$. The non-zero elements are given below:

$\bar{F}_{3,1} = cpf_{11} K_{R1} / T_{SG1}$

$\bar{F}_{3,2} = cpf_{12} K_{R1} / T_{SG1}$

$\bar{F}_{3,3} = cpf_{13} K_{R1} / T_{SG1}$

$\bar{F}_{3,4} = cpf_{14} K_{R1} / T_{SG1}$

$\bar{F}_{4,1} = cpf_{11} / T_{SG1}$

$\bar{F}_{4,2} = cpf_{12} / T_{SG1}$

$\bar{F}_{4,3} = cpf_{13} / T_{SG1}$

$\bar{F}_{4,4} = cpf_{14} / T_{SG1}$

$\bar{F}_{5,1} = -2T_{RS1}\ cpf_{21} / (T_{GH1} T_{RH1})$

$\bar{F}_{5,2} = -2T_{RS1}\ cpf_{22} / (T_{GH1} T_{RH1})$

$\bar{F}_{5,3} = -2T_{RS1}\ cpf_{23} / (T_{GH1} T_{RH1})$

$\bar{F}_{5,4} = -2T_{RS1}\ cpf_{24} / (T_{GH1} T_{RH1})$

$\bar{F}_{6,1} = cpf_{21} T_{RS1} / (T_{GH1} T_{RH1})$

$\bar{F}_{6,2} = cpf_{22} T_{RS1} / (T_{GH1} T_{RH1})$

$\bar{F}_{6,3} = cpf_{23} T_{RS1} / (T_{GH1} T_{RH1})$

$\bar{F}_{6,4} = cpf_{24} T_{RS1} / (T_{GH1} T_{RH1})$

$\bar{F}_{7,1} = cpf_{21} / T_{GH1}$

$\bar{F}_{7,2} = cpf_{22} / T_{GH1}$

$\bar{F}_{7,3} = cpf_{23} / T_{GH1}$

$\bar{F}_{7,4} = cpf_{24} / T_{GH1}$

$\bar{F}_{9,1} = T_{CR1} cpf_{31} X_{G1} / (b_{g1} Y_{G1} T_{F1})$

$\bar{F}_{9,2} = T_{CR1} cpf_{32} X_{G1} / (b_{g1} Y_{G1} T_{F1})$

$\bar{F}_{9,3} = T_{CR1} cpf_{33} X_{G1} / (b_{g1} Y_{G1} T_{F1})$

$\bar{F}_{9,4} = T_{CR1} cpf_{34} X_{G1} / (b_{g1} Y_{G1} T_{F1})$

$\bar{F}_{10,1} = cpf_{31} X_{G1} / (b_{g1} Y_{G1})$

$\bar{F}_{10,2} = cpf_{32} X_{G1} / (b_{g1} Y_{G1})$

$\bar{F}_{10,3} = cpf_{33} X_{G1} / (b_{g1} Y_{G1})$

$\bar{F}_{10,4} = cpf_{34} X_{G1} / (b_{g1} Y_{G1})$

$\bar{F}_{11,1} = cpf_{31} / b_{g1}$

$\bar{F}_{11,2} = cpf_{32}/b_{g1}$

$\bar{F}_{11,3} = cpf_{33}/b_{g1}$

$\bar{F}_{11,4} = cpf_{34}/b_{g1}$

$\bar{F}_{14,1} = cpf_{41}K_{R2}/T_{SG2}$

$\bar{F}_{14,2} = cpf_{42}K_{R2}/T_{SG2}$

$\bar{F}_{14,3} = cpf_{43}K_{R2}/T_{SG2}$

$\bar{F}_{14,4} = cpf_{44}K_{R2}/T_{SG2}$

$\bar{F}_{15,1} = cpf_{41}/T_{SG2}$

$\bar{F}_{15,2} = cpf_{42}/T_{SG2}$

$\bar{F}_{15,3} = cpf_{43}/T_{SG2}$

$\bar{F}_{15,4} = cpf_{44}/T_{SG2}$

$\bar{F}_{16,1} = -2T_{RS2}\ cpf_{51}/(T_{GH2}T_{RH2})$

$\bar{F}_{16,2} = -2T_{RS2}\ cpf_{52}/(T_{GH2}T_{RH2})$

$\bar{F}_{16,3} = -2T_{RS2}\ cpf_{53}/(T_{GH2}T_{RH2})$

$\bar{F}_{16,4} = -2T_{RS2}\ cpf_{54}/(T_{GH2}T_{RH2})$

$\bar{F}_{17,1} = T_{RS2}\ cpf_{51}/(T_{GH2}T_{RH2})$

$\bar{F}_{17,2} = T_{RS2}\ cpf_{52}/(T_{GH2}T_{RH2})$

$\bar{F}_{17,3} = T_{RS2}\ cpf_{53}/(T_{GH2}T_{RH2})$

$\bar{F}_{17,4} = T_{RS2}\ cpf_{54}/(T_{GH2}T_{RH2})$

$\bar{F}_{18,1} = cpf_{51}/T_{GH2}$

$\bar{F}_{18,2} = cpf_{52}/T_{GH2}$

$\bar{F}_{18,3} = cpf_{53}/T_{GH2}$

$\bar{F}_{18,4} = cpf_{54}/T_{GH2}$

$\bar{F}_{20,1} = T_{CR2}cpf_{61}X_{G2}/(b_{g2}Y_{G2}T_{F2})$

$\bar{F}_{20,2} = T_{CR2}cpf_{62}X_{G2}/(b_{g2}Y_{G2}T_{F2})$

$\bar{F}_{20,3} = T_{CR2}cpf_{63}X_{G2}/(b_{g2}Y_{G2}T_{F2})$

$\bar{F}_{20,4} = T_{CR2}cpf_{64}X_{G2}/(b_{g2}Y_{G2}T_{F2})$

$\bar{F}_{21,1} = cpf_{61}X_{G2}/(b_{g2}Y_{G2})$

$\bar{F}_{21,2} = cpf_{62}X_{G2}/(b_{g2}Y_{G2})$

$\bar{F}_{21,3} = cpf_{63}X_{G2}/(b_{g2}Y_{G2})$

$\bar{F}_{21,4} = cpf_{64}X_{G2}/(b_{g2}Y_{G2})$

$\bar{F}_{22,1} = cpf_{61}/b_{g2}$

$\bar{F}_{22,2} = cpf_{62}/b_{g2}$

$\bar{F}_{22,3} = cpf_{63}/b_{g2}$

$\bar{F}_{22,4} = cpf_{64}/b_{g2}$

$\bar{F}_{24,1} = (cpf_{41} + cpf_{51} + cpf_{61})$

$\bar{F}_{24,2} = (cpf_{42} + cpf_{52} + cpf_{62})$

$\bar{F}_{24,3} = -(cpf_{13} + cpf_{23} + cpf_{33})$

$\bar{F}_{24,4} = -(cpf_{14} + cpf_{24} + cpf_{34})$

$\bar{F}_{25,1} = a_{12}(cpf_{41} + cpf_{51} + cpf_{61})$

$\bar{F}_{25,2} = a_{12}(cpf_{42} + cpf_{52} + cpf_{62})$

$\bar{F}_{25,3} = -a_{12}(cpf_{13} + cpf_{23} + cpf_{33})$

$\bar{F}_{25,4} = -a_{12}(cpf_{14} + cpf_{24} + cpf_{34})$

The matrix $\tilde{C}$ is defined as

$$\tilde{C} = \begin{bmatrix} 1 & 0 & 0 & 0 & 0 & 0 & 0 & 0 & 0 & 0 & 0 & 0 & 0 & 0 & 0 & 0 & 0 & 0 & 0 & 0 & 0 & 0 & 0 & 0 & 0 \\ 0 & 0 & 0 & 0 & 0 & 0 & 0 & 0 & 0 & 0 & 0 & 1 & 0 & 0 & 0 & 0 & 0 & 0 & 0 & 0 & 0 & 0 & 0 & 0 & 0 \\ 0 & 0 & 0 & 0 & 0 & 0 & 0 & 0 & 0 & 0 & 0 & 0 & 0 & 0 & 0 & 0 & 0 & 0 & 0 & 0 & 0 & 0 & 1 & 0 & 0 \\ 0 & 0 & 0 & 0 & 0 & 0 & 0 & 0 & 0 & 0 & 0 & 0 & 0 & 0 & 0 & 0 & 0 & 0 & 0 & 0 & 0 & 0 & 0 & 1 & 0 \end{bmatrix}$$

The matrix $\tilde{Q}$ is of the dimension 25×25, where $\tilde{Q}_{i,j}$ is the element of i^{th} row and j^{th} column of the matrix $\tilde{Q}$. The non-zero elements are given below:

$\tilde{Q}_{1,1} = 1 + B_1^2$

$\tilde{Q}_{1,23} = B_1$

$\tilde{Q}_{12,12} = 1 + B_2^2$

$\tilde{Q}_{12,23} = B_2 a_{12}$

$\tilde{Q}_{23,1} = B_1$

$\tilde{Q}_{23,12} = B_2 a_{12}$

$\tilde{Q}_{23,23} = 1 + a_{12}^2$

$\tilde{Q}_{24,24} = 1$

$\tilde{Q}_{25,25} = 1$

and the matrix $\tilde{R}$ is an identity matrix of the dimension 6×6.

REFERENCES

[1] A. Yazdizadeh, M. H. Ramezani, and E. Hamedrahmat, "Decentralized load frequency control using a new robust optimal MISO PID controller," *Int. J. Electrical Power and Energy Systems*, vol. 35, pp. 57 –65, 2012.

[2] D. P. Kothari and I. J. Nagrath, *Modern Power System Analysis*, 4th ed. McGraw Hill, 2011.

[3] D. P. Kothari and J. S. Dhillon, *Power System Optimization*, 2nd ed. New Delhi, India: Prentice Hall, 2010.

[4] Ibraheem, P. Kumar, and D. P. Kothari, "Recent philosophies of automatic generation control strategies in power systems," *IEEE Trans Power Syst*, vol. 20, no. 1, pp. 346 –357, 2005.

[5] H. Bevrani and T. Hiyama, *Intelligent Automatic Generation Control*. New York: CRC Press Taylor and Francis, 2011.

[6] H. Bevrani, *Robust Power System Frequency Control*. New York: Springer, 2009.

[7] O. Elgerd, *Electric Energy System Theory: an introduction*, 2nd ed. New York: McGraw-Hill, 1983.

[8] O. Elgerd and C. Fosha, "Optimum megawatt frequency control of multi-area electric energy systems," *IEEE Trans Power Appl. Syst.*, vol. 89, no. 4, pp. 556 –563, 1970.

[9] L. C. Saikia, J. Nanda, and S. Mishra, "Performance comparison of several classical controllers in AGC for multi-area interconnected thermal system," *Electrical Power and Energy Systems*, vol. 33, pp. 394 –401, 2011.

[10] P. Kundur, *Power System Stability and Control*, fifth reprint ed. New Delhi India: Tata McGraw Hill, 2008.

[11] B. Tyagi and S. C. Srivastava, "A LQG based load frequency controller in a competitive electricity environment," *Int. J. Emerging Elect. Power Syst.*, vol. 2, 2005. [Online]. Available: http://www.bepress.com/ijeeps/vol2/iss2/art1044

[12] A. Khodabakhshian and R. Hooshmand, "A new PID controller design for automatic generation control of hydro power systems," *Int. J. Electrical Power and Energy Systems*, vol. 32, pp. 375 –382, 2010.

[13] T. A. Muthana, F. H. Mohamed, and Z. Mohamed, "Decentralized load frequency controller for a multi-area interconnected power system," *Int. J. Electrical Power and Energy Systems*, vol. 33, pp. 198 –209, 2011.

[14] K. T. H. Bevrani, Y. Mitani, "Robust AGC: Traditional structure versus restructured scheme," *IEEJ Trans. on Power and Energy*, vol. 124, no. 5, pp. 751 –761, 2004.

[15] J. Nanda, S. Mishra, and L. C. Saikia, "Maiden application of bacterial foraging-based optimization technique in multi-area automatic generation control," *IEEE Trans. Power Syst*, vol. 24, no. 2, pp. 602 –609, 2009.

[16] N. Jaleeli, D. N. Ewart, and L. H. Fink, "Understanding automatic generation control," *IEEE Trans. Power System*, vol. 7, no. 3, pp. 1106 –1112, 1992.

[17] H. Bevrani, "Decentralized robust load-frequency control synthesis in restructured power systems," Ph.D. dissertation, Department of Electrical Engineering Graduate School of Engineering Osaka University, 2004.

[18] P. Bhatt, S. P. Ghoshal, R. Roy, and S. Ghosal, "Load frequency control of interconnected restructured power system along with DFIG and coordinated operation of TCPS-SMES," *IEEE Conf proc.,PEDES*, 2010.

[19] P. Bhatt, R. Roy, and S. P. Ghoshal, "Optimized multiarea AGC simulation in restructured power systems," *Int. Journal of Electrical Power and Energy Systems*, vol. 32, no. 4, pp. 311 –322, 2010.

[20] V. Donde, M. A. Pai, and I. A. Hiskens, "Simulation and optimization in an AGC system after deregulation," *IEEE Trans. Power Syst.*, vol. 16, no. 3, pp. 481 –489, 2001.

[21] R. D. Christie and A. Bose, "Load frequency control issues in power system operation after deregulation," *IEEE Trans. Power Syst.*, vol. 11, no. 3, pp. 1191 –1200, 1996.

[22] N. Bekhouche, "Automatic generation control before after deregulation," *34th Southeastern Symp.System Theory*, pp. 321 –323, 2002.

[23] C. Concordia and L. K. Kirchmayer, "Tie line power and frequency control of electric power systems," *Amer. Inst. Elect. Eng. Trans.*, vol. pt. II,72, pp. 562 –572, 1953.

[24] L. K. Kirchmayer, *Economic Control of Interconnected Systems*. New York: Wiley, 1959.

[25] N. Cohn, "Some aspects of tie-line bias control on interconnected power systems," *Amer. Inst. Elect. Eng. Trans.*, vol. 75, pp. 1415 –1436, 1957.

[26] ——, "Considerations in the regulation of interconnected area," *IEEE Trans. Power Syst.*, vol. PAS-86, pp. 1527 – 1538, 1967.

[27] J. E. Van Ness, "Root loci of load frequency control systems," *IEEE Trans. Power App. Syst.*, vol. PAS-82, no. 5, pp. 712 –726, 1963.

[28] G. Quazza, "Noninteracting controls of interconnected electric power systems," *IEEE Trans. Power App. Syst.*, vol. PAS-85, no. 7, pp. 727 –741, 1966.

[29] N. Cohn, "Techniques for improving the control of bulk power transfers on interconnected systems," *IEEE Trans. Power App. Syst.*, vol. PAS-90, no. 6, pp. 2409 –2419, 1971.

[30] H. G. Kwatny, K. C. Kalnitsky, and A. Bhatt, “An optimal tracking approach to load frequency control,” *IEEE Trans. Power App. Syst.*, vol. PAS-94,, pp. 1635 –1643, 1975.

[31] C. Concordia, L. K. Kirchmayer, and E. A. Szymanski, “Effect of speed governor dead-band on tie-line power and frequency control performance,” *Amer. Inst. Elect. Eng. Trans.*, vol. 76, pp. 429 –435, 1957.

[32] H. Golpira, H. Bevrani, and H. Golpira, “Application of GA optimization for automatic generation control design in an interconnected power system,” *Energy Conversion and Management*, vol. 52, pp. 2247 –2255, 2011.

[33] S. C. Tripathy, T. S. Bhatti, C. S. Jha, O. P. Malik, and G. S. Hope, “Sampled data automatic generation control analysis with reheat steam turbines and governor dead band effects,” *IEEE Trans Power Appl. Syst.*, vol. 103(5), pp. 1045 –1051, 1984.

[34] D. Das, J. Nanda, M. L. Kothari, and D. P. Kothari, “Automatic generation control of hydrothermal system with new area control error considering generation rate constraint,” *Elect. Mach. Power Syst.*, vol. 18, no. 6, pp. 461 –471, 1990.

[35] “IEEE power engineering systems committee report, dynamic models for steam and hydro turbines for power systems studies,” *IEEE Trans. Power App. Syst*, vol. PAS-92, 1973.

[36] “IEEE power engineering systems committee report, hydraulic turbine and turbine control models for system dynamics,” *IEEE Trans. Power. Syst.*, vol. PWRS-7, 1992.

[37] “Working group on prime mover and energy supply models for system dynamic performance studies, dynamic models for combined cycle plants in power system studies,” *IEEE Trans. Power Syst.*, vol. 9, no. 3, pp. 1698 –1708, 1994.

[38] H. L. M and B. G. R, “Utility experience with gas turbine testing and modeling,” *Proceedings of IEEE Power Engineering Society Winter Meeting*, vol. 2, no. 2, pp. 671 –677, 2001.

[39] C. Fosha and O. Elgerd, "The megawatt frequency control problem: a new approach via optimal control theory," *IEEE Trans Power Appl Syst*, vol. 89, no. 4, pp. 563 – 577, 1970.

[40] E. C. Tacker, C. C. Lee, T. W. Reddoch, T. O. Tan, and P. M. Julich, "Optimal control of interconnected electric energy systems: A new formulation," *Proc. IEEE*, vol. 60, no. 10, pp. 1239 – 1241, 1972.

[41] E. V. Bohn and S. M. Miniesy, "Optimum load frequency sample data control with randomly varying system disturbances," *IEEE Trans. Power App. Syst.*, vol. PAS-91, no. 5, pp. 1916 – 1923, 1972.

[42] K. Yamashita and T. Taniguchi, "Optimal observer design for load frequency control," *Int. J. Elect. Power Energy Syst.*, vol. 8, no. 2, pp. 93 –100, 1986.

[43] A. Feliachi, "Load frequency control using reduced order models and local observers," *Int. J. Energy Syst.*, vol. 7, no. 2, pp. 72 –75, 1987.

[44] A. Rubaai and V. Udo, "An adaptive control scheme for LFC of multiarea power systems. part i: Identification and functional design, part-ii: Implementation and test results by simulation," *Elect. Power Syst. Res*, vol. 24, no. 3, pp. 183 –197, 1992.

[45] S. Velusami and K. Ramar, "Design of observer-based decentralized load-frequency controllers for interconnected power systems," *Int. J. Power Energy Syst.*, vol. 17, no. 2, pp. 152 –160, 1997.

[46] Y. Hain, R. Kulessky, and G. Nudelman, "Identification-based power unit model for load-frequency control purposes," *IEEE Trans. Power Syst.*, vol. 15, no. 4, pp. 1313 – 1321, 2000.

[47] V. R. Moorthi and R. P. Aggarawal, "Suboptimal and near optimal control of a load frequency control system,," *Proc. Inst. Elect. Eng.*, vol. 119, pp. 1653 – 1660, Nov. 1972.

[48] S. S. Choi, H. K. Sim, and K. S. Tan, "Load frequency control via constant limited-state feedback," *Elect. Power Syst. Res.*, vol. 4, no. 4, pp. 265 – 269, 1981.

[49] M. Aldeen and H. Trinh, "Load frequency control of interconnected power systems via constrained feedback control schemes," *Int J Comput Elect Eng*, vol. 20, no. 1, pp. 71 –88, 1994.

[50] G. Shirai, "Load frequency control using liapunovs second method: Bang-bang control of speed changer position," *Proc. IEEE*, vol. 67, no. 10, pp. 1458 – 1459, october 1979.

[51] A. Kumar, O. P.Malik, and G. S. Hope, "Discrete variable-structure controller for load frequency control of multi-area interconnected power system ." *Proc. Inst. Elect. Eng. C*, vol. 134, no. 2, pp. 116 –122, 1987.

[52] S. M. Miniesy and E. V. Bohn, "Two level control of interconnected power plants," *IEEE Trans. Power App. Syst.*, vol. PAS-90, pp. 2742 –2748, June 1971.

[53] N. N. Bengiamin and W. C. Chan, "Multilevel load frequency control of interconnected power system," *Proc. Inst. Elect. Eng.*, vol. 125, no. 6, pp. 521 –526, 1978.

[54] G. Shirai, "Load frequency control using generator and voltage controls via a new approach," *Proc. IEEE*, vol. 66, no. 10, pp. 1293 – 1295, October 1978.

[55] N. Premakumaran, K. Parthasarathy, H. P. Khincha, and M. R. Chidambara, "Some aspects of multi-level load frequency control of a power system," *Proc. Inst. Elect. Eng. C*, vol. 129, no. 5, pp. 290 –294, november 1982.

[56] C. Ross, "A comprehensive direct digital load frequency controller," *Proc. IEEE, PICA Conf.*, pp. 231 – 238, 1967.

[57] C. W. Ross and T. A. Green, "Dynamic performance evaluation of a computer controlled electric power system," *IEEE Trans. Power App. Syst.*, vol. PAS-91, pp. 1156 – 1165, 1972.

[58] F. P. Demello, R. J. Mills, and W. F. BRells, "Automatic generation control, part iprocess modeling," *IEEE Trans. Power App. Syst.*, vol. PAS-92, pp. 710 – 715, 1973.

[59] L. M. Smith, L. H. Fink, and R. P. Schulz, "Use of computer model of interconnected power system to assess generation control strategies," *IEEE Trans. Power App. Syst.*, vol. 94, no. 5, 1975.

[60] C. W. Taylor and R. L. Cresap, "Real-time power system simulations for automatic generation control," *IEEE Trans. Power App. Syst.*, vol. PAS-95, pp. 375 – 384, 1976.

[61] A. Kumar, "Discrete load frequency control of interconnected power system," *Int. J. Energy Syst.*, vol. 9, no. 2, pp. 73 – 77, 1989.

[62] M. L. Kothari, J. Nanda, D. P. Kothari, and D. Das, "Discrete mode automatic generation control of a two area reheat thermal system with new area control error," *IEEE Trans. Power App. Syst.*, vol. 4, no. 2, pp. 730 –738, May 1989.

[63] D. C. H. Prowse, "Improvements to a standard automatic generation control filter algorithm," *IEEE Trans. Power Syst.*, vol. 8, no. 3, pp. 1204 – 1210, 1993.

[64] L. Hari, M. L. Kothari, and J. Nanda, "Optimum selection of speed regulation parameters for automatic generation control in discrete mode considering generation rate constraints," *Proc. Inst. Elect. Eng. C*, vol. 138, no. 5, pp. 401 – 406, 1991.

[65] Y. Wang, R. Zhou, and C. Wen, "Robust load-frequency controller design for power systems," *Proc. Inst. Elect. Eng. C*, vol. 140, no. 1, pp. 111 – 116, 1993.

[66] ——, "New robust adaptive load frequency control with system parameter uncertainties," *Proc. Inst. Elect. Eng.*, vol. 141, no. 3, pp. 184 –190, May 1994.

[67] G. Ray and C. S. Rani, "Stabilizing decentralized robust controllers of interconnected uncertain power systems based on the hessenberg form:simulated results," *Int. J. Syst. Sci*, vol. 32, no. 3, pp. 387 –399, 2001.

[68] T. C. Yang, Z. T. Ding, and H. Yu, "Decentralised power system load frequency control beyond the limit of diagonal dominance," *Int. J. Elect. Power Energy Syst.*, vol. 24, pp. 173 –184, 2002.

[69] C. W. Ross, “Error adaptive control computer for interconnected power system,” *IEEE Trans. Power App. Syst.*, vol. PAS-85, p. 749, 1966.

[70] J. Kanniah, S. C. Tripathy, and O. P. Malik, “Microprocessor based adaptive load frequency control,” *Proc. Inst. Elect. Eng. C*, vol. 131, no. 4, pp. 121 – 128, 1984.

[71] I. Vajk, M. Vajta, and L. Keviczky, “Adaptive load frequency control of hungarian power system,” *Automatica*, vol. 21, no. 2, pp. 129 –137, 1985.

[72] C. T. Pan and C. M. Liaw, “An adaptive controller for power system and load frequency control,” *IEEE Trans. Power Syst.*, vol. 4, no. 1, pp. 122 –128, 1989.

[73] R. R. Shoults and J. A. J. Ibarra, “Multi-area adaptive LFC developed for a comprehensive agc simulator,” *IEEE Trans. Power App. Syst.*, vol. 8, no. 2, pp. 541 – 547, 1993.

[74] C. M. Liaw, “Design of a reduced-order adaptive LFC for an interconnected hydrothermal power system,” *Int. J. Contr.*, vol. 60, no. 6, pp. 1051 – 1063, 1994.

[75] H. Shayeghi and H. A. Shayanfar, “Application of ANN technique for interconnected power system load frequency control,” *Int J Eng.*, vol. 16, no. 3, pp. 247 – 254, 2003.

[76] ——, “Application of ANN technique based on -synthesis to load frequency control of interconnected power system,” *Electr Power Energy Syst*, vol. 28, pp. 503 – 511, 2006.

[77] S. Ramesh and A. Krishnan, “Fuzzy rule based load frequency control in a parallel AC-DC interconnected power systems through hvdc link,” *International Journal of Computer Applications*, vol. 1, no. 4, 2010.

[78] C. S. Chang and W. Fu, “Area load frequency control using fuzzy gain scheduling of PI controllers,” *Electr Power Syst Res*, vol. 47, pp. 145 – 152, 1997.

[79] E. Cam and I. Kocaarslan, “Load frequency control in two area power system using fuzzy logic controller,” *J. Energy Conversion and Management*, vol. 45, pp. 233 – 245, 2005.

[80] P. Bhatt, R. Roy, and S. Ghoshal, "GA/particle swarm intelligence based optimization of two specific varieties of controller devices applied to two-area multi-units automatic generation control," *Int. Journal of Electrical Power and Energy Syst.*, vol. 32, no. 4, pp. 299 – 310, May 2010.

[81] L. C. Saikia, N. Sinha, and J. Nanda, "Maiden application of bacterial foraging based fuzzy idd controller in AGC of a multi-area hydrothermal system," *Electrical Power and Energy Systems*, vol. 45, pp. 98 – 106, 2013.

[82] M. Bettayeb, A. Quddus, and Randhawa, "Time-weighted optimal state and output feed-back control of power systems," *Int. J. Electric Power Systems Research*, vol. 52, pp. 77 – 86, 1999.

[83] R. Shahnazi and H. Khaloozadeh, "Output feedback control with disturbance rejection of a class of nonlinear mimo systems," *Automatic Control and Computer Sciences*, vol. 42, no. 3, pp. 138 – 144, 2008.

[84] B. Tyagi and S. C. Srivastava, "A decentralized automatic generation control scheme for competitive electricity markets," *IEEE Trans. on Power Systems*, vol. 21, no. 1, pp. 312 –320, 2006.

[85] M. Shiroei, M. R. Toulabi, and A. M. Ranjbar, "Robust multivariable predictive based load frequency control considering generation rate constraint," *Int. J. Electrical Power and Energy Syst.*, vol. 46, pp. 405 – 413, 2013.

[86] N. Hasan, Ibraheem, P. Kumar, and Nizamuddin, "Sub-optimal automatic generation control of interconnected power system using constrained feedback control strategy," *Int. J. Electrical Power and Energy Syst.*, vol. 43, pp. 295 – 303, 2012.

[87] E. Rakhshani and J. Sadeh, "Reduced-order observer control for two-area LFC system after deregulation," *Control Intell. Syst.*, vol. 38, no. 4, pp. 185 – 193, 2010.

[88] C. S. Chang, W. Fu, and F. Wen, “Load frequency control using genetic-algorithm based fuzzy gain scheduling of PI controllers,” *Electr Mach Power Syst*, vol. 26, no. 1, pp. 39–52, 1998.

[89] K. Challa and P. N. Rao, “Analysis and design of controller for two area thermal-hydro-gas AGC system,” *IEEE Conf. proceedings, PEDES*, 2010.

[90] K. P. S. Parmar, S. Majhi, and D. P. Kothari, “Load frequency control of a realistic power system with multi-source power generation,” *International Journal of Electrical Power and Energy Systems*, vol. 42, pp. 426 –33, 2012.

[91] ——, “Automatic generation control of an interconnected hydrothermal power system,” *IEEE Conf. proceedings, INDICON*, 2010.

[92] ——, “Multi-area load frequency control in a power system using optimal output feedback method,” *IEEE Conf. proceedings, PEDES*, 2010.

[93] ——, “Improvement of dynamic performance of LFC of the two area power system: an analysis using MATLAB,” *International Journal of Computer Applications*, vol. 40, no. 10, pp. 28 –32, February 2012.

[94] ——, “LFC of an interconnected power system with thyristor controlled phase shifter in the tie line,” *International Journal of Computer Applications*, vol. 41, no. 9, pp. 27 –30, 2012.

[95] H. Shayeghi, H. Shayanfar, and A. Jalili, “Load frequency control strategies: A state-of-the-art survey for the researcher,” *Energy Conversion and Management*, vol. 50, pp. 344 – 353, 2009.

[96] S. K. Aditya and D. Das, “Battery energy storage for load frequency control of an interconnected power system,” *Electr Power Syst Res*, vol. 58, no. 3, pp. 179 – 185, 2001.

[97] S. C. Tripathy, R. Balasubramanian, and P. S. C. Nair, “Effect of superconducting magnetic energy storage on automatic generation control considering governor dead-band and boiler dynamics,” *IEEE Trans Power Syst*, vol. 7, no. 3, pp. 1266 – 1273, 1992.

[98] S. C. Tripathy, “Improved load frequency control with capacitive energy storage,” *J. Energy Conversion and Management*, vol. 38, no. 6, pp. 551 – 562, 1997.

[99] M. Farahani and S. Ganjefar, “Solving LFC problem in an interconnected power system using superconducting magnetic energy storage,” *Physica C*, vol. 487, pp. 60 – 66, 2013.

[100] I. Chidambaram and B. Paramasivam, “Optimized load-frequency simulation in restructured power system with redox flow batteries and interline power flow controller,” *Int. J. Electrical Power and Energy Syst.*, vol. 50, pp. 9 – 24, 2013.

[101] T. S. Bhatti and D. P. Kothari, “Variable structure load-frequency control of isolated wind-diesel-microhydro hybrid power systems,” *J. Institution of Engineers (India)*, vol. 83, pp. 52 – 56, 2002.

[102] S. Ganapathy and S. Velusami, “Design of MOEA based decentralized load-frequency controllers for interconnected power systems with AC-DC parallel tie-lines,” *International Journal of Recent Trends in Engineering*, vol. 2, no. 2, pp. 357 –361, 2009.

[103] P. Kumar and Ibraheem, “Dynamic performance evaluation of 2-area interconnected power systems: a comparative study,” *Electrical Engineering Division, J. Institution of Engineers (India)*, vol. 78, pp. 199 –209, 1998.

[104] Ibraheem and P. Kumar, “Dynamic performance enhancement of hydropower systems with asynchronous tie-lines,” *J Electr Power Compon Syst*, vol. 31, no. 7, pp. 605 – 626, 2003.

[105] K. Y. Lim, Y. Wang, and R. Zhou, “Decentralized robust load-frequency control in coordination with frequency-controllable HVDC links,” *Electr Power Energy Syst*, vol. 19, no. 7, pp. 423 – 431, 1997.

[106] K. Subbaramaiah, V. C. J. Mohan, and V. C. V. Reddy, "Comparison of performance of SSSC and TCPS in automatic generation control of hydrothermal system under deregulated scenario," *International Journal of Electrical and Computer Engineering*, vol. 1, no. 1, pp. 21 –30, 2011.

[107] C. S. Rao, "Improvement of dynamic performance of AGC of hydrothermal system employing capacitive energy storage and TCPS," *Innovative Systems Design and Engineering*, vol. 2, no. 6, pp. 63 –71, 2011.

[108] R. J. Abraham, D. Das, and A. Patra, "Damping oscillations in tie power and area frequencies in a thermal power system with SMES-TCPS combination," *J. Electrical Systems*, vol. 7, no. 1, pp. 71 –80, 2011.

[109] ——, "AGC of a hydrothermal system with thyristor controlled phase shifter in the tie-line," *IEEE conf. proceedings*, 2006.

[110] R. D. Christie and A. Bose, "Load frequency control in hybrid electric power markets," *Proc. IEEE, Int. Conf. Contr. App*, vol. 11, pp. 432 – 436, 1996.

[111] B. H. Bakken and O. S. Grande, "Automatic generation control in a deregulated power system," *IEEE Trans. Power Syst.*, vol. 13, no. 4, pp. 1401 – 1406, 1998.

[112] J. Kumar, K. Ng, and G. Sheble, "AGC simulator for price-based operation part 1: A model," *IEEE Trans.Power Syst.*, vol. 12, no. 2, pp. 527 –532, 1997.

[113] S. Chanana and A. Kumar, "A price based automatic generation control using unscheduled interchange price signals in indian electricity system," *International Journal of Engineering, Science and Technology*, vol. 2, no. 2, pp. 23 – 30, 2010.

[114] S. Debbarma, L. C. Saikia, and N. Sinha, "AGC of a multi-area thermal system under deregulated environment using a non-integer controller," *Electric Power Systems Research*, vol. 95, pp. 175 – 183, 2013.

[115] B. Tyagi and S. C. Srivastava, "Automatic generation control for multiarea system in a deregulated electricity market," *Proc. Int. Conf. Bulk Power Transmission System Integration Developing Countries, Cigre Regional Meeting,*, pp. VIII–18–VIII–29, 2001.

[116] K. S. S. Ramakrishna and T. S. Bhatti, "Automatic generation control of single area power system with multi-source power generation," *Proc. IMechE: J. Power and Energy*, vol. 222 part A, pp. 1 –11, 2008.

[117] K. S. S. Ramakrishna, P. Sharma, and T. S. Bhatti, "Automatic generation control of interconnected power system with diverse sources of power generation," *Int. J. of Engineering Science and Technology*, vol. 2, no. 5, pp. 51 –65, 2010.

[118] T. E. Bechert and N. Chen, "Area automatic generation control by multi-pass dynamic programming," *IEEE Trans. Power App. Syst.*, vol. PAS-96, pp. 1460 –1468, 1977.

[119] S. Mishra, G. Mallesham, and P. Sekhar, "Biogeography based optimal state feedback controller for frequency regulation of a smart microgrid," *IEEE Transactions on Smart Grid*, vol. 4, no. 1, pp. 628 – 637, 2013.

[120] F. Llewis and V. L. Syrmos, *Optimal Control*. New Jersy , Englewood cliffs: Prentice hall, 1995.

[121] *Control Toolbox, MATLAB Software*. MathWoks, Inc. MATLAB, vol. Version 7.13 (R2011b).

[122] Y. K. Singh and B. B. Chaudhuri, *MATLAB Programming*. New Delhi: Prentice hall, 2007.

[123] S. K. Sinha, "Automatic generation control in regulated and restructured power system," Ph.D. dissertation, IIT Roorkee,India, 2010.

[124] K. R. Sudha and R. V. Santhi, "Robust decentralized load frequency control of interconnected power system with generation rate constraint using type-2 fuzzy approach," *Int. J. Electrical Power and Energy Systems*, vol. 33, pp. 699 –707, 2011.

[125] Y. L. Karanvas and D. P. Papadopoulos, " AGC for autonomous power system using combined intelligent techniques," *Electr Power Syst Res*, vol. 62, no. 2, pp. 225 – 239, 2002.

[126] H. Shabani, B. Vahidi, and M. Ebrahimpour, "A robust PID controller based on imperialist competitive algorithm for load-frequency control of power systems," *ISA Transactions*, vol. 52, pp. 88 – 95, 2013.

[127] C. S. Rao, S. S. Nagaraju, and P. Raju, "Improvement of dynamic performance of AGC under open market scenario employing TCPS and AC-DC parallel tie line," *International Journal of Recent Trends in Engineering*, vol. 1, no. 1, 2009.

[128] H. D. Mathur and H. V. Manjunath, "Study of dynamic performance of thermal units with asynchronous tie lines using fuzzy based controller," *J. Electrical Systems*, vol. 3, no. 3, pp. 124 –130, 2007.